



Durham E-Theses

Symmetry violation in quark models of mesons

Rimmer, Anthony B.

How to cite:

Rimmer, Anthony B. (1981) *Symmetry violation in quark models of mesons*, Durham theses, Durham University. Available at Durham E-Theses Online: <http://etheses.dur.ac.uk/7666/>

Use policy

The full-text may be used and/or reproduced, and given to third parties in any format or medium, without prior permission or charge, for personal research or study, educational, or not-for-profit purposes provided that:

- a full bibliographic reference is made to the original source
- a [link](#) is made to the metadata record in Durham E-Theses
- the full-text is not changed in any way

The full-text must not be sold in any format or medium without the formal permission of the copyright holders.

Please consult the [full Durham E-Theses policy](#) for further details.

SYMMETRY VIOLATION IN QUARK

MODELS OF MESONS

SYMMETRY VIOLATION IN QUARK

MODELS OF MESONS

The copyright of this thesis rests with the author.
No quotation from it should be published without
his prior written consent and information derived
from it should be acknowledged.

A Thesis submitted to
the University of Durham

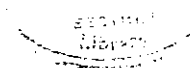
by

Anthony B.Rimmer, B.Sc. (Durham)

For the Degree of Doctor of Philosophy

Department of Physics
University of Durham

December, 1981.



CONTENTS

	<u>Pages</u>
ABSTRACT	i
ACKNOWLEDGEMENT	iii
CHAPTER 1 :	
1.1 PARTICLE CLASSIFICATION AND THE RELATIVISTIC QUARK MODEL	1
1.2 THE ADDITION OF CHARM AND HIGHER SYMMETRIES	5
1.3 THE OZI RULE	6
1.4 POTENTIAL MODELS	8
1.5 QUARK MODEL DETERMINATION OF HADRON PROPERTIES	10
1.5.1 Radiative Decays in the Quark Model	11
1.5.2 Inelastic Meson Baryon Scattering	14
1.6 QUANTUM CHROMODYNAMICS	16
1.6.1 Introduction	16
1.6.2 Symmetry Properties of the QCD Lagrangian	19
CHAPTER 2 : ISOSCALAR MESON MIXING I.GROUND STATE MIXING MODELS	23
2.1 INTRODUCTION	23
2.2 CONVENTIONAL MIXING IN THE NON-RELATIVISTIC QUARK MODEL	24
2.3 THE ANNIHILATION INTERACTION	29
2.4 FLAVOUR DEPENDENCE OF THE ANNIHILATION PARAMETER	31
2.5 MIXING WITH A FLAVOUR DEPENDENT A	34
2.5.1 The Quadratic Mass Matrix	34
2.5.2 The Linear Mass Matrix	41

CHAPTER 3	: ISOSCALAR MESON MIXING	
	II. THE INCLUSION OF RADIAL EXCITATIONS	43
	3.1 INTRODUCTION	43
	3.2 RADIAL EXCITATIONS - THE EXPERIMENTAL SCENE	45
	3.2.1 Heavy Vector Mesons	46
	3.2.2 Pseudoscalar Meson Excitations	49
	3.3 MODELS WITH RADIAL EXCITATIONS	50
	3.3.1 General Features	50
	3.3.2 Extending the Cohen and Lipkin Models	56
	3.3.3 The Extended Quadratic Model	58
	3.3.4 The Extended Linear Model	60
CHAPTER 4	: THE LINEAR MIXING MODEL AND MESON PROPERTIES	65
	4.1 INTRODUCTION	65
	4.2 RADIATIVE DECAY PREDICTIONS AND THE VALUE OF ρ	66
	4.3 HADRONIC INTERACTIONS	78
	4.3.1 Isoscalar Production Processes	78
	4.3.2 Strong Decay Processes	82
CHAPTER 5	: ISOSPIN VIOLATION - THE CONSTITUENT QUARK MODEL	92
	APPROACH	
	5.1 INTRODUCTION	92
	5.2 QUARK MASSES	93
	5.3 ISOSPIN VIOLATING MASS DIFFERENCES	98
	5.4 ISOSPIN VIOLATION IN THE RADIAL MIXING MODEL	100
	5.4.1 Isospin Violating Mixing	101
	5.4.2 Isomultiplet Mass Differences	106
	5.4.3 $\omega \rightarrow 2\pi$ Decay	109
	4.3.3 The Isospin Violating Decay $\psi' \rightarrow \pi^0 \psi$	109

	<u>Pages</u>
CHAPTER 6 : THE CURRENT ALGEBRA APPROACH TO $\rho = \Gamma(\psi \rightarrow \eta' \gamma) / \Gamma(\psi \rightarrow \eta \gamma)$ AND $R = \Gamma(\psi' \rightarrow \pi^0 \psi) / \Gamma(\psi' \rightarrow \eta \psi)$	113
6.1 INTRODUCTION	113
6.2 CURRENT AND DIVERGENCE DEFINITIONS	118
6.3 AXIAL VECTOR WARD IDENTITIES	123
6.4 SOLUTION OF THE SU(3) VIOLATING EQUATIONS	128
6.5 SOLUTION OF THE ISOSPIN VIOLATING EQUATIONS	132
CHAPTER 7 : SUMMARY AND CONCLUSIONS	136
APPENDICES :	145
REFERENCES :	155

ABSTRACT

Constituent and current quark models are employed to discuss many of the SU(3) and SU(2) violating strong and electromagnetic properties of pseudoscalar and vector mesons. The conventional ground state isoscalar meson mixing models are reviewed and extended to include radial excitations in the mass matrix. A phenomenological analysis of symmetry breaking in the models allows a successful simultaneous description of both the vector and pseudoscalar mass spectra, although attempts made to include the high statistics Crystal Ball result for the ratio $\rho = \Gamma(\psi \rightarrow \eta'\gamma)/\Gamma(\psi \rightarrow \eta\gamma) = 5.88 \pm 1.46$ fail. A detailed description of meson radiative decay processes and the ratio of strong production amplitudes $\bar{\sigma}(\pi^- p \rightarrow \eta' n)/\bar{\sigma}(\pi^- p \rightarrow \eta n)$ in a linear radial mixing model indicates that a consistent description of isoscalar meson properties can be made when $\rho = 3.1$, a value considerably less than the Crystal Ball result but in agreement with that obtained by the Dasp collaboration. The model parameters obtained in this analysis allow a satisfactory description of strong two body vector to pseudoscalar meson decays, and subsequent prediction of relationships between amplitudes for similar decays of the radial states. The model does not, however, provide an adequate account of the $I \neq 0$ D, D^*, F, F^* and to a lesser extent K and K^* meson states, a failing shared by all similar constituent models which are examined. Deficiencies in this description of meson structure which may explain the discrepancies are discussed.

The linear mass model used to predict $\rho = 3.1$ provides an ideal framework for an examination of isospin violating meson properties. The phenomenological addition of strong and electromagnetic isospin violating parameters to the mass matrix allows the prediction of pseudoscalar and vector isoscalar-isovector mixing angles and isomultiplet mass differences. A satisfactory description of these mass differences and the branching ratio $B(\omega \rightarrow 2\pi)$ results, however, a prediction made for the ratio $R = \Gamma(\psi' \rightarrow \pi^0 \psi)/\Gamma(\psi' \rightarrow \eta \psi)$ is much

smaller than measured values. The importance of contributions to these results from the isospin violating strong interactions is stressed.

A current algebra approach to the ratios ρ and R is also undertaken. Axial Ward identities which include contributions from the triangle anomaly yield relations between the pseudoscalar meson masses and decay constants. These are included with equations describing $P \rightarrow 2\gamma$ decays and the ratio ρ which together are solved for the decay constants and topological charge components of the π^0, η and η' . These allow a prediction for the ratio R which agrees with that obtained using the constituent quark model approach but is only half the magnitude of present experimental measurements.

ACKNOWLEDGEMENTS

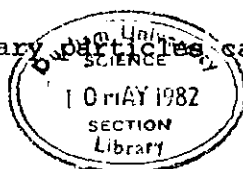
It is my pleasure to thank Fred Gault for his support and guidance during my too brief excursion to the world of particle physics. My thanks to him also for many stimulating discussions during the course of this work, of which a part was completed with his collaboration. To Mike Pennington, Tim Spiller, Phil Done, Alan Martin, Peter Collins and Fred, again, I offer my gratitude for creating the happy, convivial atmosphere in which this work was performed and to my wife, Maria, my thanks for the understanding and encouragement given during the trying period in which this manuscript was completed.

The Science and Engineering Research Council receive my thanks for providing the financial support which allowed me to accept the opportunity of gaining research experience in such a fascinating field offered by this university.

CHAPTER 11.1 PARTICLE CLASSIFICATION AND THE NON-RELATIVISTIC QUARK MODEL

The present theories of the electroweak (Weinberg-Salam⁽¹⁾) and strong (Quantum Chromodynamics⁽²⁾) interactions have been used with reasonable success to describe the dynamical behaviour of many physical systems. However, in certain regimes the dynamical predictions of these theories break down, and in such conditions recourse is often made to a study of their invariance properties. This is particularly true in the case of quantum chromodynamics (QCD) where the perturbative techniques applied in the high energy regime to explain such processes as deep inelastic lepton-proton scattering cannot be used to describe the nature of bound states at low energies. A study of the properties of such states is the purpose of this investigation where symmetry principles and, when available, techniques peculiar to the non-relativistic quark model are used to derive relationships between amplitudes describing many of the strong and electromagnetic interactions of bound states, particular attention being paid to the way in which the various symmetries are broken.

The classification schemes of hadron states in particle physics have a long history. The earliest known hadrons, the proton and neutron, were observed to have very similar masses and strong interactions, properties which suggested they form a doublet, which was later recognised as a multiplet of the SU(2) algebra of isospin which transforms these states into one another. In the course of time further particles were discovered which, like the proton and neutron, were also classified in isospin multiplets, each multiplet containing states with approximately the same mass and similar strong interactions but differing in their electromagnetic properties. With the discovery of an increasing number of elementary particles came the recognition that groups of



isospin multiplets with different values of strangeness, but with the same eigenvalues of all other quantum numbers conserved in the strong interactions, could be collected to form larger multiplets of particles with roughly similar masses. The symmetry algebra which correctly described this larger multiplet structure was suggested independently by Gell-Mann and Ne'eman⁽³⁾ in 1961 to be that of SU(3).

Of interest here are the spin zero and spin one pseudoscalar and vector mesons, which, in the SU(3) classification belong to one of only two multiplets, a singlet or an octet. This scheme is well explained in terms of the non-relativistic quark model^(3,4,5,6) in which hadrons are regarded as composites of a fundamental triplet $\underline{3}$ of quarks and/or a triplet $\bar{\underline{3}}$ of anti-quarks⁽⁷⁾. Conventionally these quarks are denoted u, d and s where the three different types are said to have different flavours. The observed hadrons are constructed such that baryons are bound states of three quarks while mesons are composed of a quark-antiquark pair such that, with the assigned quark properties in Table 1.1, the hadron classification scheme which results reproduces that observed experimentally. The pseudoscalar and vector mesons are then formed by combining quarks and antiquarks in different arrangements to fill the multiplets of the SU(3) product representations given by

$$\underline{3} \otimes \bar{\underline{3}} = \underline{8} \oplus \underline{1} \quad (1.1)$$

Table 1.1 : Quark quantum number assignments

Quark Flavour	Isospin		Strange- ness S	Hyper- charge Y = B+ S	Charge Q	Baryon Number B	Spin-Parity J ^P
	I	I ₃					
u	½	+ ½	0	1/3	2/3	1/3	1/2 ⁺
d	½	- ½	0	1/3	-1/3	1/3	1/2 ⁺
s	0	0	-1	-2/3	-1/3	1/3	1/2 ⁺

It is useful, for future applications, to write the meson wavefunctions in terms of their underlying quark structure. The full wavefunction is formed from a product^(4,5,6) of four parts :

(i) The spatial wavefunction, whose structure depends upon the detailed dynamics of the quark motion inside the hadron. The information required for its construction is unknown at present, however, a simplifying assumption is frequently made which involves giving a common spatial wavefunction to all members of a given multiplet such that their overlap integrals, which appear in many quark model applications, can be set equal to unity.

(ii) The spin wavefunction⁽⁴⁾. The pseudoscalar mesons are spin singlet states with

$$|0, 0\rangle = \frac{1}{\sqrt{2}} \left[|\uparrow\downarrow\rangle - |\downarrow\uparrow\rangle \right] \quad (1.2)$$

while the vectors with spin one form a triplet

$$\begin{aligned} |1, 1\rangle &= |\uparrow\uparrow\rangle \\ |1, 0\rangle &= \frac{1}{\sqrt{2}} \left[|\uparrow\downarrow\rangle + |\downarrow\uparrow\rangle \right] \\ |1, -1\rangle &= |\downarrow\downarrow\rangle \end{aligned} \quad (1.3)$$

where the notation $|S, s_3\rangle$ with S the total spin and s_3 its third component is used to define the spin states.

(iii) The unitary spin wavefunction, which provides the explicit quark structure of a hadron state. The $SU(3)$ pseudoscalar and vector mesons have

unitary spin wavefunctions

$$\begin{aligned}
 |\pi^+\rangle &= |\bar{u}d\rangle & |\pi^0\rangle &= \frac{1}{\sqrt{2}} |u\bar{u}-d\bar{d}\rangle & |\pi^-\rangle &= |\bar{d}u\rangle \\
 |\rho^+\rangle & & |\rho^0\rangle & & |\rho^-\rangle & \\
 \\
 |k^+\rangle &= |\bar{u}s\rangle & |k^0\rangle &= |\bar{d}s\rangle & |\bar{k}^0\rangle &= |\bar{s}d\rangle & |k^-\rangle &= |\bar{s}u\rangle & (1.4) \\
 |k^{*+}\rangle & & |k^{*0}\rangle & & |\bar{k}^{*0}\rangle & & |k^{*-}\rangle & \\
 \\
 |8\rangle &= -\frac{1}{\sqrt{6}} |u\bar{u} + d\bar{d} - 2s\bar{s}\rangle & |1\rangle &= \frac{1}{\sqrt{3}} |u\bar{u} + d\bar{d} + s\bar{s}\rangle
 \end{aligned}$$

where $|8\rangle$ and $|1\rangle$ denote the SU(3) octet and singlet states respectively,

(iv) The colour wavefunction. Various theoretical and experimental arguments have been proposed for the inclusion of colour degrees of freedom in the quark model. The symmetric nature of the space-spin-unitary spin wavefunctions associated with ground state baryons requires such a proposal^(5,8) if quarks are to obey Fermi-Dirac statistics, the additional colour wavefunction having the required anti-symmetric form. Theoretical calculations of $\Gamma(\pi^0 \rightarrow 2\gamma)$ ⁽⁹⁾ and $R_{e^+e^-} = \sigma(e^+e^- \rightarrow \text{hadrons}) / \sigma(e^+e^- \rightarrow \mu^+\mu^-)$ ⁽⁸⁾ when compared with experiment suggest that each quark flavour (u,d or s) should come in three different colours, denoted here by red (R), green (G) and blue (B). The absence of coloured hadrons has led to the hypothesis that all physical observables are colour singlets, thus assigning the colour degrees of freedom to a colour group, SU(3)_c, the colour singlet wavefunction for mesons is formed from

$$\underline{3} \otimes \bar{\underline{3}} = \underline{1} \oplus \underline{8}$$

where the singlet state is given by

$$|1\rangle = \frac{1}{\sqrt{3}} |RR + GG + BB\rangle \quad (1.5)$$

By treating quarks as dynamical objects and assigning each a half integer spin the internal symmetry group $SU(3)$ was conveniently extended⁽¹⁰⁾ (by the inclusion of $SU(2)_{\text{spin}}$) to $SU(6)$. Meson states now fall into multiplets given by

$$\underline{6} \otimes \bar{\underline{6}} = \underline{35} \oplus \underline{1} \quad (1.6)$$

where the $\underline{35}$ representation of $SU(6)$ is decomposed into

$$\underline{35} \supset \underline{3}_8 + \underline{1}_8 + \underline{3}_1 \quad (1.7)$$

The $\underline{3}_8$ and $\underline{3}_1$ contain the vector mesons (the superscript corresponds to $2s + 1$) while the $\underline{1}_8$ and singlet $\underline{1}_1$ of $(1,6)$ contain the pseudoscalar mesons.

In addition to their intrinsic spin the quarks forming a $q\bar{q}$ pair within a meson can have a non-zero orbital angular momentum \vec{L} , the total spin of the meson being given by $\vec{J} = \vec{L} + \vec{S}$. Higher spin systems with $L \neq 0$ will also fall into the $SU(3)$ classification scheme and occupy $\underline{8}$ and $\underline{1}$ multiplets, however, only the properties of $L = 0$ states are discussed here.

1.2 THE ADDITION OF CHARM AND HIGHER SYMMETRIES

In 1964 Bjorken and Glashow⁽¹¹⁾ and others⁽¹²⁾, working on the assumption that a quark-lepton symmetry may exist in nature, suggested the introduction of a further quark to the (u,d,s) triplet to match the four leptons (e, ν_e, μ, ν_μ) which were known at the time. This new quark, the c -quark, and associated quantum number, charm⁽¹³⁾, required that the $SU(3)$ classification scheme should be enlarged to $SU(4)$ and hence that many new hadron states containing the c -quark should exist. The idea was given further theoretical support in 1970 when it was noted by Glashow et al⁽¹⁴⁾ that the introduction of the charmed quark to the Weinberg Salam model of electroweak interactions would eradicate the unwanted strangeness

changing neutral current present in the theory, however it had to wait until 1974 for experimental verification, when the first state to fit into the proposed SU(4) classification, the $J/\psi^{(15)}$ was discovered.

The u, d, s and c-quarks form the fundamental representation $\underline{4}$ of SU(4) while the pseudoscalar and vector mesons occupy the product representations given by

$$\underline{4} \otimes \bar{\underline{4}} = \underline{15} \oplus \underline{1} \quad (1.8)$$

where the SU(3) content of the $\underline{15}$ is given by

$$\underline{15} \supset \underline{8} \oplus \underline{1} \oplus \underline{3} \oplus \bar{\underline{3}} \quad (1.9)$$

The $\underline{8}$ and $\underline{1}$ of SU(3) containing the 'old' mesons have charm, $C = 0$ while the $\underline{3}$ and $\bar{\underline{3}}$ which contain the new D and F pseudoscalars, or D^* and F^* vectors have $C = -1$ and $+1$ respectively.

The discovery⁽¹⁶⁾ of further narrow width meson states in the mass region 9.46 GeV and above in 1977 has necessitated the extension of SU(4) to SU(5) with the introduction of another quark, the b-quark, with associated quantum number beauty. Mesons states, as before, occupy the product representations given by

$$\underline{5} \otimes \bar{\underline{5}} = \underline{24} \oplus \underline{1} \quad (1.10)$$

Working on the principle of a quark-lepton symmetry the discovery of a further charged lepton⁽¹⁷⁾, the τ , and the expected existence of its associated neutrino ν_τ , suggests that six quarks should exist. The additional sixth quark, the top quark, will require the extension of SU(5) to SU(6).

1.3 THE OZI RULE

The considerable symmetry breaking observed in the SU(3) (and higher) multiplets induces the unitary spin wavefunctions of the $I = Y = 0$ mesons to mix. The mixing observed in the pseudoscalar nonet is of a complicated nature,

and is discussed in detail in subsequent chapters, however, the mixing amongst the vector, octet and singlet states is believed to be much simpler, the physical ω and ϕ which result consisting of almost pure quark configurations,

$$\begin{aligned} |\omega\rangle &\approx \frac{1}{\sqrt{2}} |u\bar{u} + d\bar{d}\rangle \\ |\phi\rangle &\approx s\bar{s} \end{aligned} \tag{1.11}$$

Both of these particles have finite widths decaying principally via the strong interactions into pseudoscalar mesons, for example, both the ω and ϕ decay into three pions. Their partial decay widths for this mode are quite different, however, that of the ω being more than an order of magnitude larger than that of the ϕ . Just why these partial widths are so different is explained qualitatively by the Okubo, Zweig, Iizuka (OZI) rule⁽¹⁸⁾.

The OZI rule is most simply formulated in terms of quark-line diagrams in which a quark (or an anti-quark) is described by a line upon which the quantum numbers of the quark remain the same. Its essential content is then the statement that OZI allowed processes are described by connected diagrams, as in Fig 1.1(a), while disconnected diagrams, Fig 1.1(b), represent processes which are OZI forbidden.

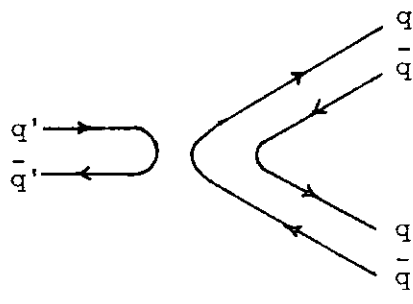
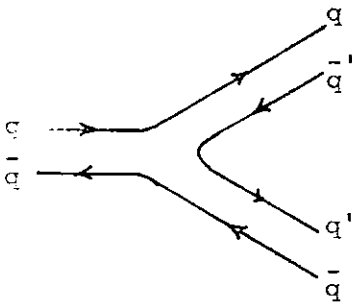


Fig 1.1(a): An OZI allowed process

Fig 1.1(b) : An OZI forbidden process

The decay modes of ω and ϕ to 3π are then described by Fig 1.2.

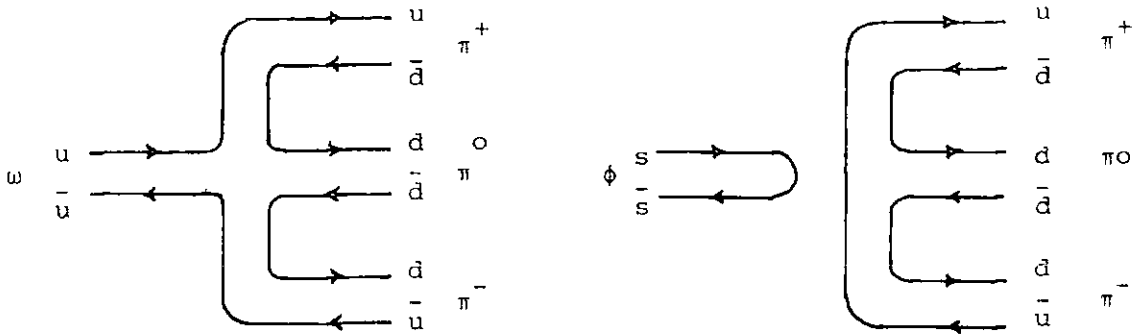


Fig 1.2 : Quark line diagrams for $\omega \rightarrow 3\pi$ and $\phi \rightarrow 3\pi$ decay.

With the quark structure given in (1.11) $\omega \rightarrow 3\pi$ is seen to be an allowed process while $\phi \rightarrow 3\pi$ is forbidden by the OZI rule, which thus qualitatively explains its relative suppression.

The small, but non-zero value observed for the decay width $\Gamma(\phi \rightarrow 3\pi)$ (and $\Gamma(\phi \rightarrow \pi\gamma)$ and other OZI forbidden processes) indicates that the quark structure of the ω and ϕ given in (1.11) does not represent the whole picture. An admixture of u and d quarks in the ϕ wavefunction is necessary to explain these non-zero rates. Just how such deviations from the mixing scheme of (1.11) arise is described in chapters 2 and 3.

1.4 POTENTIAL MODELS

Although the exact nature of the forces which bind a quark and an antiquark to form a meson are unknown, they are often approximated by assuming a specific form for the binding potential $V(r)$ and employing non-relativistic methods, identifying the bound $q\bar{q}$ quarkonium states as eigenstates of the Schrödinger equation. Such a non-relativistic description is usually applied to the heavy quark systems, for example to the $c\bar{c}$ and $b\bar{b}$ families^(19,20) where it has met with great success, however, it has also been used for the lighter $s\bar{s}$ quark system⁽²¹⁾ where predictions of many as yet unidentified quark states are made.

Several functional forms for the potential $V(r)$ have been investigated,

the most common examples are,

(i) Power-Law potentials of the form

$$V(r) = ar^m \quad (1.12)$$

Several examples corresponding to different values of m have been analysed in detail⁽²⁰⁾,

(a) $m = 2$, the harmonic potential. It is possible to solve the non-relativistic equation of motion corresponding to this potential exactly giving the energy eigenvalues

$$E = (2n + \ell + 3/2)\omega \quad (1.13)$$

where ω is the angular frequency of the motion. The values taken by the principal quantum number n and orbital quantum number ℓ denote the degree of radial and orbital excitation respectively, of the system.

(b) $m = 1$, the linear potential. This is a popular choice of potential in quark confinement schemes where it is assumed to apply at large distance scales.

(c) $m = -1$, the Coulomb potential. This is a further commonly used potential which is assumed to simulate the $q\bar{q}$ interaction at short distance scales. Cases (b) and (c) are often used collectively to provide an interaction potential

$$V(r) = a_1 r^{-1} + a_2 r \quad (1.14)$$

which describes how the force between quark and antiquark varies with their separation. The parameter a_1 is frequently set at $a_1 = -4/3 \alpha_s$ and α_s and a_2 determined by fits to the spectrum of states. In this manner the ψ and Υ systems have been successfully reproduced⁽²⁰⁾.

A quantity which will be of considerable value in later applications is the variation of the non-relativistic wavefunction evaluated at zero separation of the $q\bar{q}$ pair with radial quantum number n . This is given for

the power-law potentials by⁽²⁰⁾

$$|\psi_n(0)|^2 \sim (n - 1/4)^{2(m-1)/(m+2)} \quad 0 < m < \infty$$

and

$$|\psi_n(0)|^2 \sim \left[n - \frac{(1+m)}{2(m+2)} \right]^{(m-2)/(2+m)} \quad -2 < m < 0$$

(1.15)

(ii) The logarithmic potential. It has been suggested by Quigg and Rosner⁽²⁰⁾ that the empirical observations in the ψ and Υ systems

$$M_{\psi'} - M_{\psi} \approx M_{\Upsilon'} - M_{\Upsilon} \quad \text{and} \quad M_{\psi''} - M_{\psi} \approx M_{\Upsilon''} - M_{\Upsilon}$$

could have important implications for the inter-quark potential. They exploited this weak dependence of level splitting upon the reduced mass μ of the constituent $q\bar{q}$ pair to derive

$$V(r) = C \ln(r/r_0) \quad (1.16)$$

(which is the unique form for which level spacing is independent of μ).

Setting the interaction strength $C \approx 3/4$ GeV reproduces the level structure of both the ψ and Υ families in reasonable agreement with experiment.

For this potential the variation of $|\psi_n(0)|^2$ with n is given by

$$n |\psi_n(0)|^2 \approx \text{constant} \quad (1.17)$$

1.5 QUARK MODEL DETERMINATION OF HADRON PROPERTIES

The quark model hypothesis has been exploited in many applications to derive hadron properties in terms of those of the underlying quarks. Two approaches can be taken. The quarks can be treated as a useful mnemonic for classifying the numerous elementary particles and hadron properties investigated by exploiting the group structure of the classification scheme

or, the quarks can be treated as dynamical objects, the interactions of which determine the properties of the particles they compose. Both of these approaches will be used here.

1.5.1 Radiative Decays in the Quark Model

One of the most basic assumptions which recurs in many applications of the non-relativistic quark model is the additivity assumption⁽⁴⁾ which allows a particular property of a composite hadron to be described by the sum of contributions from the constituent quarks or antiquarks. In a quark model description of radiative decay processes this assumption is incorporated by writing the operator which causes a transition between mesons $V \rightarrow P + \gamma$ as a sum of operators causing single quark transitions $q_a \rightarrow q_a + \gamma$, Fig 1.3.

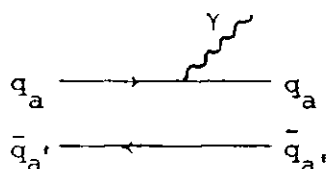


Fig 1.3 : Radiative transition in the non-relativistic quark model.

Thus,

$$\langle P + \gamma | O | V \rangle = \langle P | \sum_a O_a(\gamma) | V \rangle \quad (1.18)$$

where $O_a(\gamma)$ is responsible for the spin-flip process $q_a \rightarrow q_a + \gamma$ and $|V\rangle$ and $|P\rangle$ are the meson wavefunctions described in section 1.1.

Following Kokkedee⁽⁴⁾ the interaction operator $O_a(\gamma)$ is written in non-relativistic form as

$$O_a(\gamma) = \mu_a \frac{e_a}{e} \vec{\sigma}_a \cdot (\vec{k} \times \vec{\epsilon}) e^{i\vec{k} \cdot \vec{r}_a} \quad (1.19)$$

where e_a/e gives the magnitude of the quark charge in units of e , $\vec{\sigma}_a$ is the quark spin operator, μ_a is a scale parameter closely connected with the quark magnetic moment and \vec{k} and $\vec{\epsilon}$ are the photon momentum and polarisation respectively. Unlike the treatment of reference 4 SU(3) symmetry breaking effects are included in the operator through the flavour dependence of μ_a . The matrix elements (1.18) are calculated by substituting meson wavefunctions

(1.2), (1.3) and (1.4) and assuming that (i) the overlap of spatial wavefunctions occurring in (1.18) equals unity and (ii) $\vec{k} \cdot \vec{r} \ll 1$, that is $e^{i\vec{k} \cdot \vec{r}} \approx 1$ (the long photon wavelength approximation). Squaring the results obtained, summing over photon polarisations and averaging over the initial vector meson polarisations yields the required squared matrix element $|M_{V \rightarrow P\gamma}|^2$. Including the relevant phase space factors gives the partial width

$$\Gamma(V \rightarrow P\gamma) = |M_{V \rightarrow P\gamma}|^2 \cdot \frac{k}{2\pi} \quad (1.20)$$

with

$$k = \frac{M_V^2 - M_P^2}{2M_V} \quad (1.21)$$

Precisely the same result is obtained in all cases by applying the more convenient form

$$\Gamma(V \rightarrow P\gamma) = \frac{k^3}{3\pi} |A|^2 \quad (1.22)$$

$$\text{where } A = \langle P | \frac{1}{e} \sum_a \mu_a \mathbf{e}_a \sigma_{3a} | V ; s_3 = 0 \rangle \quad (1.23)$$

and σ_{3a} represents the third component of the spin operator. Denoting general vector and pseudoscalar wavefunctions by

$$\begin{aligned} |V, s_3 = 0 \rangle &= \left[\alpha |u\bar{u}\rangle + \beta |d\bar{d}\rangle + \gamma |s\bar{s}\rangle \right] \frac{1}{\sqrt{2}} (|++\rangle + |--\rangle) \\ |P \rangle &= \left[a |u\bar{u}\rangle + b |d\bar{d}\rangle + c |s\bar{s}\rangle \right] \frac{1}{\sqrt{2}} (|++\rangle - |--\rangle) \end{aligned} \quad (1.24)$$

the matrix element (1.23) gives

$$A = \frac{2}{3} (2\mu_u \alpha a - \mu_d \beta b - \mu_s \gamma c)$$

The μ_a are related by noting that the individual quark magnetic moments are

inversely proportional to the quark mass, thus,

$$\frac{\mu_a}{\mu_b} = \frac{m_b}{m_a} \quad (1.25)$$

giving

$$A = \frac{2}{3} \mu \left(2 \alpha a - \beta b - \frac{m_u}{m_s} \gamma c \right) \quad (1.26)$$

where $\mu_u = \mu_d \equiv \mu$. μ is determined from an evaluation of the proton magnetic moment to give $\mu = \mu_p = 2.79e/2M_p$.

As an example of the application of (1.22) and (1.26) consider the transition $\omega \rightarrow \pi^0 \gamma$ for which (assuming $|\omega\rangle$ is given by (1.11))

$\alpha = \beta = a = -b = 1/\sqrt{2}$ and $\gamma = c = 0$. Thus $A = \mu$ and $\Gamma(\omega \rightarrow \pi \gamma) = 1.11 \text{ MeV}$.

Experiment⁽²²⁾ suggests $\Gamma(\omega \rightarrow \pi \gamma) = 0.87 \pm 0.08 \text{ MeV}$, in reasonable agreement with the predicted width.

The decay processes $P \rightarrow V \gamma$ are calculated using

$$\Gamma(P \rightarrow V \gamma) = \frac{k^3}{\pi} |A|^2 \quad (1.27)$$

where A is again given by (1.23) and

$$k = \frac{M_P^2 - M_V^2}{2M_P} \quad (1.28)$$

$\Gamma(V \rightarrow P \gamma)$ differs from $\Gamma(P \rightarrow V \gamma)$ by a factor of 1/3 because of the average over the spin components of the initial state vector meson in the former case.

An analysis of the extent to which the assumptions made in the derivation of (1.22) hold true has been performed by Barnes⁽²³⁾, who finds that the straightforward calculations are significantly changed by

(i) relaxing the long photon wavelength assumption. Bag model calculations⁽²³⁾ suggest that the decay rates given above could be reduced by a factor of approximately 0.7 if this assumption is not made.

(ii) including recoil effects of the final state meson. Feynman, Kislinger and Ravndal⁽²⁴⁾ have investigated these effects in a relativistic harmonic oscillator quark model and find

$$\Gamma(V \rightarrow P\gamma, \text{ with recoil}) = \left(\frac{2 M_V}{M_V + M_P} \right)^3 \Gamma(V \rightarrow P\gamma, \text{ without recoil}) \quad (1.29).$$

This correction factor may have a considerable effect when $M_V \gg M_P$.

1.5.2 Inelastic Meson Baryon Scattering

A combination of the ideas inherent in the non-relativistic quark model and the additivity assumption have been used quite successfully to predict relations between cross-sections for various high energy elastic⁽²⁵⁾ and inelastic⁽²⁶⁾ scattering processes. Of particular interest here are sum rules relating the amplitudes for inelastic reactions of the type

$$A + B \rightarrow C + D \quad (1.30)$$

where A and C are mesons and B and D are baryons. The target and incident particles are assumed to have a composite quark structure, the quarks of the incident particles scattering coherently on quarks in the target such that the total scattering amplitude is simply the sum of all possible quark scattering amplitudes. The transition matrix element describing (1.30) is thus written as⁽²⁶⁾,

$$\langle (q_a \bar{q}_a) B | (q_c \bar{q}_c) D \rangle = \langle q_a B | q_c D \rangle \delta_{a,c'} + \langle \bar{q}_a B | \bar{q}_c D \rangle \delta_{ac} \quad (1.31)$$

This form implies that any process requiring a simultaneous change in the state of both the quark (q_a) and antiquark (\bar{q}_a) in meson A is forbidden, so any process involving the exchange of more than one unit of charge and/or strangeness is not allowed.

The additivity assumption applied to meson baryon scattering, as represented in (1.31), is only expected to work in the high energy ($s \rightarrow \infty$)

and small scattering angle ($t \rightarrow 0$) limits. Generally, the inelastic processes (1.30) are strongly peripheral, their differential cross-sections are dominated by forward diffraction like peaks in just the region where the additivity assumption is expected to hold. Thus, meaningful comparisons of the model predictions can only be made if peripheralism is exhibited in all the processes considered.

As an example of the application of (1.31) to physical processes the strangeness exchange sum rule

$$\bar{\sigma}(k^- X \rightarrow \eta X') + \bar{\sigma}(k^- X \rightarrow \eta' X') = \bar{\sigma}(k^- X \rightarrow \pi^0 X') + \bar{\sigma}(\pi^- X \rightarrow k^0 X') \quad (1.32)$$

is derived, where X and X' are initial and final state baryons and $\bar{\sigma}$ represents the square of the transition amplitude. The required meson wavefunctions are given in (1.2) and (1.4) with the addition that those of the physical η and η' mesons are linear combinations of the octet and singlet wavefunctions given in (1.4) such that (see chapter 2 for a full discussion)

$$|\eta\rangle = \cos\theta |8\rangle + \sin\theta |1\rangle \quad (1.33)$$

$$|\eta'\rangle = -\sin\theta |8\rangle + \cos\theta |1\rangle$$

Comparing (1.31) and (1.32) requires the identification

$$q_a = s ; q_c = u ; \bar{q}_{a'} = \bar{u} ; \bar{q}_{c'} = \bar{s} \quad (1.34)$$

so that, including spin wavefunctions, the strangeness exchange transition

amplitudes are

$$\begin{aligned}
 \langle k^-_X | \eta_{X'} \rangle &= \frac{1}{2} \left\{ \frac{\cos\theta}{\sqrt{6}} + \frac{\sin\theta}{\sqrt{3}} \right\} S_1 + \frac{1}{2} \left\{ \frac{\sin\theta}{\sqrt{3}} - \frac{2\cos\theta}{\sqrt{6}} \right\} S_2 \\
 \langle k^-_X | \eta'_{X'} \rangle &= \frac{1}{2} \left\{ \frac{\cos\theta}{\sqrt{3}} - \frac{\sin\theta}{\sqrt{6}} \right\} S_1 + \frac{1}{2} \left\{ \frac{\cos\theta}{\sqrt{3}} + \frac{\sin\theta}{\sqrt{6}} \right\} S_2 \quad (1.35) \\
 \langle k^-_X | \pi^0_{X'} \rangle &= \frac{1}{2\sqrt{2}} S_1 \\
 \langle \pi^-_X | k^0_{X'} \rangle &= \frac{1}{2} S_2
 \end{aligned}$$

where

$$\begin{aligned}
 S_1 &\equiv \langle (s\uparrow)_X | (u\uparrow)_{X'} \rangle + \langle (s\uparrow)_X | (u\downarrow)_{X'} \rangle \\
 S_2 &\equiv \langle (\bar{u}\uparrow)_X | (\bar{s}\uparrow)_{X'} \rangle + \langle (\bar{u}\uparrow)_X | (\bar{s}\downarrow)_{X'} \rangle
 \end{aligned} \quad (1.36)$$

Thus

$$\begin{aligned}
 \bar{\sigma}(k^-_X \rightarrow \eta_{X'}) + \bar{\sigma}(k^-_X \rightarrow \eta'_{X'}) &= \frac{1}{8} \left[S_1^2 + 2S_2^2 \right] \\
 &= \bar{\sigma}(k^-_X \rightarrow \pi^0_{X'}) + \bar{\sigma}(\pi^-_X \rightarrow k^0_{X'})
 \end{aligned}$$

independent of the octet-singlet mixing angle, as required.

1.6 QUANTUM CHROMODYNAMICS

1.6.1 Introduction

Quantum Chromodynamics⁽²⁾ is a non-abelian quantum field theory of the strong interactions which embodies the two fundamental concepts of quarks and colour. The spin = 1/2 quarks which carry fractional charge each form colour triplets of $SU(3)_c$, which is assumed to be an exact symmetry. The strong interactions between the coloured quarks are mediated by an octet of coloured vector gluons, one gluon associated with each generator of the group $SU(3)_c$. Further, all physical observables are assumed to be colour singlets (the confinement hypothesis) so the fundamental fields do not appear as physical states. The connection between the fundamental world of quarks and gluons and the real world of interacting hadrons is unknown at

present but is expected to be established with an understanding of the confinement problem⁽²⁷⁾.

The quark fields $q_i^\alpha(x)$ carry two types of indices, α the colour index, $\alpha = R, G, B$, and i the flavour index, $i = u, d, s, c, b, \dots$, while the gluon fields $A_\mu^a(x)$ carry space-time (μ) and $SU(3)_c$ (a) indices and do not couple to flavour. By requiring the $SU(3)_c$ gauge symmetry to be a local symmetry the Lagrangian of QCD is written as⁽⁸⁾

$$\begin{aligned} \mathcal{L}_{\text{QCD}}(x) = & -\frac{1}{4} F_{\mu\nu}^a(x) F_a^{\mu\nu}(x) + i \sum_{i=1}^{n_f} \bar{q}_i^\alpha(x) \gamma^\mu (D_\mu)_{\alpha\beta} q_i^\beta(x) \\ & - \sum_{i=1}^{n_f} m_i \bar{q}_i^\alpha(x) q_i^\alpha(x) + \left\{ \begin{array}{l} \text{gauge fixing and} \\ \text{Fadeev-Popov terms} \end{array} \right\} \end{aligned} \quad (1.37)$$

where (i) $F_{\mu\nu}^a(x)$, $a = 1, \dots, 8$ are the Yang-Mills field strengths constructed from gluon fields and their derivatives

$$F_{\mu\nu}^a(x) = \partial_\mu A_\nu^a(x) - \partial_\nu A_\mu^a(x) + g f_{abc} A_\mu^b(x) A_\nu^c(x) \quad (1.38)$$

with f_{abc} the $SU(3)_c$ structure constants

$$\left[\frac{\lambda^a}{2}, \frac{\lambda^b}{2} \right] = i f_{abc} \frac{\lambda^c}{2} \quad (1.39)$$

and g the QCD coupling constant. $\lambda^a/2$ are the eight generators of the $SU(3)_c$ algebra.

(ii) $(D_\mu)_{\alpha\beta}$ is the covariant derivative

$$(D_\mu)_{\alpha\beta} = \delta_{\alpha\beta} \partial_\mu - ig \sum_a \frac{1}{2} \lambda_{\alpha\beta}^a A_\mu^a(x) \quad (1.40)$$

and (iii) m_i are the bare quark masses. The quark-gluon coupling g and the masses m_i of the quarks are the only free parameters contained in the

Lagrangian (1.37).

Quantizing ^(8,28) the theory in a covariant manner gives rise to the gauge fixing term in (1.37). Requiring that the resulting Lagrangian remain locally gauge invariant forces the introduction of the Fadeev-Popov term.

The first term in (1.37) contains expressions describing the self interactions of the gluon fields represented in Fig 1.4, while the second

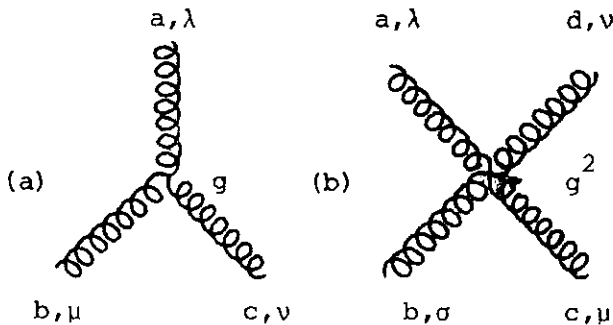


Fig 1.4: Gluon self interactions involving (a) 3 gluons and (b) 4 gluons.

contains an expression describing the quark-gluon interaction, Fig 1.5. An

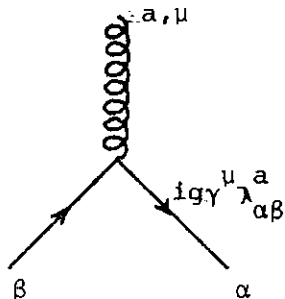


Fig 1.5 : The quark-gluon interaction.

important feature of these interactions is that their strengths are all characterised by just one universal coupling g .

The gluon self coupling represented by Fig 1.4(a) is responsible for a further important feature of this theory - asymptotic freedom ⁽²⁹⁾ - by which the effective interaction strength \bar{g} becomes smaller with decreasing separation (R) such that the theory becomes free, i.e. $\bar{g} \rightarrow 0$ as $R \rightarrow 0$. Thus, while the strong interactions are 'strong' at some distance scale set by, for example, the pion mass, at shorter distances the interactions become weaker allowing the dynamics of many physical systems (for example e^+e^- annihilation and deep inelastic lepto-production ⁽³⁰⁾) to be described using a perturbation expansion in the effective coupling.

1.6.2 Symmetry Properties of the QCD Lagrangian

When the quark mass term m_i is set equal to zero the Lagrangian (1.37) is invariant under the following set of global gauge transformations

$$(a) \quad q(x) \rightarrow \exp(-i\omega^A T^A) q(x) \quad (1.41)$$

$$(b) \quad q(x) \rightarrow \exp(-i\omega_5^A T^A \gamma_5) q(x) \quad (1.42)$$

$$(c) \quad q(x) \rightarrow \exp(-i\omega) q(x) \quad (1.43)$$

$$(d) \quad q(x) \rightarrow \exp(-i\omega_5 \gamma_5) q(x) \quad (1.44)$$

where ω and ω^A are constant gauge parameters and T^A are generators of the flavour group $SU(n)$. The associated Noether currents are

$$(a) \quad V_\mu^A(x) = \bar{q}^i(x) \gamma_\mu T_{ij}^A q^j(x) \quad (1.45)$$

$$(b) \quad A_\mu^A(x) = \bar{q}^i(x) \gamma_\mu \gamma_5 T_{ij}^A q^j(x) \quad (1.46)$$

$$(c) \quad V_\mu(x) = \bar{q}_i(x) \gamma_\mu q_i(x) \quad (1.47)$$

$$(d) \quad A_\mu(x) = \bar{q}_i(x) \gamma_\mu \gamma_5 q_i(x) \quad (1.48)$$

$V_\mu^A(x)$ and $A_\mu^A(x)$ are the usual vector and axial vector currents, which, in this limit, are conserved and have associated charges

$$Q^A = \int d^3x V_0^A(\vec{x}, t) \quad (1.49)$$

$$Q_5^A = \int d^3x A_0^A(\vec{x}, t) \quad (1.50)$$

which satisfy the commutation relations,

$$\begin{aligned}
 \left[Q^A(t), Q^B(t) \right] &= if^{ABC} Q^C(t) \\
 \left[Q^A(t), Q_5^B(t) \right] &= if^{ABC} Q_5^C(t) \\
 \left[Q_5^A(t), Q_5^B(t) \right] &= if^{ABC} Q^C(t)
 \end{aligned} \tag{1.51}$$

$V_\mu(x)$ in (1.47) is the conserved baryonic current whose associated charge

$$Q_B = \int d^3x v_0(\vec{x}, t) \tag{1.52}$$

is the generator of the $U_B(1)$ group, while $A_\mu(x)$ in (1.48) is the axial baryonic current⁽³¹⁾ which is not conserved, even in the $m_i \rightarrow 0$ limit, due to the presence of anomalies⁽³²⁾ arising from the triangle graph Fig 1.6.

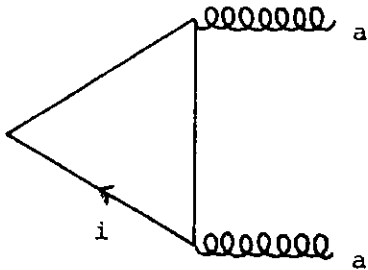


Fig 1.6 : Triangle graph associated with the axial anomaly.

Following the usual procedure, the charges (1.49) and (1.50) can be arranged into left-handed, Q_L^A , and right-handed, Q_R^A , combinations⁽³³⁾ which are generators of the chiral $SU_L(n) \times SU_R(n)$ symmetry, a global symmetry of the QCD Lagrangian in the absence of quark mass terms. There are two possible realisations⁽³⁴⁾ of this chiral symmetry group on physical states corresponding to whether the charges which generate the symmetry annihilate the vacuum or not. In the former case, with

$$Q^A |0\rangle = 0 \quad ; \quad Q_5^A |0\rangle = 0 \tag{1.53}$$

a Wigner-Weyl realisation is obtained where the physical states are classified according to irreducible representations of the group generated by the charges

(Coleman's Theorem⁽³⁵⁾). Then, in the limit $m_i \rightarrow 0$ mass degenerate parity doublets would be expected in the physical spectrum. The alternative possibility where

$$Q^A |0\rangle \neq 0 ; \quad Q_5^A |0\rangle \neq 0 \quad (1.54)$$

results in a Nambu-Goldstone realisation where a spin zero massless particle is associated with each generator which does not annihilate the vacuum (Goldstone's Theorem)⁽³⁶⁾.

The physical picture appears to be a mixture of these two possibilities with

$$Q^A |0\rangle = 0 \quad \text{and} \quad Q_5^A |0\rangle \neq 0 \quad (1.55)$$

so that physical states are observed in degenerate multiplets corresponding to the Wigner-Weyl realisation of the group generated by Q^A together with a number of massless Goldstone bosons, one for each generator Q_5^A which does not annihilate the vacuum (there will be n^2-1 such generators for $SU(n)$).

In reality massless Goldstone bosons and degenerate $SU(n)$ multiplets are not seen in the hadron spectrum and the chiral $SU(n) \times SU(n)$ symmetry of the QCD Lagrangian is broken by the appearance of non-zero quark mass terms. This Lagrangian contains just two free parameters, the bare coupling g and the quark masses m_i . It is believed⁽³⁷⁾ that the non-zero quark masses m_u , m_d and m_s can be treated perturbatively (ignoring higher mass m_i terms) to a good approximation leaving the theory with just one dimensionless parameter g and hence no parameter which can define a scale for dimensional quantities. Such a scale is usually set by the arbitrary renormalisation parameter μ (which is used to define the renormalised coupling g), its magnitude being taken, in general, as a few GeV. The smallness of the quark mass terms m_u , m_d and m_s compared to μ reflects the observation that $SU(3) \times SU(3)$ remains

an approximate symmetry of the strong interactions.

Accepting $SU(3) \times SU(3)$ as an approximate symmetry of the hadron spectrum allows the observed symmetry breaking to be explained in terms of the relative magnitudes of m_u , m_d and m_s . The breaking can be thought of as occurring in three stages⁽³⁸⁾. Firstly, with $m_u = m_d = 0$ and $m_s \neq 0$ the degeneracy of the hadron multiplets will be lifted, the splitting depending upon the number of strange quarks contained in each hadron. Also, the Goldstone Kaon and eta will obtain masses but the non-strange pi triplet will remain massless. Secondly, setting $m_u = m_d \neq 0$ will shift the multiplet and η and K levels slightly and give the π a mass, thus breaking the previous $SU(2) \times SU(2)$ symmetry down to $SU(2)$. The observed splittings within $SU(2)$ multiplets can then be accommodated by setting $m_u \neq m_d$, Fig 1.7. This is the pattern of symmetry breaking originally suggested by Gell-Mann, Oakes and Renner⁽³⁸⁾.

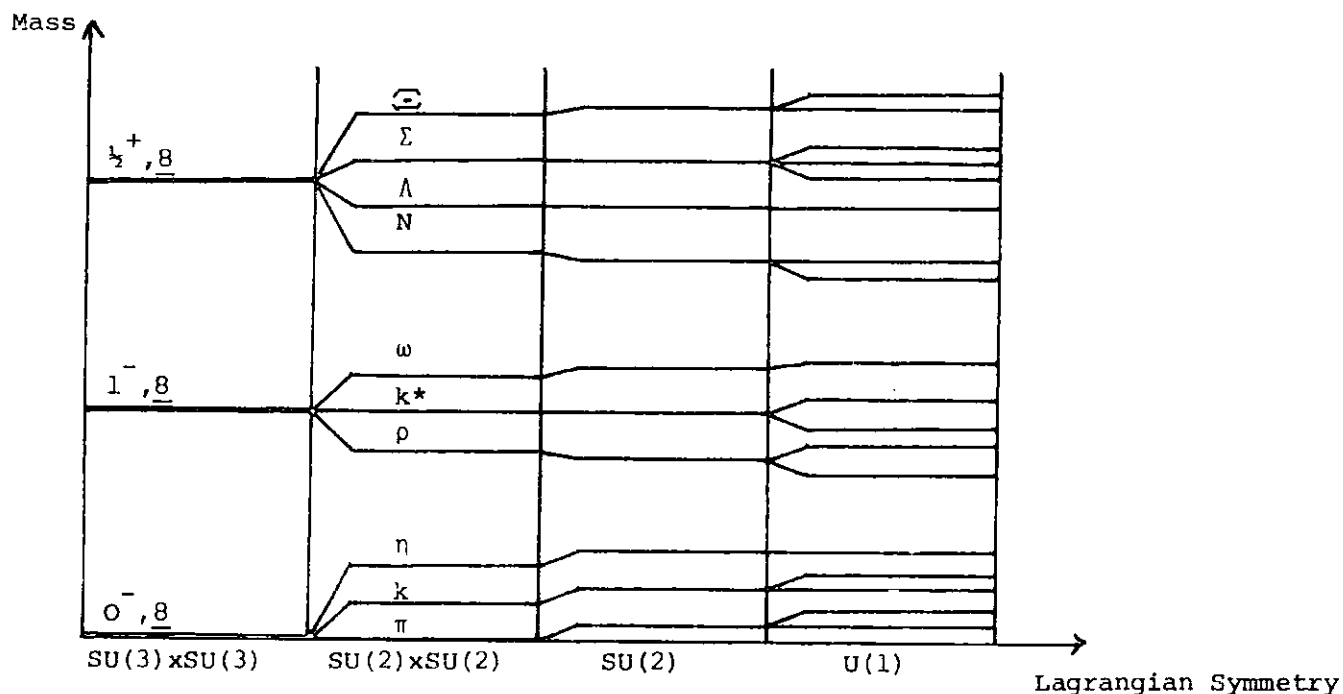


Fig 1.7 : Symmetry breaking in the hadron spectrum.

CHAPTER 2ISOSCALAR MESON MIXINGI. GROUND STATE MIXING MODELS2.1 INTRODUCTION

The non-relativistic quark model in which quarks are considered to be the fundamental building blocks of hadronic matter provides an excellent framework in which many quantitative predictions of meson properties can be made⁽⁴⁾. The picture presented here describes the mesons as composite particles constructed from a quark and an anti-quark which are strongly bound (confined) by the exchange of coloured gluons.

The description of the quark structure of mesons presented by the spin-unitary-spin wavefunctions of Chapter 1 (equations (1.2), (1.3) and (1.4)) assumes that the only forces acting between the quark and anti-quark are those which leave $SU(6)$ ($SU(3)_{\text{flav.}} \otimes SU(2)_{\text{spin}}$) an unbroken symmetry. In nature this is not so, however for considerable splittings are observed both between the central masses of the pseudoscalar and vector octets and between the masses of isospin multiplets within these $SU(3)$ multiplets. The symmetry violating forces which produce these effects are also responsible for isoscalar meson mixing, the subject investigated here.

Some of the initial problems encountered with mixing schemes developed in the non-relativistic quark model revolved around the question of whether the mixing should be described in terms of linear or quadratic masses. The construction of early models favoured a quadratic approach and many arguments have been suggested to justify this choice, for example, since free mesons propagate according to the Klein-Gordon equation, which is quadratic in mass, it would perhaps be more appropriate to treat the mixing problems of mesons in terms of quadratic masses. The point is well

summarised by Dalitz⁽⁵⁾, "it is a matter of experience that the discussion works best in terms of $(\text{mass})^2$ ".

The approach to mixing schemes has been revised in recent years with the inclusion of further terms, describing the possible annihilation of a $q\bar{q}$ pair contained in an isoscalar meson, in the basic Hamiltonian⁽³⁹⁾, and in most recent models allowance has been made for the possible mixing of ground-state wavefunctions with their radial excitations (Chapter 3). The view taken here is that the failure of the early linear mixing models was due to their simplistic construction and the problem of whether mixing should be described in terms of linear or quadratic masses is left open.

A drawback in all the mixing prescriptions described is their non-relativistic nature. At best, the models to be proposed can only give an average description of meson properties, and it is hoped that relativistic effects will, to some extent, be included in the parameters of the model⁽⁴⁰⁾ which are fixed by fitting to the physical properties of the systems they describe. The favourable predictions of the more sophisticated models may bear witness to this.

2.2 CONVENTIONAL MIXING IN THE NON-RELATIVISTIC QUARK MODEL

When states in $SU(6)$ multiplets have the same eigenvalues of all quantities conserved in the strong interactions they can be mixed by symmetry breaking forces. This is the case for the octet and singlet pseudoscalar and vector mesons which are mixed when $SU(3)$ is broken (note, however, that non-strange mesons with different spin have different G-parity so there will be no mixing between the vectors and pseudoscalars). As a result, the wavefunctions of the physical $I = Y = 0$ mesons will not be those given by (1.4) but will be the resultants of linear combinations of these wavefunctions⁽⁴⁾.

To investigate the degree to which mixing occurs, an analysis is made of quark model predictions for meson masses. For convenience, the

strong binding forces which act between quark and anti-quark are separated into three groups,

(i) Strong forces which confine the quarks to the hadrons but leave all the mesons within SU(6) multiplets degenerate in mass. With just these forces acting the quarks will also have equal masses.

(ii) Spin dependent forces which lift the degeneracy between SU(3) multiplets within SU(6) multiplets. The part of the Hamiltonian operator^(4,39) describing these interactions is expected to take the form $B \bar{\sigma}_a \cdot \bar{\sigma}_b$ for quarks a and b, where B characterises the strength of this hyperfine interaction.

(iii) SU(3) breaking forces which produce mass differences between isospin multiplets. These forces are assumed to be manifest entirely in the $m_s - m_u$ quark mass difference⁽⁴⁾.

When these forces act together the mass of a meson A (in the regime of linear masses) is given by

$$M_A = \langle \psi(A) | \sum_a m_a + B \bar{\sigma}_a \cdot \bar{\sigma}_b | \psi(A) \rangle \quad (2.1)$$

where $\psi(A)$ represents the product of spin, unitary spin and spatial wave-functions for meson A and m_a is the mass of a quark of type a. In order to investigate quadratic mass mixing m_a is replaced by m_a^2 .

The conventional analysis of isoscalar meson mixing follows a set procedure,

(a) Firstly write down the masses of SU(3) states as given by (2.1), including their mixing elements. For the pseudoscalars these are,

$$\begin{aligned} M_\pi &= 2 m_u + aB \\ M_K &= m_u + m_s + aB \\ M_8 &= \frac{2}{3} (m_u + 2m_s) + aB \\ M_1 &= \frac{2}{3} (2m_u + m_s) + aB \\ \delta M_{81} &= -\frac{2\sqrt{2}}{3} (m_u - m_s) \\ \delta M_{8\pi} &= \delta M_{1\pi} = 0 \end{aligned} \quad (2.2)$$

where M_8 and M_1 are the masses of the octet and singlet states respectively. Similar expressions are obtained for the vectors by making the replacements $\pi \rightarrow \rho$ and $k \rightarrow k^*$ and noting that a , the eigenvalue of the $\bar{\sigma}_a \cdot \bar{\sigma}_b$ operator takes on the values $a = -\frac{3}{4}$ for the pseudoscalars and $+1/4$ for the vectors. Note that the hyperfine interaction lifts the degeneracy between SU(3) multiplets but does not mix states within an SU(3) multiplet. The overlap of spatial wavefunctions occurring in the mixing element δM_{81} is assumed, for the present to be unity.

(b) Write the unitary spin wavefunctions of the physical $I = Y = 0$ mesons as linear combinations of the octet and singlet states,

$$\begin{bmatrix} |\eta\rangle \\ |\eta'\rangle \end{bmatrix} = \begin{bmatrix} \cos\theta & \sin\theta \\ -\sin\theta & \cos\theta \end{bmatrix} \begin{bmatrix} |8\rangle \\ |1\rangle \end{bmatrix} \quad (2.3)$$

(c) Obtain the mass matrix in the basis of physical states by diagonalising the mass matrix in the SU(3) basis ($M_{\text{SU}(3)}$) with the rotation matrix given in (2.3), where

$$M_{\text{SU}(3)} = \begin{bmatrix} M_8 & \delta M_{81} \\ \delta M_{81} & M_1 \end{bmatrix} \quad (2.4)$$

(d) Requiring the off diagonal elements of the physical mass matrix to be zero yields an expression for the mixing angle

$$\tan 2\theta = \frac{-2\delta M_{81}}{M_1 - M_8} = 2\sqrt{2} \quad (2.5)$$

giving $\theta = 35.3^\circ$. With a Hamiltonian operator as given in (2.1) this mixing angle will be the same for both vectors and pseudoscalars, it corresponds to the angle for ideal or magic mixing where the meson wavefunctions contain

purely non-strange or purely strange quarks,

$$\begin{aligned} |\eta'\rangle \text{ or } |\omega\rangle &= \frac{1}{\sqrt{2}} (u\bar{u} + d\bar{d}) \\ |\eta\rangle \text{ or } |\phi\rangle &= s\bar{s} \end{aligned} \quad (2.6)$$

and the corresponding masses have the following values (in GeV),

$$\begin{aligned} M_{\eta'} &= M_{\pi} = 0.14 & M_{\eta} &= 2M_k - M_{\pi} = 0.86 \\ M_{\omega} &= M_{\rho} = 0.77 & M_{\phi} &= 2M_k^* - M_{\rho} = 1.01 \end{aligned} \quad (2.7)$$

Predictions for the vector masses agree well with their experimental values, but the model fails completely for the pseudoscalars where even the pattern of mass breaking $M_{\pi} < M_k < M_{\eta} < M_{\eta'}$ is not reproduced.

Related to this problem is that of the prediction of the $m_s - m_u$ mass difference given by

$$m_s - m_u = M_k^* - M_{\rho} = 116 \text{ MeV} \quad (2.8)$$

$$\text{and } m_s - m_u = M_k - M_{\pi} = 354 \text{ MeV}$$

Attempts were made to solve this discrepancy⁽⁴⁾ by treating the problem in terms of (mass)² rather than linear masses giving

$$m_s^2 - m_u^2 = M_{k^*}^2 - M_{\rho}^2 = 1.93 \times 10^5 \text{ MeV} \quad (2.9)$$

$$\text{and } m_s^2 - m_u^2 = M_k^2 - M_{\pi}^2 = 2.24 \times 10^5 \text{ MeV}$$

which appear to be mutually consistent, adding weight to arguments in favour of a quadratic rather than a linear mixing formalism. The view is taken here, however, that the failure of the model to produce a consistent mass difference in (2.8) is not due to its linear mass nature but due to the inadequate

description of hadronic structure afforded by (2.1). The apparently consistent prediction in (2.9) thus appears fortuitous. In later investigations both quadratic and linear mixing procedures are investigated.

A phenomenological analysis⁽⁴¹⁾ of the meson mass spectrum in terms of the Gell-Mann/Okubu mass formula leads to the mixing angles in Table 2.1.

J^P	Nonet Members	$\theta(\text{Linear})$	$\theta(\text{quadratic})$
0^-	π, k, η, η'	-24°	-11°
1^-	ρ, k^*, ω, ϕ	36°	39°

Table 2.1 : Linear and Quadratic octet-singlet mixing angles.

The non-relativistic quark model can reproduce these values⁽⁴⁾, but to do so it is necessary to replace the hyperfine interaction by a general interaction U which takes on different values when operating on singlet and octet states. The meson mass is then

$$M_A = \langle \psi(A) | \sum_a m_a + U(\alpha) | \psi(A) \rangle \quad (2.10)$$

where $\alpha = 1$ or 8 corresponding to whether U operates on singlet or octet states respectively. Diagonalising this mass matrix, and allowing for a possible spatial wavefunction overlap integral less than unity yields the results in Table 2.2 which agree well with those in Table 2.1.

	Pseudoscalars		Vectors	
	Linear	Quadratic	Linear	Quadratic
	I	0.45	0.48	1
θ	-23°	-10°	38°	40°

Table 2.2 : Overlap integral (I) and mixing angle (θ), results of the mass matrix (2.10).

2.3 THE ANNIHILATION INTERACTION

The attempt to understand the mass spectrum and mixing angle of the pseudoscalar mesons using the simple quark model in section 2.2 has failed. The situation can be improved^(39,42,43,44), however, and the pseudoscalar mixing angle⁽⁴³⁾ 'explained' by assuming that the strong interactions binding a $q\bar{q}$ pair in a meson are described by QCD. The Hamiltonian operator of the simple quark model must now be modified to allow for the possible annihilation (in isoscalar mesons) of $q\bar{q}$ pairs into gluons which may subsequently hadronize to produce a different $q\bar{q}$ pair.

Representing the annihilation amplitude by A, and assuming for the moment that this amplitude is SU(3) invariant then in the subspace of states $u\bar{u}$, $d\bar{d}$ and $s\bar{s}$ its contribution to the interaction Hamiltonian takes the form⁽⁴²⁾

$$H_A = \begin{bmatrix} A & A & A \\ A & A & A \\ A & A & A \end{bmatrix} \quad (2.11)$$

Changing into the basis of SU(3) states gives

$$H_A^{SU(3)} = \begin{bmatrix} 0 & 0 & 0 \\ 0 & 0 & 0 \\ 0 & 0 & 3A \end{bmatrix} \quad (2.12)$$

This interaction contributes only to the mass of the singlet in the SU(3) basis, thus

$$M_{SU(3)} = \begin{bmatrix} \frac{2}{3} (m_u + 2m_s) + aB & -\frac{4}{\sqrt{18}} (m_u - m_s) I \\ -\frac{4}{\sqrt{18}} (m_u - m_s) I & \frac{2}{3} (2m_u + m_s) + aB + 3A \end{bmatrix} \quad (2.13)$$

where I is the overlap integral of the spatial wavefunctions. The condition in (2.10) that the general interaction $U(8) \neq U(1)$ is thus equivalent to adding the annihilation interaction to the basic model.

This is very similar to the linear mixing model introduced by de Rujula, Georgi and Glashow⁽³⁹⁾. In its quadratic form it also resembles the model of Isgur⁽⁴³⁾ where the hyperfine splitting term $B\bar{\sigma}_a \cdot \bar{\sigma}_b$ is replaced by a parameter s which takes on different values in the pseudoscalar and vector nonets. Both of these models are discussed in detail in Chapter 3 where they are extended to include mixing between the ground-state isoscalars and their radial excitations.

The magnitude of A can be obtained by equating the trace of (2.13) with that of the physical mass matrix to yield, for the pseudoscalars (P) and vectors (V),

$$A_P = 173 \text{ MeV} \quad A_V = 7 \text{ MeV}$$

in the linear case, and

$$A_P = 243 \text{ MeV}^2 \quad A_V = 21 \text{ MeV}^2$$

in the quadratic case. The mixing angles in Table 2.2 are obtained as before.

These values of A_p and A_v are in qualitative agreement with the expectations of QCD⁽⁴⁴⁾ where $J^P = 1^-$ (0^-) states couple to no fewer than 3(2) gluons in the virtual annihilation process, Fig 2.1.

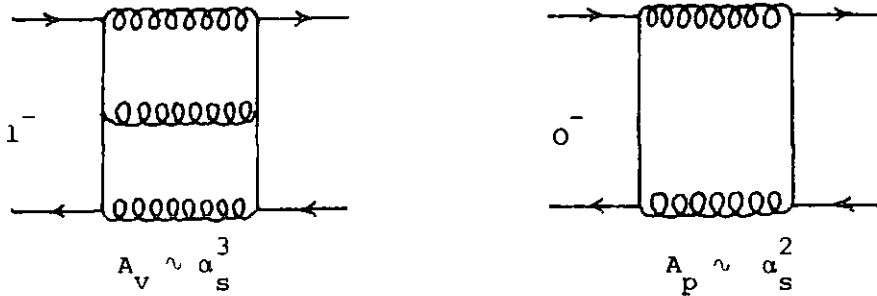


Fig 2.1 : Annihilation of $q\bar{q}$ pairs in 1^- and 0^- isoscalar states.

The annihilation amplitudes, while only playing a small role in the vector nonet where the predominant symmetry breaking interaction is that causing the $m_s - m_u$ mass difference, are crucial to our understanding of the η and η' masses.

2.4 FLAVOUR DEPENDENCE OF THE ANNIHILATION PARAMETER

The introduction of ideas from QCD, in particular the annihilation mechanism, has provided a much firmer theoretical basis for mixing models of mesons and also a possible explanation of the pseudoscalar mixing scheme. Thus far the annihilation term has been assumed to be independent of quark flavour, however, a more realistic approach, which produces improved results for the meson mass spectra^(43,45), is to break this SU(3) invariance.

An analysis of the two gluon decay of a $J^P = 0^-$ state has been made by Barbieri et al⁽⁴⁶⁾, who find⁽⁴⁷⁾,

$$\Gamma(0^-, M) = \frac{\alpha_s}{M^2} |\psi(0)|^2 \quad (2.14)$$

where α_s defines the strength of the quark-gluon coupling, M is the mass of the decaying meson and $\psi(r)$ is the non-relativistic wavefunction for the 0^- state normalised to $\int_0^\infty r^2 |\psi_s(r)|^2 dr = 1$. Assuming that the annihilation

term will have a similar dependence, the proposal

$$A_P \sim \frac{\alpha_s^2}{M^2} |\psi_s(0)|^2 \quad (2.15)$$

is made. For $J^P = 1^-$ decay, α_s^2 is replaced⁽⁴⁸⁾ by α_s^3

Equation (2.15) can be simplified considerably by noting the empirical observation⁽⁴⁹⁾ for vector (V) to e^+e^- decay,

$$\Gamma(V \rightarrow e^+e^-)/e_q^2 \approx \text{const. (11 KeV)} \quad (2.16)$$

which holds for ρ, ω, ϕ, ψ and Υ where e_q is the charge of the quark of flavour q (in units of e) contained in V . The Van Royen-Weisskopf formula⁽⁵⁰⁾ gives

$$\Gamma(V \rightarrow e^+e^-) = \frac{16\pi\alpha^2}{M_V^2} |\psi(0)|^2 e_q^2 \quad (2.17)$$

thus $|\psi(0)|^2 \propto M_V^2$ (2.18)

A similar observation can be made for the charged pseudoscalars⁽⁵¹⁾ (where $|\psi(0)|^2$ is determined from the leptonic decay to $l\nu$), Fig 2.2.(2.15) then implies

$$\begin{aligned} A_P &\sim \alpha_s^2 \\ A_V &\sim \alpha_s^3 \end{aligned} \quad (2.19)$$

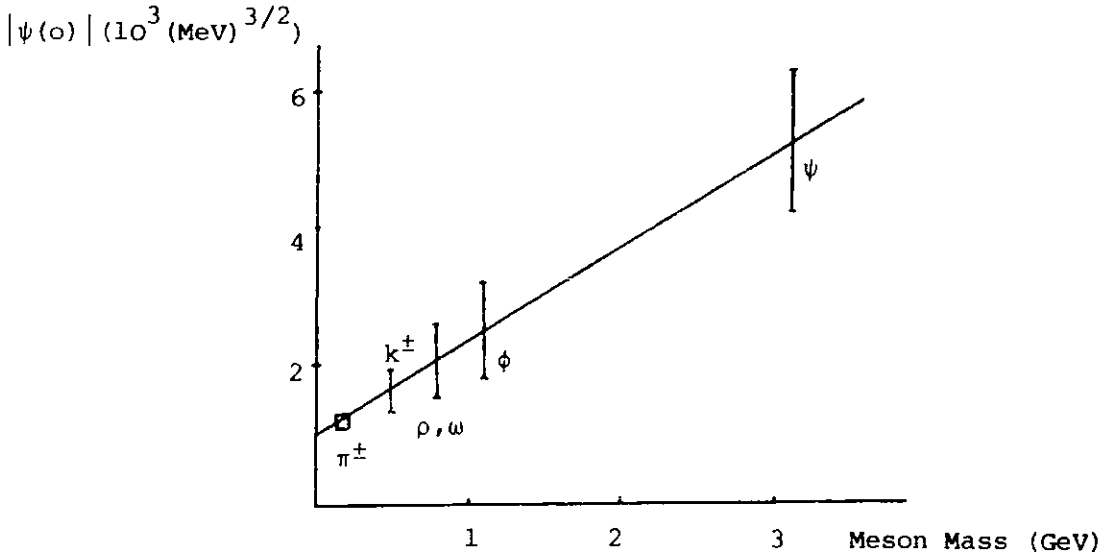


Fig 2.2 : A plot showing the linear dependence of $|\psi(o)|$ on meson mass.

These relations are often written in terms of the constituent quarks which comprise the mesons⁽⁵²⁾

$$A_{aa'}^P \sim \alpha_s(m_a^2) \alpha_s(m_{a'}^2) \quad (2.20)$$

$$A_{aa'}^V \sim \left[\alpha_s(m_a^2) \alpha_s(m_{a'}^2) \right]^{3/2}$$

a behaviour which suggests that $A_{aa'}$ factorises⁽⁵³⁾

$$A_{aa'}^2 = A_{aa} A_{a'a'} \quad (2.21)$$

The flavour dependence of the annihilation term is then given by the variation of α_s with mass scale. This variation is not known precisely but evidence from, for example, ϕ , ψ and τ leptonic decays suggests a decrease with increasing mass in line with the idea of asymptotic freedom, which is embodied, in first order QCD, in the formula⁽³⁹⁾

$$\alpha_s(M_2) = \left[1 - \frac{25}{12\pi} \alpha_s(M_1) \ln \left(\frac{M_1}{M_2} \right) \right]^{-1} \alpha_s(M_1) \quad (2.22)$$

Also, an investigation by de Rujula, Georgi and Glashow⁽³⁹⁾ in the opposite limit as $M \rightarrow 0$ has suggested that $A \sim M^2$ leading to an overall variation with

mass along the lines of that shown in Fig 2.3.

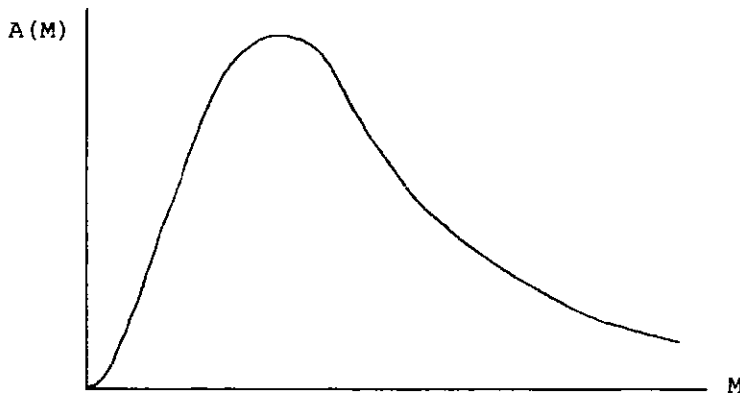


Fig 2.3 : The expected variation of Annihilation parameter with mass scale.

2.5 MIXING WITH A FLAVOUR DEPENDENT A

The simple mixing model of section 2.3 is extended to include the flavour dependence of the annihilation interaction⁽⁵²⁾. The paucity of quantitative estimates of the variation of α_s with mass scale implies that the SU(3) violation of A must be determined phenomenologically by introducing a new parameter A_{aa} , in each sector of the mass matrix such that, assuming isospin symmetry is not violated, the previous parameter A is replaced by $A_{uu} = A_{dd}$, A_{ss} and, including charm states, A_{cc} . Off diagonal elements such as A_{us} are determined using (2.21). This increase in the number of parameters in the model necessitates the introduction of new constraints upon which their values can be fixed. The merits of different constraints are discussed with reference to their effect upon the variation of A_{aa} , which is required to comply qualitatively with that discussed in section 2.4. The properties of quadratic and linear mass matrices are analysed separately.

2.5.1 The Quadratic Mass Matrix

(a) The Pseudoscalars

The quadratic mass matrix is

$$\langle q_a, \bar{q}_b | M^2 | q_a, \bar{q}_b \rangle = M_{ab}^2 \delta_{aa'} \delta_{bb'} + A_{aa'} \delta_{ab} \delta_{a'b'} \quad (2.23)$$

with $A_{aa'}$, the mass contribution from the annihilation term and M_{ab}^2 the

contribution from quark masses, and the hyperfine splitting term which is understood to contribute only to the common mass of the multiplet under consideration. In what follows M_{ab}^2 is determined phenomenologically, taking on different values in different multiplets.

Assuming isospin conservation, the values of M_{ab}^2 can be determined from the observed particle masses

$$M_{uu}^2 = M_{dd}^2 = M_{\pi^0}^2 = 0.0182 \text{ GeV}^2 \quad (2.24)$$

$$M_{ss}^2 = 2M_{k^0}^2 - M_{\pi^0}^2 = 0.4778 \text{ GeV}^2$$

An analysis of the mixing problem is made in several stages :

(i) By confining the problem to just u, d and s quarks and ignoring the flavour dependence of the annihilation term, i.e. $A_{aa'} = A$, the physical η and η' masses are determined solely by the value of A, all other mass contributions being fixed in (2.24). Making an isospin transformation on the 3x3 mass matrix (2.23) gives an $I = 1 \pi^0$ state and a 2x2 $I = 0$ submatrix, equivalent to (2.13) with quadratic masses, and the overlap of spatial wave-functions set equal to unity. A can be determined either from the trace condition

$$2M_k^2 + 3A = M_\eta^2 + M_{\eta'}^2 \quad (2.25)$$

or the determinant condition

$$(M_\pi^2 + 2A)(2M_k^2 - M_\pi^2 + A) - 2A^2 = M_\eta^2 M_{\eta'}^2 \quad (2.26)$$

giving $A = 0.24 \text{ GeV}^2$ or 0.27 GeV^2 respectively. By substituting either of these values back into (2.23) and diagonalising, the η and η' masses are given to within 20% of their experimental values.

(ii) The fit to the η and η' masses can be made perfect by including the flavour dependence of A. Assuming that A factorises then $A_{uu} = 0.28 \text{ GeV}^2$

and $A_{ss} = 0.17 \text{ GeV}^2$. A trend of decreasing annihilation strength with increasing mass scale is observed in agreement with the concept of asymptotic freedom in QCD.

The assumption that the annihilation term factorises can be seen to be reasonable by following a similar analysis of the problem which has been made by Fritzsche and Jackson⁽⁴⁵⁾. They do not impose factorisation and thus introduce an additional unknown, A_{us} , which is determined by using the pseudoscalar mixing angle as a third constraint. The η and η' states can be decomposed as follows

$$|\eta\rangle = \cos\alpha |NS\rangle + \sin\alpha |S\rangle : \quad |\eta'\rangle = -\sin\alpha |NS\rangle + \cos\alpha |S\rangle \quad (2.27)$$

where $|NS\rangle \equiv \frac{1}{\sqrt{2}} |u\bar{u} + d\bar{d}\rangle$ and $|S\rangle \equiv |s\bar{s}\rangle$, or

$$|\eta\rangle = \cos\theta |8\rangle + \sin\theta |1\rangle : \quad |\eta'\rangle = -\sin\theta |8\rangle + \cos\theta |1\rangle \quad (2.28)$$

where $\theta = \theta_I + \alpha - \pi/2$ and the ideal mixing angle $\theta_I = \sin^{-1}(1/\sqrt{3}) = 35.3^\circ$.

Fritzsche and Jackson performed two fits corresponding to the mixing angles

$\alpha = 45^\circ$ ($\theta = -9.7^\circ$) and $\theta = -11^\circ$ ($\alpha = 43.7^\circ$) which gave $A_{uu} = 0.29$, $A_{us} = 0.21$, $A_{ss} = 0.13 \text{ GeV}^2$ and $A_{uu} = 0.30$, $A_{us} = 0.21$, $A_{ss} = 0.12 \text{ GeV}^2$ respectively.

In both fits A_{us} is reasonably close to the value expected from factorisation.

(iii) Thus far the charmonium state η_c has been excluded from the analysis. Since $A/M_{cc}^2 \ll 1$ (with $M_{cc}^2 \approx 9 \text{ GeV}^2$) including this state will have little effect on the η - η' mixing pattern. M_{cc}^2 can be found in the same manner as M_{ss} to give

$$M_{cc}^2 = 2M_{D^0}^2 - M_{\pi^0}^2 = (2.63)^2 \text{ GeV}^2 \quad (2.29)$$

This determination raises a fundamental problem, however, for assuming

factorisation, a fit to the mass spectrum yields $A_{uu} = 0.36$, $A_{ss} = 0.22$ and $A_{cc} = 1.74 \text{ GeV}^2$ which does not follow the expected variation with mass scale.

The problem is intractable, unless the view is taken that the model description of hadron structure is, in general, too simple and that it is unable to cope with meson states which are constructed from quarks with unequal mass. This is not an unreasonable proposal, as will become clear in future analyses. The mass contribution $M_{qq'}^2$ to hadron masses has a dependence upon the hyperfine splitting term described in section 2.2 such that

$$M_{qq'}^2 = M_q^2 + M_{q'}^2 + B \bar{\sigma}_q \cdot \bar{\sigma}_{q'}$$

In this particular model B is taken to be a constant throughout a given $SU(4)$ multiplet, however, such a proposal is incorrect and, as will be seen B takes different values in different sections of the mass matrix. Following this reasoning, the result $A_{cc} > A_{ss}$ when $M_{cc} = 2.63 \text{ GeV}$ can be ignored and a new phenomenological determination of M_{cc} made using different constraints. However, if the description of M_{cc} in (2.29) is not to be trusted, the value of M_{ss} quoted in (2.24) must also be in doubt, so a different determination of this parameter is made.

In order to find the value of M_{ss} , M_{cc} and A_{cc} , additional constraints are required. Considering first the situation with just u , d and s quarks and assuming factorisation of the annihilation terms, M_{ss} can be fixed by a fit to the pseudoscalar mixing angle, $\theta = -11^\circ$. This gives $A_{uu} = 0.29$, $A_{ss} = 0.16$ and $M_{ss}^2 = 0.460 \text{ GeV}^2$, that is a decrease of 4% from 0.478 GeV^2 given in (2.24). Following this trend, if M_{cc}^2 is also lower than the value determined in (2.29) there will be no hope of consistency with perturbative QCD which requires $A_{uu} > A_{ss} > A_{cc}$ so the value of $\theta = -11^\circ$ is discarded.

Another constraint is provided by the ratio of radiative ψ decays,

$$\rho \equiv \frac{\Gamma(\psi \rightarrow \eta' \gamma)}{\Gamma(\psi \rightarrow \eta \gamma)} \quad (2.30)$$

which can be written as^(45,52)

$$\rho = \left(\frac{k_{\eta'}}{k_{\eta}} \right)^3 \left(\frac{\epsilon'}{\epsilon} \right)^2 \quad (2.31)$$

where k_p represents the centre of mass photon momentum in $\psi \rightarrow P\gamma$ and ϵ, ϵ' give the amount of $c\bar{c}$ in the η and η' unitary spin wavefunctions respectively. With a strange/non-strange mixing angle $\alpha = 45^\circ$ ϵ and ϵ' can be expressed as

$$\epsilon = - \frac{\sqrt{2} A_{uc} - A_{sc}}{1/\sqrt{2} (M_{\eta}^2 + M_{\eta'}^2) - \sqrt{2} M_{cc}^2} \quad (2.32)$$

$$\epsilon' = - \frac{\sqrt{2} A_{uc} + A_{sc}}{1/\sqrt{2} (M_{\eta}^2 + M_{\eta'}^2) - \sqrt{2} M_{cc}^2}$$

so their ratio ϵ'/ϵ is independent of M_{cc}^2 . This independence is lost when $\alpha \neq 45^\circ$, however, a 10% variation in M_{cc}^2 about $M_{cc} = 3.0$ GeV produces very little effect in ϵ'/ϵ .

Many experimental determinations have been made for ρ , not all of which are mutually consistent (see discussion in Chapter 4). For the purposes of this analysis the Crystal Ball result⁽⁵⁴⁾ $\rho = 5.88 \pm 1.46$ is chosen, giving $\epsilon'/\epsilon = 2.66 \pm 0.31$. By fixing $M_{cc} \approx 2.98$ GeV this result for ρ determines $M_{ss}^2 = 0.51 \pm 0.03$ GeV² which gives a mixing angle of $\theta = -(16 \pm 2)^\circ$. Requiring consistency with perturbative QCD such that $A_{ss} > A_{cc}$ limits M_{cc} to the range 2.98 - 2.97 GeV where the first value corresponds to $A_{cc} = 0$. The magnitude of A_{cc} is fixed by fitting to the individual decay rate $\Gamma(\psi \rightarrow \eta'\gamma)$, which can be expressed in the non-

relativistic quark model as

$$\Gamma(V \rightarrow P\gamma) = \left\{ \frac{4\alpha}{3} \right\} k^3 \left\{ \frac{e_q}{m_q} \right\}^2 \Omega^2 \quad (2.33)$$

where e_q and m_q are quark charges and masses, and Ω is the overlap integral of spatial wavefunctions, taken to be unity in most applications. For ψ decay $e_c = 2/3$ and m_c is taken as 1.53 GeV. Crystal Ball⁽⁵⁴⁾ data gives

$$\Gamma(\psi \rightarrow \eta' \gamma) = 460 \pm 110 \text{ eV}$$

which fixes A_{cc} at 0.011 GeV^2 .

To summarise, if the inability of the model to cope with meson states made up of quarks of unequal mass is accepted, it is possible to fit the pseudoscalar mass spectrum and the radiative ratio ρ in a way which is consistent with perturbative QCD. The parameters obtained from the fit are

$$\begin{aligned} A_{uu} &= 0.261 \text{ GeV}^2 : A_{ss} = 0.173 \text{ GeV}^2 : A_{cc} = 0.011 \text{ GeV}^2 \\ M_{ss}^2 &= 0.507 \text{ GeV}^2 : M_{cc}^2 = 8.84 \text{ GeV}^2 \end{aligned} \quad (2.34)$$

which imply the following unitary spin wavefunctions,

$$\begin{aligned} |\eta\rangle &= 0.784 |NS\rangle + 0.621 |S\rangle + 3.7 \times 10^{-3} |\bar{c}\bar{c}\rangle \\ |\eta'\rangle &= -0.621 |NS\rangle + 0.784 |S\rangle - 1.0 \times 10^{-2} |\bar{c}\bar{c}\rangle \\ |\eta_c\rangle &= -9.1 \times 10^{-3} |NS\rangle + 5.5 \times 10^{-3} |S\rangle + 0.999 |\bar{c}\bar{c}\rangle \end{aligned} \quad (2.35)$$

Ignoring the $\bar{c}\bar{c}$ contributions, these give the η - η' mixing angles

$$\alpha = 38.4^\circ : \theta = -16.3^\circ \quad (2.36)$$

which are in reasonable agreement with $\theta = (-18.2 \pm 1.4)^\circ$ obtained from the ratio of differential cross-sections for $\pi^- p \rightarrow \eta' n$ and $\pi^- p \rightarrow \eta n$ ⁽⁵⁵⁾.

(b) The Vector Mesons

The gross features of the mixing of vector mesons are well described in the simplest mixing models where the ω - ϕ mass mixing elements are determined solely by the SU(3) violating quark mass difference $m_s - m_u$. The annihilation contributions will thus be small, an observation which is supported by QCD where a $q\bar{q}$ pair which comprises a vector meson must annihilate into three gluons, rather than two as in the pseudoscalar case, so that $A_{aa} \sim \alpha_s^3$. Problems are encountered when the fine details, that is, the relative magnitudes of the annihilation terms are investigated.

Following the previous analysis M_{aa}^2 could be determined by

$$M_{uu}^2 = M_{dd}^2 = M_{\rho^0}^2 = 0.602 \text{ GeV}^2$$

$$M_{ss}^2 = 2M_{k^*}^2 - M_{\rho}^2 = 0.990 \text{ GeV}^2$$

where again M_{aa}^2 represents the sum of quark mass and hyperfine splitting terms. It is clear that the mass contribution to the $I = 0$ states from the annihilation terms need only be very small in order to reproduce the experimental masses. A fit to M_{ω}^2 and M_{ϕ}^2 , assuming factorisation of A_{aa} , gives $A_{uu} = 0.008 \text{ GeV}^2$ and $A_{ss} = 0.050 \text{ GeV}^2$.

If, as in the pseudoscalar case, this determination of M_{aa}^2 is taken to be inadequate because of the models inability to cope with k^* states, and a 5% increase in M_{ss}^2 is made (comparable to the increase required for the pseudoscalars) then A_{ss} will be reduced essentially to zero. When this treatment is extended to the charm sector the pattern observed with the pseudoscalars recurs here and an increase of about 28% in the value $M_{cc}^2 = 2M_{D^*}^2 - M_{\rho}^2$ is required if A_{cc} is to be less than A_{ss} . This suggests again that the model cannot cope with meson states composed of quarks with unequal mass.

2.5.2 The Linear Mass Matrix

(a) The Pseudoscalars

The linear mass matrix which describes the mixing of pseudoscalar states is (52)

$$\langle q_a, \bar{q}_b | M | q_a, \bar{q}_b \rangle = M_{ab} \delta_{aa'} \delta_{bb'} + A_{aa'} \delta_{ab} \delta_{a'b'} \quad (2.37)$$

It is possible to determine M_{aa} as before

$$\begin{aligned} M_{uu} &= M_{dd} = M_{\pi^0} = 0.135 \text{ GeV} \\ M_{ss} &= 2M_{K^0} - M_{\pi^0} = 0.861 \text{ GeV} \\ M_{cc} &= 2M_{D^0} - M_{\pi^0} = 3.592 \text{ GeV} \end{aligned} \quad (2.38)$$

Ignoring the charm sector and accepting (2.38), a fit to the η, η' masses gives $A_{uu} = 0.236 \text{ GeV}$ and $A_{ss} = 0.043 \text{ GeV}$ which imply a linear mixing angle $\theta = -32^\circ$, compared with the standard mixing angle of -24° . As in the quadratic case, M_{cc} obtained from (2.38) will not allow the η_c to be included in this analysis, but the problem here centres around M_{cc} being too large rather than too small as before. Again, this indicates that the model cannot accommodate meson states composed of quarks of different flavours, and further constraints are required to fix the values of M_{ss} and M_{cc} .

By fitting to $\epsilon'/\epsilon = 2.66 \pm 0.31$, $\Gamma(\psi \rightarrow \eta' \gamma) = 460 \pm 110 \text{ eV}^{(54)}$ and the η and η' masses and requiring $M_{\eta_c} \approx M_{cc} + A_{cc}$ the following parameters are obtained,

$$\begin{aligned} A_{uu} &= 0.321 \text{ GeV} \quad : \quad A_{ss} = 0.065 \text{ GeV} \quad : \quad A_{cc} = 6.3 \times 10^{-3} \text{ GeV} \\ M_{ss} &= 0.669 \text{ GeV} \quad : \quad M_{cc} = 2.979 \text{ GeV} \end{aligned} \quad (2.39)$$

which imply the wavefunctions

$$\begin{aligned}
 |\eta\rangle &= 0.668 |NS\rangle + 0.744 |S\rangle + 3.6 \times 10^{-3} |c\bar{c}\rangle \\
 |\eta'\rangle &= -0.774 |NS\rangle + 0.668 |S\rangle - 9.5 \times 10^{-3} |c\bar{c}\rangle \\
 |\eta_c\rangle &= -9.5 \times 10^{-3} |NS\rangle + 3.7 \times 10^{-3} |S\rangle + 0.999 |c\bar{c}\rangle
 \end{aligned} \tag{2.40}$$

(b) The Vector Mesons

The linear model of the vector mesons suffers from the same problems as the quadratic model, the annihilation terms being sufficiently small to make even a qualitative comparison with QCD expectations difficult. The results are essentially the same as those of (2.13) with $I = 1$ and the annihilation terms set equal to zero.

CHAPTER 3ISOSCALAR MESON MIXINGII. THE INCLUSION OF RADIAL EXCITATIONS3.1 INTRODUCTION

The incorporation of ideas abstracted from QCD in ground-state mixing models has led to the addition of further terms to the mass matrix, the annihilation terms described in Chapter 2. A phenomenological analysis of the isoscalar mixing problems indicates that these terms are relatively much smaller in the vector meson case than in the pseudoscalar meson case in agreement with the predictions of first order perturbative QCD where, naively, $A_V(M^2) \sim \alpha_s(M^2) A_P(M^2)$ at some mass scale M . The smallness of A_V implies only a slight deviation from ideal mixing, while the larger A_P forces the non-ideal mixing pattern on the $J^P = 0^-$ isoscalar states. This simple picture presents an explanation of why the mixing schemes for 1^- and 0^- states are so different.

Problems with these ground state mixing procedures were noticed in 1977, however, when Lipkin⁽⁵⁶⁾ made an analysis of measurements of various production cross-sections. Relations between different charge exchange and strangeness exchange cross-sections near the forward direction have been derived using the quark model additivity assumption for scattering amplitudes⁽²⁶⁾ to give, for the pseudoscalars,

$$\begin{aligned} \bar{\sigma}(\pi^- p \rightarrow \pi^0 n) + \bar{\sigma}(\pi^- p \rightarrow \eta n) + \bar{\sigma}(\pi^- p \rightarrow \eta' n) \\ = \bar{\sigma}(k^+ n \rightarrow k^0 p) + \bar{\sigma}(k^- p \rightarrow \bar{k}^0 n) \end{aligned} \quad (3.1)$$

$$\bar{\sigma}(k^- p \rightarrow \eta \Lambda) + \bar{\sigma}(k^- p \rightarrow \eta' \Lambda) = \bar{\sigma}(\pi^- p \rightarrow k^0 \Lambda) + \bar{\sigma}(k^- p \rightarrow \pi^0 \Lambda) \quad (3.2)$$

where $\bar{\sigma}$, which is proportional to the square of the transition amplitude

must be multiplied by phase space factors before a comparison is made with experiment. Similar relations hold when vector mesons occur in the final state, and are given by making the replacements $\pi \rightarrow \rho$, $\eta \rightarrow \omega$, $\eta' \rightarrow \phi$ and $k \rightarrow k^*$. Lipkin found that such sum rules are well satisfied for the vectors, but fail for the pseudoscalars where contributions to (3.1) and (3.2) from the η and η' are consistently too small. An extensive, complementary, analysis of (3.2) made by Marzano et al⁽⁵⁷⁾ over the range $0 \leq |t'| \leq 1.5 \text{ (GeV/c)}^2$ has confirmed this result. The breakdown of these sum rules for the pseudoscalars but not for the vectors has been taken as evidence to suggest that the conventional pseudoscalar mixing schemes used to derive the rules are inadequate. The consistently small contributions from the η and η' indicates that the wavefunctions of these particles may contain inert components⁽⁵⁶⁾ which do not contribute to the overlap with the initial state meson.

Several hypotheses have been made to explain the physical structure of such components, for example, Capps⁽⁵⁸⁾ has suggested the mixing of the η and η' with a tenth gluonic meson would lead to a significant inert glue component in the η' wavefunction. This idea is not pursued here because of lack of evidence for a tenth pseudoscalar. An alternative solution to the problem, suggested by Lipkin⁽⁵⁶⁾, involves the mixing of radial excitations of the isoscalar mesons with their ground-states. That ground-state mixing alone is unjustified becomes apparent when charmonium states are included in the analysis, mixing $\bar{c}c$ states solely with the ground-states of the lower mass mesons will only provide a partial description of the problem since many radial excitations of the light quark mesons are expected (section 3.2) to exist in the mass range 1-3 GeV.

The extent to which the excitations will mix with their ground-states depends upon the type of symmetry breaking interaction which causes the mixing. In the vector case the predominant interaction is that causing the $m_s - m_u$ mass difference which has no radial dependence, so the mass mixing elements due

to this interaction between the ground-states and radial excitations will contain an overlap of spatial wavefunctions, which is expected to be small. Thus, the vectors should be well described by ground-state mixing schemes. In the pseudoscalar case, however, the annihilation interaction competes with the $m_s - m_u$ mass difference in breaking the symmetry. The mass mixing element derived from this interaction does not contain a spatial wavefunction overlap between initial and final states but instead has a dependence on the wavefunction near the origin which may allow significant mixing. Radial excitations can hence be expected to play an important role in the pseudoscalar mixing problem, particularly in the case of the η' where experiment indicates that the mass difference between the lowest mass, first radially excited isoscalar and the η' is of the same order as that between the η and η' . This will be seen to explain the discrepancies encountered in the production cross-section analyses mentioned earlier.

Models describing the mixing between ground-states and their radial excitations have been constructed, based on both logarithmic^(52,59) and harmonic⁽⁶⁰⁾ confining potentials. The properties of both quadratic and linear versions of the former are investigated in detail in section 3.3, but firstly a review is made of the present experimental status of meson radial excitations.

3.2 RADIAL EXCITATIONS - THE EXPERIMENTAL SCENE

Within the quark model framework radial excitations of a $q_1 \bar{q}_2$ pair are expected for all quarks of flavour q_1 . Many such excitations are already well determined in the ψ and Υ spectra, excitations up to $n = 4$ ($n = 1$ for ground-state) having been observed in the case of the ψ , however, evidence of the existence of the excitations of light quark mesons is such that only one state finds a firm place within the Particle Data Group tables⁽⁶¹⁾, all other assignments being tentative, and many unconfirmed⁽⁶²⁾.

The experimental status of radially excited states can be conveniently grouped into two sections. Firstly, the excitations of the vector mesons for

which, despite the lack of firm evidence, there are a great many experimental results, and secondly the pseudoscalars whose excitations have only been observed in four experiments at the present time.

3.2.1 Heavy Vector Mesons

The excitations of the charmonium and upsilonium systems are well established and will not be discussed here. Candidates for those of the ρ , ω and ϕ are ;

(i) $\rho'(1250)$

The existence of a radial excitation of the ρ at approximately 1250 MeV has been hinted in many experiments but the assignment of a vector resonance at this mass has still to be confirmed. Strong evidence for this state has been given by the SLAC-LBL photoproduction experiment⁽⁶³⁾ which examined the reaction $\gamma p \rightarrow p \pi^+ \pi^- + \text{neutrals}$. A broad peak ($\Gamma \approx 150$ MeV) is observed centred at 1250 MeV in the $\pi^+ \pi^-$ missing mass plot, however, a spin analysis of the resonance could not be made so its J^P assignment is uncertain, it may possibly be the $1^+ B(1235)$ state. Observation of the interference pattern of the $e^+ e^-$ final state in $\gamma p \rightarrow e^+ e^- p$ by a Desy-Frascati experiment⁽⁶⁴⁾ has led to the positive $J^P = 1^-$ assignment of an enhancement centred at 1266 ± 5 MeV with width 110 ± 35 MeV. Another $J^P = 1^-$ assignment has been claimed for an enhancement observed in the Daresbury photoproduction experiment⁽⁶⁵⁾ in the $\gamma p \rightarrow \pi^+ \pi^- \pi^0 \pi^0 p$ channel with mass approximately 1.3 GeV and width 0.3 GeV. Further evidence is given by a CERN experiment⁽⁶⁶⁾ which studied the same reaction and found $M \approx 1.25$ GeV and $\Gamma \approx 0.3$ GeV. Other, older observations can be found in reference 67.

Definite evidence for an enhancement in the $M = 1250$ MeV mass region exists, however its interpretation as a $\rho'(1250)$ is uncertain. Analyses are complicated by the effects of the $J^P = 1^+$ B meson with mass 1235 MeV.

(ii) ρ' (1600)

This is the only light radial excitation which is sufficiently well established to be included in the Particle Data Group tables. Many observations of its mass and width have been made in e^+e^- , photoproduction and π^-p experiments where, in most cases, its decay to $\pi^+\pi^-\pi^+\pi^-$, $\pi^+\pi^-\pi^0\pi^0$ or $\pi^+\pi^-$ is observed. Most recent experiments give the following results.

(a) $M = 1598 \begin{smallmatrix} + 24 \\ - 22 \end{smallmatrix}$ MeV, $\Gamma = 175 \begin{smallmatrix} + 98 \\ - 53 \end{smallmatrix}$ MeV obtained from a phase shift analysis⁽⁶⁸⁾ of $\pi^-p \rightarrow \pi^+\pi^-n$.

(b) $M = 1666 \pm 39$ MeV, $\Gamma = 700 \pm 160$ MeV obtained from $e^+e^- \rightarrow \pi^+\pi^-\pi^+\pi^-$ experiments⁽⁶⁹⁾.

(c) $M = 1540 \pm 30$ MeV, $\Gamma = 478 \pm 135$ MeV obtained by a Daresbury group⁽⁶⁵⁾ investigating $\gamma p \rightarrow \pi^+\pi^-\pi^+\pi^-p$.

(d) $M = 1600 \pm 10$ MeV, $\Gamma = 283 \pm 14$ MeV obtained from a Fermilab⁽⁷⁰⁾ experiment studying $\pi^+\pi^-$ and $\pi^+\pi^-\pi^+\pi^-$ final states in γC photoproduction.

(e) $M = 1590 \pm 20$ MeV, $\Gamma = 230 \pm 80$ MeV obtained in a $\gamma p \rightarrow \pi^+\pi^-p$ CERN experiment⁽⁷¹⁾.

(iii) ω Excitations

Experiments performed in the mid 1970's to identify such states all obtained evidence for an ω' in the mass region 1780 MeV,

(a) $M \approx 1780$ MeV⁽⁷²⁾ (b) $M = 1792 \begin{smallmatrix} + 31 \\ - 14 \end{smallmatrix}$ MeV, $\Gamma = 79 \begin{smallmatrix} + 77 \\ - 29 \end{smallmatrix}$ MeV⁽⁷³⁾

(c) $M = 1778 \pm 14$ MeV, $\Gamma = 150 \pm 40$ MeV⁽⁷⁴⁾.

where all enhancements were observed in $e^+e^- \rightarrow \pi^+\pi^-\pi^+\pi^-\pi^0$ processes. Later experiments⁽⁷⁵⁾, which analysed the same decay mode of the excitation but in a different production process, $\gamma p \rightarrow \pi^+\pi^-\pi^+\pi^-\pi^0p$, have obtained a slightly lower mass of

$$M \approx 1700 \text{ MeV}, \quad \Gamma \approx 500 \text{ MeV}$$

(iv) ϕ Excitations

As in the ω case evidence for such excitations is scarce and the picture is confused. Reference 76 gives $M = 1690$ MeV, $\Gamma = 120$ MeV for a possible ϕ enhancement observed in $\gamma p \rightarrow k^+ k^- p$. The $k^+ k^- \pi$ channel in the same experiment also shows an enhanced peak at $M \approx 1.9$ GeV with $\Gamma \approx 0.4$ GeV. Evidence for the lower mass enhancement has also been noted in $e^+ e^-$ and photoproduction experiments where 3π and 5π final states are observed. Such OZI violating decays have been explained by deviations from the ideal ω' - ϕ' mixing scheme. The enhancements observed can be interpreted as possible candidates for both ω and ϕ excitations, but their narrow width (50 - 100 MeV) indicates that a ϕ assignment is preferable. The results are⁽⁷⁵⁾

$$\begin{aligned}
 M &= 1652 \pm 17 \text{ MeV}, & \Gamma &= 42 \pm 17 \text{ MeV} & \text{from } e^+ e^- \rightarrow 3\pi \text{ mode,} \\
 M &= 1665 \pm 6 \text{ MeV}, & \Gamma &= 37 \pm 21 \text{ MeV} & \text{from } e^+ e^- \rightarrow 4\pi^+ \pi^0 \text{ mode,} \\
 M &\approx 1660 \text{ MeV}, & \Gamma &\approx 50 \text{ MeV} & \text{from } \gamma p \rightarrow 4\pi^+ \pi^0 p \text{ and} \\
 M &\approx 1690 \text{ MeV}, & \Gamma &\approx 130 \text{ MeV} & \text{from } \gamma p \rightarrow \pi^+ \pi^- \pi^0 p.
 \end{aligned}$$

The interpretation of these vector meson results is not straightforward. Barring complications with the $J^P = 1^+$ B(1235) state there appears to be a first excitation of the ρ at about 1250 MeV with width ≈ 100 MeV, and another, presumably second, excitation at about 1600 MeV with width ≈ 300 MeV. The isospin assignments of these states appear to be clear cut, which raises a problem with their ω and ϕ partners. If the excitations are taken to mix ideally then an ω' (1250) would be expected, but no such state has been observed. Similarly, there is little evidence for an ω' (1600), only the most recent experiment suggests a value of about 1700 MeV, all previous results producing ω candidates with masses around 1780 MeV. Also, assuming an ideal mixing pattern, a ϕ' would be expected at

$$\begin{aligned}
 M_{\phi'} &= M_{\rho'}(1250) + 2(m_s - m_u) \\
 &\approx 1530 \text{ MeV}
 \end{aligned}$$

Only one tentative identification⁽⁷⁷⁾ has been made for such a state, which has not been confirmed by other experiments. Following similar lines the second ϕ excitation which would partner the $\rho''(1600)$ is expected at $M_{\phi}'' \approx 1880$ MeV. Such a state is observed in the photoproduction experiment of reference 76, but this identification leaves a difficulty with the interpretation of the lower mass $I = 0$ states at about 1650 MeV. Their mass fits in well with the expected ω'' , however, their narrow width presents a puzzle.

Accepting all the uncertainties associated with these states in the mass range 1200-2100 MeV, the following assignments are suggested,

$M_{\rho}' \approx 1250$ MeV	Ref. 63, 64, 65, 66, 67.
$M_{\rho}'' \approx 1600$ MeV	Ref. 65, 68, 69, 70, 71.
$M_{\omega}'' \approx 1650$ MeV	Ref. 75.
$M_{\phi}'' \approx 1900$ MeV	Ref. 76.

3.2.2 Pseudoscalar Meson Excitations

Evidence for $J^P = 0^-$ excitations is rare, only four experiments having made speculative identifications at the present time. Firstly, an investigation of the reaction $\pi^- p \rightarrow \eta \pi^+ \pi^- n$ at 8.45 GeV/c by Stanton et al⁽⁷⁸⁾ has revealed an $IJ^P = 00^-$ state with $M = 1275$ MeV and $\Gamma \approx 70$ MeV, with evidence for a second excitation at about 1400 MeV.

A second experiment⁽⁷⁹⁾ examining $\pi^- p \rightarrow 3\pi p$ has suggested the existence of a π' with $M = 1275 \pm 50$ MeV and $\Gamma = 508 \pm 100$ MeV. An examination of the same channel in an independent study⁽⁸⁰⁾ has found evidence for a 0^- excitation at approximately 1400 MeV with width ≈ 600 MeV.

Finally, a recent experiment performed by the Crystal Ball group⁽⁸¹⁾ has provided evidence for a possible isoscalar radial excitation observed in $\psi \rightarrow \gamma k^+ k^- \pi^0$. Preliminary results indicate $M = 1440 \begin{smallmatrix} + 20 \\ - 15 \end{smallmatrix}$ MeV and $\Gamma = 70 \begin{smallmatrix} + 20 \\ - 30 \end{smallmatrix}$ MeV with a $J^{PC} = 0^{-+}$ assignment. The resonance is observed

to decay predominantly via $\delta\pi^0$ (with subsequent $\delta \rightarrow k\bar{k}$ or $\delta \rightarrow \eta\pi$ decays) as expected for an isoscalar radial excitation⁽⁵⁹⁾. Evidence for a first radially excited η_c candidate is also given with $M = 3592 \pm 5$ MeV and $\Gamma < 9$ MeV (95% confidence level), where the decay $\psi' \rightarrow \eta'_c \gamma$ is observed.

Despite the lack of experimental data radial excitations of the pseudoscalars are just as firmly defined within quark models as are those of the vectors. The mixing models to be discussed in sections 3.3 and 3.4 make predictions for these states which could help to clarify the present situation.

3.3 MODELS WITH RADIAL EXCITATIONS

3.3.1 General Features

The inadequacy of ground-state mixing models, as indicated by investigations of the η and η' contributions to charge exchange and strangeness exchange production cross-sections⁽⁵⁶⁾, and a desire to include charmonium states in the mixing analyses has prompted the construction of phenomenological models which take into account the effects of the admixture of radially excited components in ground-state meson wavefunctions. Three fundamentally different types of model have been constructed ;

(i) a linear mixing model due to Graham and O'Donnell⁽⁶⁰⁾ based upon a confining harmonic oscillator potential,

(ii) a quadratic model in which simple modifications are made to the conventional ground state mixing model of Isgur⁽⁴³⁾, and

(iii) a linear model which involves the extension of ideas developed by de Rujula, Georgi and Glashow⁽³⁹⁾ to include radial excitations. The comparatively simple phenomenological models of Cohen and Lipkin⁽⁵⁹⁾ in (ii) and (iii) are of interest here, the more complicated ideas of Graham and O'Donnell, which involve a large number of free parameters are not pursued.

In order that significant predictions could be made by (ii) and (iii) the number of parameters they contain was kept to a minimum by

constructing the mass matrices with constituent quark mass and simple phenomenological interaction terms. The matrices were formulated in a $q\bar{q}$ basis with $q = u, d, s$, the diagonal elements being calculated explicitly in terms of quark masses with a phenomenological addition describing the splitting between the ground-states and their excitations, while the off-diagonal elements contain the interaction terms which are responsible for radial and ground state mixing.

The mass matrices, introduced by Cohen and Lipkin⁽⁵⁹⁾ are, in the quadratic case,

$$\langle q_a, \bar{q}_b, n' | M^2 | q_a \bar{q}_b, n \rangle = \delta_{aa'} \delta_{bb'} \delta_{nn'} \left[(m_a + m_b + E_n)^2 + S \right] + \delta_{ab} \delta_{a'b'} \frac{A}{nn'} \quad (3.3)$$

and in the linear case,

$$\langle q_a, \bar{q}_b, n' | M | q_a \bar{q}_b, n \rangle = \delta_{aa'} \delta_{bb'} \delta_{nn'} (m_a + m_b + E_n) + \delta_{ab} \delta_{a'b'} \frac{A}{m_a m_b \sqrt{nn'}} + \delta_{aa'} \delta_{bb'} \frac{B \vec{\sigma}_a \cdot \vec{\sigma}_b}{m_a m_b \sqrt{nn'}} \quad (3.4)$$

As before A and B are annihilation and hyperfine splitting strengths,

$|q_a \bar{q}_b, n\rangle$ is a state containing a quark of flavour a and an anti-quark of flavour b which are in the n^{th} radially excited state, where $n = 1$ represents the ground-state. S is a quark "scattering" interaction strength⁽⁴³⁾ representing $q\bar{q}$ binding mediated by gluons as depicted in Fig 3.1, $\vec{\sigma}_a$ and m_a are the spin and mass of a quark of flavour a and E_n are the excitation energies of the n^{th} radial excitation.

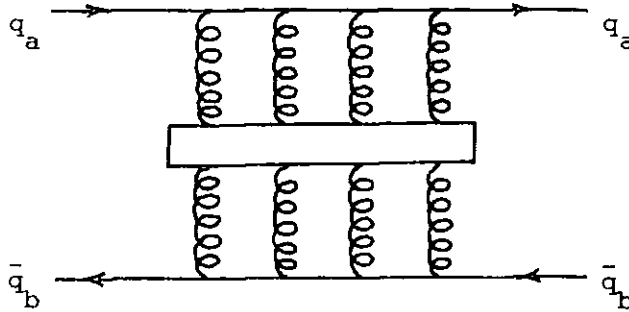


Fig 3.1 : Gluon exchange between a quark and an anti-quark.

These excitation energies are determined by setting $E_1 = 0$ to recover the predictions of the ground-state models, $E_2 = 0.59$ GeV to reproduce the ψ' - ψ splitting and $E_3 = 0.91$, $E_4 = 1.13$ GeV are obtained from the results of a logarithmic potential model developed by Quigg and Rosner⁽²⁰⁾ which describes the excitations of the charmonium system. n is allowed to run from $n = 1$ to $n = 4$.

The log. potential model also provides guidance on how the annihilation terms in (3.3) and (3.4) and the hyperfine splitting term in (3.4) behave with increasing level of excitation. The radial contributions are expected to decrease in significance as n is increased, which is just the behaviour predicted by the model. Both A and B are assumed to be associated with short range interactions and to depend upon the wavefunction at the origin $\psi_n(0)$, which in the log.potential model is proportional to $1/\sqrt{n}$. This decrease in the strength of the interaction terms ensures that the mixing of ground state configurations with radials is adequately described by the inclusion of just the first three excitations.

The interaction terms of the quadratic model are flavour independent, while those in the linear model violate SU(3) (or SU(4) including the C-quark) through the inclusion of their inverse mass dependence. They do not exhibit the full symmetry breaking expected, as outlined in Chapter 2.

The constituent quark masses appearing in (3.3) and (3.4) are deduced, for the light quarks, from the proton magnetic moment to give $m_u = m_d = 0.337$ GeV, and, for the s quark, from the equal spacing in the baryon decuplet giving $m_s - m_u = 0.140$ GeV and hence $m_s = 0.477$ GeV.

Physical particle masses are calculated by diagonalising the relevant sections of the mass matrix. For instance, the ρ and π masses are obtained in the linear model by diagonalising

$$\left[\begin{array}{cccc} 2m_u + \frac{aB}{2m_u^2} + E_1 & \frac{aB}{\sqrt{2}m_u^2} & \frac{aB}{\sqrt{3}m_u^2} & \frac{aB}{2m_u^2} \\ \frac{aB}{\sqrt{2}m_u^2} & 2m_u + \frac{aB}{2m_u^2} + E_2 & \frac{aB}{\sqrt{6}m_u^2} & \frac{aB}{\sqrt{8}m_u^2} \\ \frac{aB}{\sqrt{3}m_u^2} & \frac{aB}{\sqrt{6}m_u^2} & 2m_u + \frac{aB}{3m_u^2} + E_3 & \frac{aB}{\sqrt{12}m_u^2} \\ \frac{aB}{2m_u^2} & \frac{aB}{\sqrt{8}m_u^2} & \frac{aB}{\sqrt{12}m_u^2} & 2m_u + \frac{aB}{4m_u^2} + E_4 \end{array} \right]$$

where $a = 1/4$ for the vector states and $-3/4$ for the pseudoscalars, and B is fixed by fitting to the ρ - π mass difference. By diagonalising this sector of the mass matrix with $n = 1$, then $n = 2, 3$ and 4 , it is possible to see how the successive radials contribute to the ρ and π masses (in GeV)

$n = 1$	$\rho = 0.833$	$\pi = 0.199$	$B = 0.072 \text{ GeV}^3$
$n = 2$	$\rho = 0.795$	$\pi = 0.161$	$B = 0.063 \text{ GeV}^3$
$n = 3$	$\rho = 0.783$	$\pi = 0.149$	$B = 0.059 \text{ GeV}^3$
$n = 4$	$\rho = 0.776$	$\pi = 0.142$	$B = 0.056 \text{ GeV}^3$

As expected, the masses and interaction strength B converge to limiting values as n increases with $B_{\text{lim}} \approx 0.05 \text{ GeV}^3$, $\pi_{\text{lim}} \approx 0.14 \text{ GeV}$ and $\rho_{\text{lim}} \approx 0.77 \text{ GeV}$. The low mass prediction for the pion is an attractive feature of this linear model which is not shared by the other models discussed.

The value of S , the counterpart to B in the quadratic model, must be determined separately in the pseudoscalar and vector nonets. Its value is fixed for the pseudoscalars by fitting to the π^0 , and for the vectors by fitting to the ρ . An encouraging result of these fits is

$$S_v \approx - (1/3) S_p \quad (3.5)$$

that is, almost the entire gluon exchange interaction appears as a hyperfine interaction proportional to $\vec{\sigma}_a \cdot \vec{\sigma}_b$. This lends credence to the construction of the linear model where $B \vec{\sigma}_a \cdot \vec{\sigma}_b / m_a m_b$ which replaces S , reproduces (3.5).

Why (3.5) holds so well is indicated by the nature of the quark mass parameters m_u, m_d used in the models. These masses are obtained from the proton magnetic moment by identifying this with the quark Dirac magnetic moment $e/2m_u$. The masses which appear in this expression depend upon the nature of the potential which binds the quarks^(4,50,59). If the quarks are bound by a Lorentz four-vector potential (a Coulomb potential, for example) then the magnetic moment would be that corresponding to free particles (that is, switching on a Lorentz 4-vector potential does not change the magnetic moment) and the quark mass would not include the effect of the interaction potential. However, if the binding is due to a scalar potential this will add to the mass term in the Dirac equation

$$\begin{aligned} (m_q + \vec{\gamma} \cdot \vec{p}) \psi_q &= (E + V_v) \gamma_0 \psi_q && \text{for a 4-vector potential } V_v \\ \left[(m_q - V_s) + \vec{\gamma} \cdot \vec{p} \right] \psi_q &= E \gamma_0 \psi_q && \text{for a scalar potential } V_s \end{aligned}$$

and the mass in the magnetic moment expression will be $m_q - V_s$. The Cohen and Lipkin fit to meson masses, which produces reasonably good predictions (Table 3.1) could suggest that the spin independent confining potential which contributes to the quark masses is Lorentz scalar in nature. The spin dependent interaction terms characterised by S and B have a vector character and hence do not appear in the magnetic moment, which explains their explicit presence in the mass matrices.

In both of the models (3.3) and (3.4) the annihilation interaction strength is determined for the pseudoscalars by fitting to the η' mass, while for the vector mesons its value is set equal to zero. With the resulting parameter values the mass predictions exhibited in Table 3.1 are made.

Model	Pseudoscalar Mass (GeV)				Vector Mass (GeV)			
	π	k	η	η'	ρ	k^*	ω	ϕ
Quadratic	0.14 (fit)	0.48	0.53	0.96 (fit)	0.77	0.90	0.77	1.03
Linear	0.15	0.47	0.53	0.96 (fit)	0.77	0.89	0.77	1.01
Experimental Value	0.14	0.49	0.55	0.96	0.77	0.89	0.78	1.02

Table 3.1: Mass predictions for the Cohen and Lipkin Quadratic and Linear Mixing Models.

The vector meson results for the quadratic model are derived with the assumption that (3.5) is a good approximation. Predictions for the masses of the excited states are also produced. Cohen and Lipkin quote their results for the $n=2$ isoscalar pseudoscalar states which, in the quadratic model have masses 1260 MeV and 1420 MeV and in the linear model 1310 MeV and 1490 MeV. The lightest of these excitations is to be compared with the state observed by Stanton et al ⁽⁷⁸⁾ with mass 1275 MeV.

The linear model of reference 59 was extended to include $c\bar{c}$ states with the aim of predicting a mass for the η_c , which then had an anomalously low experimental value of 2.83 GeV. Taking the c quark mass $m_c = M_\psi/2$ gives the result $M_{\eta_c} = 3.1$ GeV, that is, the η_c has a mass essentially degenerate with that of the ψ . This prediction arises from two competing effects,

(i) the hyperfine interaction (which is reduced considerably in strength by quark mass factors when compared with its value in the $u\bar{u}$ sector) splits the ψ and η_c states, bringing the η_c below the ψ ,

(ii) the annihilation interaction makes a positive contribution to the η_c mass, essentially annulling the hyperfine splitting and leaving it almost coincident with the ψ .

3.3.2 Extending the Cohen and Lipkin Models

The experimental value of the η_c mass is presently fixed at 2.98 GeV⁽⁸²⁾, a substantial increase on its previous magnitude but still approximately 0.12 GeV below that of the ψ and much smaller than the value predicted by Cohen and Lipkin. The inability of their model to produce a ψ - η_c splitting can be understood by reconsidering the interaction terms which are responsible for the mixing of $q\bar{q}$ states. The annihilation term in the quadratic model is flavour independent while that contained in the linear model includes a flavour dependence given by the quark masses. The expected variation of the full annihilation contribution

$$A_{qq'} \sim \frac{\alpha_s^n |\psi(0)|^2}{m_q m_{q'}} \quad (3.6)$$

(with $n = 2$ for pseudoscalars and $n = 3$ for vectors) is not included in either case. Taking $\alpha_s(3 \text{ GeV}) \approx 0.19$ ⁽⁸³⁾ from ψ decays, and $\alpha_s(1 \text{ GeV}) \approx 0.22$ from the asymptotic freedom formula (2.22), and noting the empirical relation

$$|\psi_q(0)\psi_{q'}(0)| \propto M_{qq'}^2 \quad (3.7)$$

where M_{qq} , represents the magnitude of the qq element in the mass matrix, the additional dependence given to A_{qq} , in (3.6) would appear to imply that the η_c mass should be raised to a larger value than that of the ψ , however, a compensating dependence of the hyperfine splitting strength reverses this trend.

The one gluon exchange approximation in QCD suggests ⁽³⁹⁾

$$B \sim \alpha_s |\psi(0)|^2 \quad (3.8)$$

thus, the original variation of the hyperfine splitting contribution with mass scale given by

$$\frac{1}{m_u^2} : \frac{1}{m_s^2} : \frac{1}{m_c^2} \approx 22 : 11 : 1$$

will now be much less violent, (3.8) implying

$$\alpha_s (u\bar{u})M_{uu}^2 \approx \alpha_s (s\bar{s})M_{ss}^2 \approx \frac{1}{10} \alpha_s (c\bar{c})M_{cc}^2$$

where typical parameter values, as given above have been employed. The hyperfine splitting strength B is fixed in the model by the ρ - π mass difference, that is, a mass difference associated with the $u\bar{u}$ sector, therefore the additional variation given in (3.8) would substantially increase the predicted splitting between the ψ and η_c compared with the Cohen and Lipkin result. The dependence (3.8) is similar to, but more rapid than (3.6) so their combined effect would be expected to produce a ψ - η_c splitting with $M_\psi > M_{\eta_c}$.

The approach taken here involves accounting for the symmetry breaking in the interaction terms in a manner similar to that used for ground-state models such that the η_c mass can be accommodated while still maintaining a variation among the parameters which is consistent with the

expectations of perturbative QCD. The number of parameters in each model is necessarily increased so further constraints are required to fix their values. To this end the ratio $\rho = \Gamma(\psi \rightarrow \eta'\gamma) / \Gamma(\psi \rightarrow \eta\gamma)$ is used as before.

The mass matrices take essentially the same form as in (3.3) and (3.4). Whereas the same values for m_u and m_d are assumed the s and c quark masses are varied in order to provide a satisfactory description of the ϕ , ψ and η_c . The value of m_s can be upper bounded by $m_s \leq M_\phi/2 = 0.510$ GeV and, if the smallest of the baryon decuplet splittings is taken, underbounded at 0.474 GeV. Similarly the charmed quark mass can be upperbounded by $m_c \leq M_\psi/2 = 1.550$ GeV but must be less than this if the η_c is to be fitted.

3.3.3 The Extended Quadratic Model

Including symmetry breaking of the interaction terms, the mass matrix is⁽⁵²⁾

$$\langle q_a, \bar{q}_b, n' | M^2 | q_a, \bar{q}_b, n \rangle = M_{abnn'}^2 \delta_{aa'} \delta_{bb'} \delta_{nn'} + \frac{A_{aa'}}{nn'} \delta_{ab} \delta_{a'b'} \quad (3.9)$$

where

$$M_{abnn'}^2 = \left[(m_a + m_b + E_n)^2 + S \right] \quad (3.10)$$

Consider firstly the $n = 1$ case for the pseudoscalars. As before S is fixed by the pion mass at $S = -0.43 \text{ GeV}^2$ to give a reasonable prediction for the k meson mass (0.48 GeV) with m_s set initially at $m_s = 0.477$ GeV. The flavour dependent annihilation terms are fitted to the η and η' masses to give A_{uu} and A_{ss} values close to those obtained in the ground-state mixing model of section 2.5.1. Charmonium states can be included by fitting m_c and A_{cc} to the η_c mass and $\Gamma(\psi \rightarrow \eta'\gamma)$ decay rate as before. Comparing the $c\bar{c}$ components mixed into the η and η' gives the prediction $\rho \approx 7$ for the radiative ratio. As before, decreasing this value to match the Crystal Ball

result⁽⁵⁴⁾ of $\rho \approx 5.88$ involves an increase in m_s from 0.477 to 0.487 GeV. The annihilation terms and wavefunctions are essentially identical to the quadratic fit of section 2.5.1.

Switching on radial excitations up to $n = 4$ changes the value of ρ radically. Using the same value of S to give the π mass and again setting $m_s = 0.477$ GeV initially the flavour dependent annihilation terms are determined by the η, η' and η_c masses to give $A_{uu} = A_{dd} = 0.672 \text{ GeV}^2$, $A_{ss} = 0.542 \text{ GeV}^2$ and $A_{cc} = 8.68 \times 10^{-3} \text{ GeV}^2$. Mixing the ground-state with radial excitations lowers the ratio ρ from 7 for $n = 1$ to $\rho = 3.3$ for $n = 4$, well below the Crystal Ball result but in good agreement with the Dasp⁽⁸⁴⁾ result of $\rho = 3.54$. Mass predictions are essentially the same as for the flavour independent model with

$$M_{\pi_2} = 1.08 \text{ GeV} ; M_{\eta_2} = 1.29 \text{ GeV} ; M_{\eta'_2} = 1.42 \text{ GeV} ; M_{\eta_{c2}} = 3.58 \text{ GeV}$$

where the subscript indicates the $n = 2$ excitation. Wavefunctions for the ground-states are

$$\begin{aligned} |\eta\rangle &= 0.688 |NS\rangle + 0.714 |S\rangle + 1.8 \times 10^{-3} |c\bar{c}\rangle \\ |\eta'\rangle &= -0.401 |NS\rangle + 0.517 |S\rangle - 3.6 \times 10^{-3} |c\bar{c}\rangle \\ |\eta_c\rangle &= -0.018 |NS\rangle + 0.012 |S\rangle + 0.999 |c\bar{c}\rangle \end{aligned} \quad (3.11)$$

The predicted magnitude of ρ can be increased to the Crystal Ball value if m_s is reduced to 0.457 GeV which lies below the estimated underbound for this parameter, however, the predicted kaon mass is then reduced to an unsatisfactory value of 0.44 GeV. This model can clearly explain the pseudoscalar masses in a manner consistent with the expectations of QCD but the ratio $\rho = 5.58$ cannot be accommodated if a satisfactory kaon mass is required, a smaller value being preferred.

The pattern of masses for the vector states is well explained in this model by setting $A_{qq} = 0$ in all sectors of the mass matrix and fixing S with

the ρ mass to give $S = + 0.148 \text{ GeV}^2$. Then

$$M_{k^*} = 0.90 ; M_{\omega} = 0.77 ; M_{\phi} = 1.03 ; M_{\psi} = 3.07 \text{ GeV}$$

In the epsilon region A_{bb} can be reliably set equal to zero and the particle masses determined essentially by the mass of the b quark. With $m_{\eta} = 9.46 \text{ GeV}$ and $S_v = 0.148 \text{ GeV}^2$ then $M_b = 4.73 \text{ GeV}$, and hence the η_b is predicted with a mass $M_{\eta_b} = 9.4 \text{ GeV}$.

3.3.4 The Extended Linear Model

The linear model of Cohen and Lipkin⁽⁵⁹⁾ is simply extended⁽⁵²⁾ by allowing for the full symmetry breaking amongst the annihilation and hyperfine splitting strengths. Their expected variation with mass scale is given by⁽⁴⁷⁾

$$B_{aa} \sim \frac{\alpha_s(m_a^2) |\psi_a(0)|^2}{m_a^2}, \quad A_{aa} \sim \frac{\alpha_s^n(m_a^2) |\psi(0)|^2}{m_a^2}$$

where $n = 2$ for pseudoscalars and $n = 3$ for vectors. These dependencies are taken as a general guideline to the expected behaviour of the interaction terms but are not imposed upon the model. The mass matrix is

$$\langle q_a, \bar{q}_b, n' | M | q_a \bar{q}_b n \rangle = M_{abnn'} \delta_{aa'} \delta_{bb'} + \frac{A_{aa'}}{\sqrt{nn'}} \delta_{ab} \delta_{a'b'} \quad (3.12)$$

$$\text{with} \quad M_{abnn'} = (m_a + m_b + E_n) \delta_{nn'} + \bar{\sigma}_a \cdot \bar{\sigma}_b \cdot \frac{B_{ab}}{\sqrt{nn'}} \quad (3.13)$$

where the $|\psi_n(0)| \sim 1/\sqrt{n}$ dependence predicted by the log. potential is explicitly included and the quark mass terms present in the original model (3.4) are absorbed into the interaction parameters.

Equation (3.12) differs from the quadratic model through the $|\psi(0)|^2$ dependence of B_{ab} which allows the mixing of radially excited components in the ground state $I \neq 0$ as well as the $I = 0$ sector. This

mixing successfully explains the low pion mass by changing the initial hyperfine splitting between ρ and π of $(-3/4, +1/4) B_{uu}$ in the undiagonalised mass matrix to an enhanced value $\sim(-5, +1)B_{uu}$ in the physical basis.

In the $u\bar{u}$ and $c\bar{c}$ sectors B_{uu} , B_{cc} , A_{cc}^v and A_{cc}^p are essentially determined by the nature of the model. Taking a value of $m_u = 0.337$ GeV from the original Cohen and Lipkin treatment allows B_{uu} to be determined by the $I = 1$ ρ - π mass splitting, since the states in this sector do not depend upon the annihilation interaction. Its value, $B_{uu} = 0.4978$ GeV, gives good predictions for the ρ and π masses, as before. B_{cc} is fixed by the ψ - η_c splitting and by noting that A for the vectors is very small so that including $A^v \sim \alpha_s^3$ allows $A_{cc}^v = 0$ without producing any noticeable change in the particle mass spectrum. The range of charmed quark mass is limited by assuming $B_{cc} < B_{uu}$ to give $m_c = 1.50$ GeV for $B_{cc} = B_{uu}$ and $m_c = 1.54$ GeV for $B_{cc} = 0.1$ GeV. Choosing $m_c = 1.535$ GeV fixes $B_{cc} = 0.120$ GeV to give the required ψ mass and a low η_c mass which is raised to its experimental value by setting $A_{cc}^p = 0.002$ GeV.

Determining B_{uu} , B_{cc} , A_{cc}^v and A_{cc}^p in this manner leaves the remaining parameters A_{uu}^p , A_{ss}^p , A_{uu}^v , A_{ss}^v and B_{ss} to fit the η , η' , ω , ϕ masses and the radiative ratio ρ which will allow the ratio of $c\bar{c}$ components mixed into the η' and η to be fixed. The η and η' masses are independent of A_{uu}^v and A_{ss}^v , and similarly the ω and ϕ masses are independent of A_{uu}^p and A_{ss}^p while ρ depends upon all the remaining five parameters. As in the simpler Cohen and Lipkin treatment, the particle masses can easily be accommodated in the model, however, the Crystal Ball value of $\rho = 5.88 \pm 1.46$ cannot as it pushes B_{ss} against its maximum allowed value as determined by the mass of the ϕ . Lowering m_s from 0.477 GeV allows a possible solution to the problem but produces annihilation terms inconsistent with the expectations of QCD, so its present value is maintained. Fits with $B_{ss} = 0.249, 0.299, 0.339$ GeV give values of $\rho = 1.4, 3.3, 5.5$ respectively, of which the latter, with the largest ρ , is chosen. The full set of parameter values is

then,

$$\begin{aligned}
 A_{uu}^P &= 0.420, & A_{ss}^P &= 0.108, & A_{cc}^P &= 2 \times 10^{-3} \text{ GeV} \\
 A_{uu}^V &= 4 \times 10^{-3}, & A_{ss}^V &= 4 \times 10^{-4}, & A_{cc}^V &= 0.0 \text{ GeV} \\
 B_{uu} &= 0.498, & B_{ss} &= 0.339, & B_{cc} &= 0.120 \text{ GeV}
 \end{aligned} \tag{3.14}$$

giving ground-state unitary spin wavefunctions,

$$\begin{aligned}
 |\eta\rangle &= 0.472 |NS\rangle + 0.826 |S\rangle + 2.5 \times 10^{-3} |c\bar{c}\rangle \\
 |\eta'\rangle &= -0.750 |NS\rangle + 0.383 |S\rangle - 6.2 \times 10^{-3} |c\bar{c}\rangle \\
 |\eta_c\rangle &= -0.052 |NS\rangle + 0.021 |S\rangle + 0.987 |c\bar{c}\rangle
 \end{aligned} \tag{3.15}$$

and the following mass predictions for the first radial excitations,

$$\begin{aligned}
 M_{\pi_2} &= 1.13 \text{ GeV} ; & M_{\eta_2} &= 1.38 \text{ GeV} ; & M_{\eta'_2} &= 1.47 \text{ GeV} ; & M_{\eta_{c2}} &= 3.62 \text{ GeV} \\
 M_{\rho_2} &= 1.32 \text{ GeV} ; & M_{\omega_2} &= 1.33 \text{ GeV} ; & M_{\phi_2} &= 1.59 \text{ GeV} ; & M_{\psi_2} &= 3.68 \text{ GeV}
 \end{aligned} \tag{3.16}$$

In the $I \neq 0$ sector the annihilation independent k , k^* , D , D^* , F and F^* masses are determined, in principle, by B_{uu} , B_{ss} and B_{cc} through factorisation, however, their predicted splittings turn out to be larger than the corresponding experimental values and mass predictions are poor. The failure of the model for states constructed from unequal mass quarks can be attributed to many causes. The simplifications made to the original model of de Rujula, Georgi and Glashow⁽³⁹⁾ may be too drastic, a more sophisticated model being required. Also, higher order corrections to the form of the Hamiltonian

predicted by DGG may be important and it is likely that the dependence of B_{ab} upon n may be different in different sectors of the mass matrix.

The variation of $|\psi_n(0)|$ with n as predicted by a log, potential and imposed in (3.12) could be one of the principal deficiencies of the model. Assuming that A and B decrease with n as $1/\sqrt{nn'}$ for both heavy and light states is clearly simplistic as is indicated empirically in the ψ and Υ spectra. The ratio $|\psi_2(0)|^2/|\psi_1(0)|^2$ can be calculated from vector $\rightarrow e^+e^-$ decays using the Van Royen/Weiskopf formula⁽⁵⁰⁾ to give,

$$r \equiv \frac{|\psi_2(0)|^2}{|\psi_1(0)|^2} = \frac{\Gamma(V' \rightarrow e^+e^-) \cdot M_{V'}^2}{\Gamma(V \rightarrow e^+e^-) \cdot M_V^2}$$

for Υ and ψ this ratio is 0.3 and 0.6 respectively, to be compared with the predicted value of 1/2. Also, identifying the $I = 1$ state at 1600 MeV with the ρ'' allows the prediction⁽⁶⁰⁾ $r = 1.1 \pm 0.3$ compared with 1/3 expected in the model. Experimental evidence indicates that $|\psi(0)|^2$ for the lighter states falls off less rapidly with n than for the heavier states indicating, in a potential model framework, that the lighter relativistic quarks experience more of the linear confining potential which predicts⁽²⁰⁾ $|\psi_n(0)|^2 \sim \text{const.}$ than the heavier quarks which may experience more of the short range $1/r$ Coulomb-like potential which results from one gluon exchange and predicts⁽²⁰⁾ $|\psi_n(0)|^2 \sim 1/n^3$. The differences in the variation of $|\psi(0)|$ with n in different sectors of the mass matrix has important consequences for the mixing pattern. For the lighter states it is possible that more than three radial excitations would be required to correctly account for their contributions to the ground-state wavefunctions, and consequently the $(-5, +1)$ splitting which fits the ρ and π masses would change necessitating the assumption of a different value for m_u if good predictions for M_π and M_ρ are to be maintained.

Despite these problems and inadequacies a reasonable average description of meson properties may be expected. The model can fit the ground state

pseudoscalar and vector masses in a manner consistent with the expectations of lowest order QCD and with $M_{\eta_c} = 2.98$ GeV. A problem remains with the Crystal Ball value of ρ , however, which is too large for the model to cope with in a consistent manner. The matter is pursued in Chapter 4 where this ratio and many other meson properties are investigated using the wavefunctions obtained upon diagonalization of (3.12).

CHAPTER 4THE LINEAR MIXING MODEL AND MESON PROPERTIES4.1 INTRODUCTION

The radial mixing models reported in Chapter 3 adequately describe the pseudoscalar and vector meson mass spectra in a way such that the variation of their parameters with mass scale is in broad agreement with that expected from QCD. More exacting tests of the relevance of such models as descriptions of hadron structure can be made by examining their predictions for other meson properties which are sensitive to the structure of the unitary spin wavefunctions. The purpose of this chapter is to apply such tests and investigate the model predictions for radiative and hadronic decays and isoscalar meson production processes.

The examination of meson properties is conducted with the extended linear mass mixing model described in 3.3.4. This model is chosen in preference to the extended Isgur model because of its ability to mix radial excitations in the $I \neq 0$ sectors of the mass matrix, an exclusive facility which allows the prediction of a small pion mass.

The first problem to be resolved is that of the magnitude of the radiative ratio ρ . Difficulties were encountered in 3.3.4 when an attempt was made to fit the Crystal Ball measurement of this quantity, $\rho = 5.88$. In the following treatment fits are made to the various values of ρ and for each value predictions are made for other radiative decay widths which are compared with experiment, allowing a preferred magnitude to be selected. The wavefunctions obtained from the chosen fit are used to examine the discrepancy in the strangeness exchange sum rule (3.2) and the predictions for ratios of meson production amplitudes. Finally, a simple method for the examination of hadronic vector decays is formulated and predictions are made for ratios of decay widths of radially excited vector mesons.

4.2 RADIATIVE DECAY PREDICTIONS AND THE VALUE OF ρ

In the previous chapter the linear mass mixing model of Cohen and Lipkin⁽⁵⁹⁾ was extended⁽⁵²⁾ to include the flavour dependence of its various parameters and to see if it could successfully accommodate the pseudo-scalar and vector meson mass spectra and the recent Crystal Ball measurement⁽⁵⁴⁾ of $\rho = 5.88$ in a way consistent with first order perturbative QCD. The mass matrix, including symmetry breaking amongst its parameters is

$$\langle q_a, \bar{q}_b, n' | M | q_a, \bar{q}_b, n \rangle = M_{abnn'} \delta_{aa'} \delta_{bb'} + \frac{A_{aa'} \delta_{ab} \delta_{a'b'}}{\sqrt{nn'}} \quad (4.1)$$

where

$$M_{abnn'} = (m_a + m_b + E_n) \delta_{nn'} + \frac{\vec{\sigma}_a \cdot \vec{\sigma}_b}{\sqrt{nn'}} \frac{B_{ab}}{\sqrt{nn'}}$$

The pseudoscalar and vector meson mass spectra are easily reproduced but the Crystal Ball measurement of ρ provides a problem⁽⁵²⁾ in that it pushes the parameter B_{ss} against its maximum allowed value, given by the ϕ mass. In this subsequent analysis the magnitude of the s quark mass, which to a large extent determines the pattern of η - η' mixing is seen to be very sensitive to the imposed value of ρ , and predictions of the model for quantities which are strongly dependent upon η - η' mixing are used in a comparison with experiment to find a preferred value for this ratio.

The experimental status of ρ is, at present, unclear as can be seen from Table 4.1. While the measurements of $B(\psi \rightarrow \eta\gamma)$ are in broad agreement,

Experiment	$B(\psi \rightarrow \eta\gamma) \times 10^{-3}$	$B(\psi \rightarrow \eta'\gamma) \times 10^{-3}$	ρ
Desy/Heidelberg ⁽⁸⁵⁾	1.3 \pm 0.4	2.4 \pm 0.7	1.8 \pm 0.8
Dasp ⁽⁸⁶⁾	0.8 \pm 0.2	2.2 \pm 1.7	2.8 \pm 2.3
Dasp ⁽⁸⁴⁾	0.82 \pm 0.10	2.9 \pm 1.1	3.54 \pm 1.4
Mark II ⁽⁸⁷⁾	0.9 \pm 0.4	3.4 \pm 0.7	3.8 \pm 1.9
Crystal Ball ⁽⁵⁴⁾	1.2 \pm 0.2	6.9 \pm 1.7	5.9 \pm 1.5

TABLE 4.1 : Existing Branching Ratios for $\psi \rightarrow \eta(\eta')\gamma$ Radiative Decays.

the high statistics Crystal Ball determination of $B(\psi \rightarrow \eta' \gamma)$ is clearly incompatible with other measurements, being a factor of two or three larger. It is suggested⁽⁸⁷⁾ that the discrepancy between the Crystal Ball and Mark II results may, in part, be explained by the uncertainty in the relative branching fractions of the observed decay modes of the η' , the Crystal Ball collaboration⁽⁵⁴⁾ detect $\eta' \rightarrow 2\gamma$ while the Mark II group⁽⁸⁷⁾ observe $\eta' \rightarrow \rho^0 \gamma$. This argument may also apply to the other high statistics determination of $B(\psi \rightarrow \eta' \gamma)$ performed by the Desy-Heidelberg collaboration⁽⁸⁵⁾ who also observe the $\eta' \rightarrow \rho^0 \gamma$ decay mode, however, the disagreement is large while the uncertainties in $B(\eta' \rightarrow \rho^0 \gamma)$ and $B(\eta' \rightarrow 2\gamma)$ are comparatively small.

The purpose of this analysis is to exploit the sensitive dependence of η - η' mixing on ρ by comparing model predictions of meson properties which are dependent upon the structure of this mixing with their experimental values in order to, within the capacity of the model, point to a preferred value of ρ . Five fits are made corresponding to the five values of ρ in Table 4.1. In each case, the gross variation of the quark masses (which are treated as free parameters), hyperfine splitting strengths and annihilation terms are determined by the vector and pseudoscalar mass spectra, leaving the "fine tuning" of the parameters to be resolved by radiative decays, which are sensitive indicators of the structure of meson unitary spin wavefunctions. In the pseudoscalar sector the remaining parameters are determined by fitting to ρ and the corresponding radiative decay width $\Gamma(\psi \rightarrow \eta \gamma)$.

In order to determine the magnitudes of the OZI violating annihilation amplitudes (in the vector meson sector) which are responsible, for example, for $u\bar{u}$ and $d\bar{d}$ mixing in the ϕ unitary spin wavefunction, a fit is made to the radiative decay rates $\Gamma(\phi \rightarrow \pi^0 \gamma) = 5.7 \pm 2.0 \text{ KeV}$ ⁽⁸⁸⁾ and $\Gamma(\psi \rightarrow \pi^0 \gamma) = 4.6 \pm 3.0 \text{ eV}$ ⁽⁸⁴⁾. A problem is encountered here, however, for there is a competing mechanism which contributes to these decays, that of the isospin violating mixing of π^0 - η - η' . Such mixing may be induced by both the strong

and electromagnetic interactions, as noted by Isgur⁽⁴⁸⁾, leading to a π^0 state with small, but non-negligible $s\bar{s}$ and $c\bar{c}$ components (see Chapter 5).

$$|\pi^0\rangle = |\pi_u^0\rangle + \alpha|\eta_u\rangle + \beta|\eta'_u\rangle \quad (4.2)$$

where $|\pi_u^0\rangle$, $|\eta_u\rangle$ and $|\eta'_u\rangle$ are the pure isospin pseudoscalar states and α and β give a measure of the mixing. The values of α and β have been determined (references 48, 89 and Chapter 5) so it is possible to estimate the relative effects the OZI violating (but not isospin violating) and isospin violating mixing will have on the $\phi \rightarrow \pi\gamma$ and $\psi \rightarrow \pi\gamma$ decay rates. It is found that in both cases the $s\bar{s}$ and $c\bar{c}$ components in the π^0 wavefunction produce, approximately, a 15% contribution to the decay amplitudes. These corrections are included in the analysis.

In each of the five fits corresponding to different values of ρ the $J^P = 0^-$ and 1^- mass spectra are reproduced, giving the ground-state masses (in GeV)

$$\begin{aligned} M_{\pi^0} &= 0.140 : M_{\eta} = 0.549 : M_{\eta'} = 0.958 : M_{\eta_c} = 2.98^{(82)} \\ M_{\rho^0} &= 0.770 : M_{\omega} = 0.782 : M_{\phi} = 1.019 : M_{\psi} = 3.096 \end{aligned} \quad (4.3)$$

Diagonalisation of the mass matrix produces unitary spin wavefunctions in the basis of $q\bar{q}$ states, as shown in Tables 4.2 and 4.3.

Value of ρ	Particle Wavefunction
$\rho = 1.8$	$ \eta\rangle = 0.493 (u\bar{u} + d\bar{d}) - 0.669 s\bar{s} - 0.0037 c\bar{c}$ $ \eta'\rangle = 0.456 (u\bar{u} + d\bar{d}) + 0.607 s\bar{s} - 0.0055 c\bar{c}$ $ \eta_c\rangle = 0.013 (u\bar{u} + d\bar{d}) + 0.011 s\bar{s} + 0.993 c\bar{c}$
$\rho = 2.8$	$ \eta\rangle = 0.427 (u\bar{u} + d\bar{d}) - 0.748 s\bar{s} - 0.0029 c\bar{c}$ $ \eta'\rangle = 0.492 (u\bar{u} + d\bar{d}) + 0.509 s\bar{s} - 0.0054 c\bar{c}$ $ \eta_c\rangle = 0.019 (u\bar{u} + d\bar{d}) + 0.014 s\bar{s} - 0.992 c\bar{c}$
$\rho = 3.54$	$ \eta\rangle = 0.392 (u\bar{u} + d\bar{d}) - 0.783 s\bar{s} - 0.0030 c\bar{c}$ $ \eta'\rangle = 0.508 (u\bar{u} + d\bar{d}) + 0.462 s\bar{s} - 0.0062 c\bar{c}$ $ \eta_c\rangle = 0.027 (u\bar{u} + d\bar{d}) + 0.019 s\bar{s} + 0.991 c\bar{c}$
$\rho = 3.8$	$ \eta\rangle = 0.382 (u\bar{u} + d\bar{d}) - 0.792 s\bar{s} - 0.0031 c\bar{c}$ $ \eta'\rangle = 0.513 (u\bar{u} + d\bar{d}) + 0.449 s\bar{s} - 0.0067 c\bar{c}$ $ \eta_c\rangle = 0.030 (u\bar{u} + d\bar{d}) + 0.019 s\bar{s} + 0.990 c\bar{c}$
$\rho = 5.9$	$ \eta\rangle = 0.318 (u\bar{u} + d\bar{d}) - 0.842 s\bar{s} - 0.0036 c\bar{c}$ $ \eta'\rangle = 0.532 (u\bar{u} + d\bar{d}) + 0.365 s\bar{s} - 0.0097 c\bar{c}$ $ \eta_c\rangle = 0.076 (u\bar{u} + d\bar{d}) + 0.041 s\bar{s} + 0.968 c\bar{c}$

TABLE 4.2 : Pseudoscalar unitary spin wavefunctions for the various values of ρ . Ground state components only are shown. The π^0 wavefunction which is independent of ρ is $|\pi^0\rangle = 0.652 (u\bar{u} - d\bar{d})$.

Value of ρ	Particle Wavefunction
$\rho = 2.8$	$ \rho\rangle = 0.697 (u\bar{u}-d\bar{d})$ $ \omega\rangle = 0.693 (u\bar{u}+d\bar{d}) - 0.052 s\bar{s}$ $ \phi\rangle = 0.030 (u\bar{u}+d\bar{d}) + 0.991 s\bar{s}$ $ \psi\rangle = 0.999 c\bar{c}$

TABLE 4.3 : Vector unitary spin wavefunctions are virtually independent of ρ . A typical fit is shown above. Again only ground-state components are exhibited.

In order to make a comparison of the structure of η and η' wavefunctions with those obtained in more conventional schemes they can be re-expressed in a hyperfine interaction perturbed SU(3) basis⁽⁹⁰⁾ (ignoring the $c\bar{c}$ contributions) and hence written in terms of octet and singlet components (Appendix 2). In this new SU(3) basis the ground-state basis vectors contain radial excitations (the radial expansion being defined by the π^0) such that they will diagonalise the mass matrix (4.1) with $A_{ss} \equiv A_{uu}$, $B_{ss} \equiv B_{uu}$ and $m_s \equiv m_u$. The octet-singlet structure of the η and η' is shown in Table 4.4 for each of the five fits, together with similar wavefunctions obtained using the conventional ground-state mixing schemes for quadratic ($\theta = -11^\circ$) and linear ($\theta = -24^\circ$) mass matrices. As ρ is increased the η' loses more of its wavefunction to higher radial states while the η retains its ground-state components losing relatively much less of its wavefunction to higher radials. Note that the singlet $|\eta_1\rangle_1$ shows a slight variation with the value of ρ due to its dependence upon A_{uu} , its structure for $\rho = 2.8$ is quoted in Table 4.4.

Predictions⁽⁹⁰⁾ are made as before for the masses of the radial excitations of the vector and pseudoscalar mesons, although they must be treated tentatively in view of the manner in which excitation energies taken

Model	Unitary Spin Wavefunction Structure
$\rho = 1.8$	$ \eta\rangle = 0.972 \eta_8\rangle_1 + 0.188 \eta_1\rangle_1$ $ \eta'\rangle = -0.212 \eta_8\rangle_1 + 0.955 \eta_1\rangle_1$
$\rho = 2.8$	$ \eta\rangle = 0.986 \eta_8\rangle_1 + 0.093 \eta_1\rangle_1$ $ \eta'\rangle = -0.119 \eta_8\rangle_1 + 0.955 \eta_1\rangle_1$
$\rho = 3.54$	$ \eta\rangle = 0.988 \eta_8\rangle_1 + 0.050 \eta_1\rangle_1$ $ \eta'\rangle = -0.074 \eta_8\rangle_1 + 0.950 \eta_1\rangle_1$
$\rho = 3.8$	$ \eta\rangle = 0.987 \eta_8\rangle_1 + 0.039 \eta_1\rangle_1$ $ \eta'\rangle = -0.062 \eta_8\rangle_1 + 0.950 \eta_1\rangle_1$
$\rho = 5.9$	$ \eta\rangle = 0.979 \eta_8\rangle_1 + 0.030 \eta_1\rangle_1$ $ \eta'\rangle = -0.011 \eta_8\rangle_1 + 0.935 \eta_1\rangle_1$
$\theta = -11^\circ$	$ \eta\rangle = 0.982 \eta_8\rangle + 0.191 \eta_1\rangle$ $ \eta'\rangle = -0.191 \eta_8\rangle + 0.982 \eta_1\rangle$
$\theta = -24^\circ$	$ \eta\rangle = 0.914 \eta_8\rangle + 0.407 \eta_1\rangle$ $ \eta'\rangle = -0.407 \eta_8\rangle + 0.914 \eta_1\rangle$

TABLE 4.4 : The 'ground-state' octet-singlet structure of η and η' unitary spin wavefunctions. The octet and typical singlet basis vectors (in the ground-state) are
 $|\eta_8\rangle_1 = 0.376(u\bar{u} + d\bar{d}) - 0.753 s\bar{s}$ and $|\eta_1\rangle_1 = 0.493(u\bar{u} + d\bar{d} + s\bar{s})$
The subscript '1' indicates 'ground-state'

from the charmonium spectrum are applied directly to the low mass particles. The masses predicted for the first radial excitations ($n = 2$) are (in GeV),

$$\begin{aligned}
 M_{\pi_2^0} &= 1.14 ; & M_{\eta_2} &= 1.36 ; & M_{\eta_2'} &= 1.50 ; & M_{\eta_{c2}} &= 3.63 \\
 M_{\rho_2^0} &= 1.33 ; & M_{\omega_2} &= 1.34 ; & M_{\phi_2} &= 1.59
 \end{aligned}
 \tag{4.4}$$

The pseudoscalar predictions are to be compared with a possible η_2 candidate with mass 1.28 GeV⁽⁷⁸⁾, a tentatively identified π_2 ⁽⁷⁹⁾ at 1.27 GeV and a recently observed η_{c2} ⁽⁸¹⁾ with mass 3.59 GeV as outlined in section 3.2.2. The strongest candidate for a ρ_2 has a mass of approximately 1.25 GeV (identifying the $I = 1$ state at 1.6 GeV with the ρ_3) to be compared with 1.33 GeV. No excited $I = 0$ vector state has yet been observed around the predicted mass of $M_{\omega_2} = 1.34$ GeV, however, such states with a narrow width have been observed in e^+e^- and photoproduction experiments around 1.66 GeV (section 3.2.1). Their narrow width has suggested their association with the ϕ_2 ⁽⁷⁵⁾ in close agreement with the model prediction.

The predicted mass values of the $n = 3$ excitations are (in GeV)

$$\begin{aligned}
 M_{\pi_3^0} &= 1.55 ; & M_{\eta_3} &= 1.72 ; & M_{\eta_3'} &= 1.82 ; & M_{\eta_{c3}} &= 4.00 \\
 M_{\rho_3^0} &= 1.66 ; & M_{\omega_3} &= 1.67 ; & M_{\phi_3} &= 1.93 ; & M_{\psi_3} &= 4.03
 \end{aligned}
 \tag{4.5}$$

There are, at present, no experimental candidates for the pseudoscalar excitations, however, prospective $n = 3$ vectors may have been identified. A firm ρ excitation, which is associated here with the ρ_3^0 , has been observed in numerous experiments with masses ranging from 1.54 ± 0.03 ⁽⁶⁵⁾ to 1.67 ± 0.04 GeV⁽⁶⁹⁾ which coincide with the model prediction. The only sighting of an ω excitation in the mass region given in (4.5) is that due to Cosme et al⁽⁷⁵⁾ with mass approximately 1.7 GeV, all other candidates

having higher masses in the region 1.78 - 1.79 GeV. A tentatively identified ϕ_3 has been observed in $\gamma p \rightarrow k^* k \pi p$ ⁽⁷⁶⁾ with mass 1.9 GeV in agreement with the 1.93 GeV prediction above.

Predictions of the masses and wavefunctions of the k , k^* , D , D^* , F and F^* mesons are obtained by diagonalising the relevant $I \neq 0$ sectors of the mass matrix, where the only unknown parameters are the mixed quark hyperfine splitting strengths $B_{qq'}$. In each case these are evaluated by fitting to the relevant V-P mass difference so that, for example, B_{us} is determined by requiring it to reproduce the k^*-k mass splitting. The problem encountered with the ground state mixing schemes recurs here, particle mass predictions being consistently lower than their experimental values. Typical parameter values and mass predictions for the ground and first radially excited state mesons are (in GeV)

$$B_{us} = 0.329, \quad B_{uc} = 0.130, \quad B_{sc} = 0.103$$

$$M_{K_1} = 0.48 ; \quad M_{K_2} = 1.31 ; \quad M_{K_1^*} = 0.89 ; \quad M_{K_2^*} = 1.45 \quad (4.6)$$

$$M_{D_1} = 1.76 ; \quad M_{D_2} = 2.43 ; \quad M_{D_1^*} = 1.90 ; \quad M_{D_2^*} = 2.49$$

$$M_{F_1} = 1.92 ; \quad M_{F_2} = 2.57 ; \quad M_{F_1^*} = 2.03 ; \quad M_{F_2^*} = 2.62$$

while the wavefunctions for these mesons are exhibited in Table 4.5.

The unitary spin wavefunctions obtained upon diagonalisation of the mass matrix (4.1) in both $I = 0$ and $I \neq 0$ sectors can be used in a simple quark model analysis to predict the widths for the radiative transitions $V \rightarrow P\gamma$ and $P \rightarrow V\gamma$. In the past conventional quark model mixing schemes producing ideally mixed vector states have encountered difficulties when trying to explain OZI rule violating decays such as $\phi \rightarrow \pi^0 \gamma$.

$ K_1^+ \rangle = 0.956 u\bar{s}\rangle_1 + 0.236 u\bar{s}\rangle_2 :$	$ K_2^+ \rangle = 0.270 u\bar{s}\rangle_1 - 0.940 u\bar{s}\rangle_2$
$ K_1^{*+} \rangle = 0.994 u\bar{s}\rangle_1 - 0.096 u\bar{s}\rangle_2 :$	$ K_2^{*+} \rangle = 0.089 u\bar{s}\rangle_1 - 0.989 u\bar{s}\rangle_2$
$ D_1^+ \rangle = 0.991 c\bar{d}\rangle_1 + 0.108 c\bar{d}\rangle_2 :$	$ D_2^+ \rangle = 0.116 c\bar{d}\rangle_1 - 0.987 c\bar{d}\rangle_2$
$ D_1^{*+} \rangle = 0.999 c\bar{d}\rangle_1 - 0.038 c\bar{d}\rangle_2 :$	$ D_2^{*+} \rangle = 0.037 c\bar{d}\rangle_1 - 0.998 c\bar{d}\rangle_2$
$ F_1^+ \rangle = 0.994 c\bar{s}\rangle_1 + 0.087 c\bar{s}\rangle_2 :$	$ F_2^+ \rangle = 0.092 c\bar{s}\rangle_1 - 0.992 c\bar{s}\rangle_2$
$ F_1^{*+} \rangle = 0.999 c\bar{s}\rangle_1 - 0.030 c\bar{s}\rangle_2 :$	$ F_2^{*+} \rangle = 0.030 c\bar{s}\rangle_1 - 0.999 c\bar{s}\rangle_2$

TABLE 4.5 : $I \neq 0$ Meson unitary spin wavefunctions.

Later ideas, abstracted from QCD accounted for such processes by allowing them to go through the annihilation of $q\bar{q}$ pairs^(56,91) as shown in Figs 4.1 and 4.2 where the couplings of the gluons to quarks of the ϕ are presumed to be small, allowing the processes to be treated perturbatively, so only two or three gluon intermediate states need be considered.

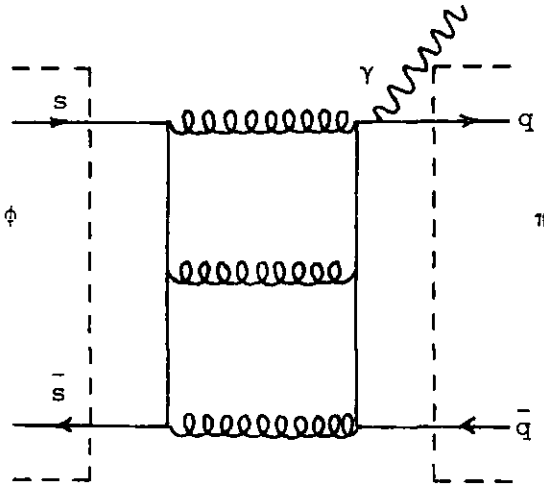


Fig 4.1 : $\phi \rightarrow \pi\gamma$ radiative transition occurring via a 3 gluon intermediate state.

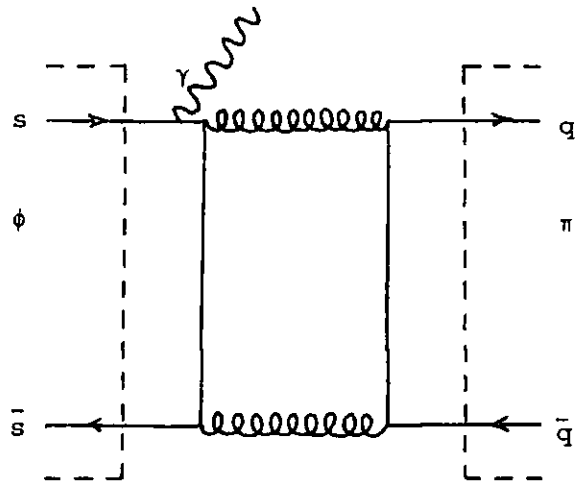


Fig 4.2 : $\phi \rightarrow \pi\gamma$ radiative transition. occurring via a 2 gluon intermediate state.

The problem is treated slightly differently here⁽⁹⁰⁾, however, the annihilation process is understood to cause mixing of, for example, $u\bar{u}$ and $d\bar{d}$ in the ϕ wavefunction, allowing the ϕ to decay directly into a π as shown in Fig 4.3 where the box represents the meson as described by the mixing program of equation (4.1).

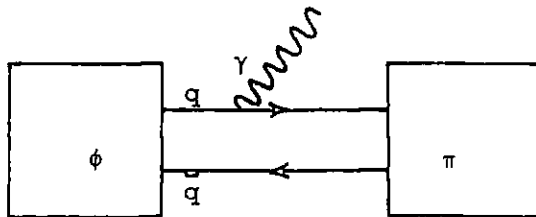


Fig 4.3 : $\phi \rightarrow \pi\gamma$ decay as described by the mixing scheme of equation (4.1).

Note that in this scheme decays such as that shown in Fig 4.3 are OZI allowed as they proceed via connected quark diagrams but are suppressed relative to, for example, $\eta' \rightarrow \rho\gamma$ because of the small annihilation amplitudes inherent in the vector mixing scheme.

Radiative decay widths are calculated by modifying the conventional quark model approach to include radial excitations, yielding the following expressions,

$$\begin{aligned}\Gamma(V \rightarrow P\gamma) &= \frac{K_1^3}{3\pi} |A(V \rightarrow P\gamma)|^2 \\ \Gamma(P \rightarrow V\gamma) &= \frac{K_2^3}{\pi} |A(P \rightarrow V\gamma)|^2\end{aligned}\tag{4.7}$$

where K_1 and K_2 are the centre of mass photon momenta, given by

$$K_1 = \frac{M_V^2 - M_P^2}{2M_V} \quad K_2 = \frac{M_P^2 - M_V^2}{2M_P}\tag{4.8}$$

The amplitudes $A(V \rightarrow P\gamma)$ and $A(P \rightarrow V\gamma)$ in which the effects of radial excitations appear are essentially the overlaps of meson unitary spin wavefunctions with the coupling of the photon to the quark charge added.

Denoting general wavefunctions for the vector (V) and pseudoscalar (P) isoscalars by

$$\begin{aligned}|V, S_3 = 0\rangle &= \sum_{i=1}^n \left[\alpha_i |u\bar{u}\rangle_i + \beta_i |d\bar{d}\rangle_i + \gamma_i |s\bar{s}\rangle_i + \delta_i |c\bar{c}\rangle_i \right] \frac{1}{\sqrt{2}} (++++)\tag{4.9} \\ |P\rangle &= \sum_{i=1}^n \left[a_i |u\bar{u}\rangle_i + b_i |d\bar{d}\rangle_i + c_i |s\bar{s}\rangle_i + d_i |c\bar{c}\rangle_i \right] \frac{1}{\sqrt{2}} (+-++)\end{aligned}$$

a typical amplitude will take the form

$$A(V \rightarrow P\gamma) = \frac{2}{3} \mu \sum_{i=1}^n \left[2\alpha_i a_i - \beta_i b_i - \frac{m}{m_s} \gamma_i c_i + 2 \frac{m}{m_c} \delta_i d_i \right] \quad (4.10)$$

To describe decays between $I_3 \neq 0$ states, denote their wavefunctions by

$$\begin{aligned} |V, S_3 = 0\rangle &= \sum_{i=1}^n f_i |q_a \bar{q}_b\rangle_i \frac{1}{\sqrt{2}} \quad (\uparrow\uparrow + \uparrow\uparrow) \\ |P\rangle &= \sum_{i=1}^n g_i |q_a \bar{q}_b\rangle_i \frac{1}{\sqrt{2}} \quad (\uparrow\uparrow - \uparrow\uparrow) \end{aligned} \quad (4.11)$$

then the amplitude for a typical decay is

$$A(V \rightarrow P\gamma) = (\mu_a e_a - \mu_b e_b) \sum_{i=1}^n f_i g_i \quad (4.12)$$

where e_a is the charge of a quark of flavour a in units of e and μ_a represents the Dirac magnetic moment of the quark. Using the notation $\mu_u = \mu$ where μ is the proton magnetic moment, as described in Chapter 1, then in general

$$\mu_a = \frac{m}{m_a} \mu \quad (4.13)$$

Predictions for the various transitions given by the wavefunctions of (4.1) (full wavefunctions are displayed in Appendix 3) are calculated for the fits to different values of ρ and compared with experiment where data is available. The results are exhibited in Table 4.6 with typical parameter values in Table 4.7.

Process	Experimental Rate (KeV)	Model Predictions (KeV)				
		$\rho = 1.8$	$\rho = 2.8$	$\rho = 3.54$	$\rho = 3.8$	$\rho = 5.9$
$\Gamma(\rho \rightarrow \pi\gamma)$	67 ± 7^a	88	88	88	88	88
$\Gamma(\rho \rightarrow \eta\gamma)$	50 ± 13^b	66	52	43	41	29
	76 ± 15^c					
$\Gamma(\omega \rightarrow \pi\gamma)$	889 ± 57	808	812	813	813	812
$\Gamma(\omega \rightarrow \eta\gamma)$	3.0 ± 2.8^b					
	29 ± 7^c	7.0	5.0	4.1	3.9	2.5
$\Gamma(\phi \rightarrow \pi\gamma)$	5.7 ± 2.0	<u>5.7</u>	<u>5.7</u>	<u>5.7</u>	<u>5.7</u>	<u>5.7</u>
$\Gamma(\phi \rightarrow \eta\gamma)$	62 ± 11	96	117	127	129	144
$\Gamma(\phi \rightarrow \eta'\gamma)$	-	0.32	0.22	0.18	0.17	0.11
$\Gamma(\psi \rightarrow \pi\gamma)$	$(4.6 \pm 3.0) \times 10^{-3}$	<u>4.6×10^{-3}</u>	<u>4.6×10^{-3}</u>	<u>4.6×10^{-3}</u>	<u>4.6×10^{-3}</u>	<u>4.6×10^{-3}</u>
$\Gamma(\psi \rightarrow \eta\gamma)^{(95)}$	0.054	<u>0.082</u>	<u>0.050</u>	<u>0.052</u>	<u>0.056</u>	<u>0.075</u>
$\Gamma(\psi \rightarrow \eta'\gamma)^{(95)}$	0.160	<u>0.151</u>	<u>0.139</u>	<u>0.183</u>	<u>0.214</u>	<u>0.435</u>
$\Gamma(\psi \rightarrow \eta_c\gamma)$	-	2.6	2.6	2.6	2.6	2.5
$\Gamma(\eta' \rightarrow \rho\gamma)$	83 ± 30	150	176	189	191	206
$\Gamma(\eta' \rightarrow \omega\gamma)$	7.6 ± 3.0	17	19	20	20	22
$\Gamma(\eta_c \rightarrow \rho\gamma)$	-	37	67	135	167	1090
$\Gamma(\eta_c \rightarrow \omega\gamma)$	-	3.2	6.7	13.4	16.6	107
$\Gamma(\eta_c \rightarrow \phi\gamma)$	-	3.0	4.2	6.9	8.3	37
$\Gamma(K^{*+} \rightarrow K^+\gamma)$	$<74.1 \pm 34.6^d$	99	98	98	98	97
$\Gamma(K^{*0} \rightarrow K^0\gamma)$	75 ± 35	170	171	172	172	173
$\Gamma(D^{*+} \rightarrow D^+\gamma)$	-	1.9	1.9	1.9	1.9	1.9
$\Gamma(D^{*0} \rightarrow D^0\gamma)$	-	35	35	35	35	35
$\Gamma(F^* \rightarrow F\gamma)$	-	0.2	0.2	0.2	0.2	0.2
$\bar{\sigma}(\pi^-\bar{p} \rightarrow \eta^-\eta)$	0.65 ± 0.13^e	0.38	0.59	0.75	0.80	1.2
$\bar{\sigma}(\pi^-\bar{p} \rightarrow \eta\eta)$						

TABLE 4.6 : Model predictions for radiative transition rates and the ratio of η, η' production amplitudes. All widths are quoted from ref. (61) unless otherwise specified and those underlined are fitted.

a. Ref. (92)

b. Constructive interference solution

d. Ref. (93)

c. Destructive interference solution

e. Ref. (94)

Parameter	Value	Parameter	Value
A_{uu}^P	0.341	A_{uu}^V	0.0099
A_{dd}^P	0.341	A_{dd}^V	0.0099
A_{ss}^P	0.112	A_{ss}^V	0.0144
A_{cc}^P	8.5×10^{-4}	A_{cc}^V	2.1×10^{-5}
B_{uu}	0.493	m_u	0.334
B_{ss}	0.287	m_s	0.472
B_{cc}	0.112	m_c	1.535

TABLE 4.7 : Parameter values for the $\rho = 2.8$ fit. A^P and A^V are the annihilation parameters corresponding to the pseudoscalar and vector sectors respectively. Off diagonal annihilation amplitudes are given by the factorisation relation⁽⁵²⁾

$$A_{aa'}^2 = A_{aa} A_{a'a'}. \quad \text{All parameters have dimensions of GeV.}$$

The predictions for the processes $\rho \rightarrow \pi\gamma$ and $\omega \rightarrow \pi\gamma$ are virtually independent of ρ , $\Gamma(\omega \rightarrow \pi\gamma)$ being consistently smaller than experiment while $\Gamma(\rho \rightarrow \pi\gamma)$ is consistently larger. As all form factors and overlap integrals are assumed to be unity in these calculations this former result is somewhat disappointing since radial mixing is expected to give values less than unity for these quantities which will further reduce the magnitude of the predicted decay widths. The predicted values of $\Gamma(\eta' \rightarrow \rho\gamma)$ and $\Gamma(\eta' \rightarrow \omega\gamma)$ also exceed those measured, however, there is some uncertainty in the value of the η' total width⁽⁶¹⁾ used to calculate the experimental results, only two^(96,97) determinations of this quantity having been made at the present time. Of the

remaining measured widths, those of the processes $\omega \rightarrow \eta\gamma$ and $\rho \rightarrow \eta\gamma$ provide a choice of values corresponding to the destructive and constructive interference solutions of the experimental analysis⁽⁹⁸⁾. A clear preference is shown for the constructive solution. These two decays and that for $\phi \rightarrow \eta\gamma$ are strongly dependent upon the magnitude of the $u\bar{u}$, $d\bar{d}$ and $s\bar{s}$ components of the η wavefunction, and hence upon the value of ρ . Comparing the predictions displayed in Table 4.6 with the corresponding experimental values, indicates an overall preference for a value of ρ smaller than the 5.9 Crystal Ball determination, although this value is not entirely ruled out.

A further experimental indicator⁽⁹⁰⁾ of the structure of η - η' mixing is provided by the ratio of the squares of the amplitudes for high energy η and η' production in the processes $\pi^- p \rightarrow \eta n$ and $\pi^- p \rightarrow \eta' n$, that is,

$$\frac{\sigma(\pi^- p \rightarrow \eta' n)}{\sigma(\pi^- p \rightarrow \eta n)} \quad (4.14)$$

Such processes are calculated in the radial mixing model in much the same manner as the ground state mixing model. Using the wavefunction notation described in (4.9) and (4.11) the amplitude for a general charge exchange process $P_1 X \rightarrow P_2 X'$ (where P_1 and P_2 are pseudoscalar mesons and X and X' appropriate baryons) is

$$A(P_1 X \rightarrow P_2 X') = \frac{1}{2} \sum_i \left[g_i b_i A_1 + g_i a_i A_2 \right] \quad (4.15)$$

where A_1 and A_2 are amplitudes describing the possible quark transitions $d \rightarrow u$ and $\bar{u} \rightarrow \bar{d}$. Isospin conservation implies $a_i = b_i$ so the ratio of amplitudes corresponding to (4.14) can be written

$$\frac{A(\pi^- p \rightarrow \eta' n)}{A(\pi^- p \rightarrow \eta n)} = \frac{\sum_i g_i^{\pi^- \eta'} a_i}{\sum_i g_i^{\pi^- \eta} a_i} \quad (4.16)$$

assuming that the amplitudes A_1 and A_2 are independent of radial excitation quantum number n .

The predictions for the ratio (4.14), which reflects the magnitude of the non-strange components of the η and η' wavefunctions are compared with experiment in Table 4.6. The value quoted here is a determination by Stanton et al⁽⁹⁴⁾ at $P_L = 8.45$ GeV/c where an extrapolation is made for this ratio from $t' > 0$ to $t' = 0$ as required by the quark model analysis. This result severely limits the values of ρ allowed, the $\rho = 2.8$ and $\rho = 3.54$ fits alone being compatible with experiment. A value of $\rho = 3.1$ would produce exact agreement, a conclusion which is in line with the inferences drawn from the evidence on radiative transitions. The model predictions for radiative decays and the ratio of production processes (4.14) thus indicate a preference for a smaller rather than larger value of ρ .

4.3 HADRONIC INTERACTIONS

The validity of the description of meson structure given by the linear mass mixing model is tested further by making a comparison of model predictions for isoscalar meson production and strong decay processes with present experimental data. Methods for calculating amplitudes for the strong decay mechanisms $V \rightarrow PP$ and $V \rightarrow VP$ are developed using a simple additive quark model approach and their precision tested with the known experimental $V \rightarrow PP$ widths. Subsequent predictions are made for ratios of decay widths for the first radially excited vector mesons.

4.3.1 Isoscalar Production Processes

The disagreement between the predictions of conventional ground-state mixing models and experimental measurements for sum rules involving strong production processes has been used as evidence⁽⁵⁶⁾ for the possibility of radial mixing in meson wavefunctions. The modifications made by such mixing have subsequently been analysed in the framework of both linear and quadratic models by Cohen and Lipkin⁽⁵⁹⁾. They find, for the linear model

(which is of interest here), that the conventional strangeness exchange sum rule (1.32) becomes,

$$\bar{\sigma}(k^- p \rightarrow \Lambda \eta) + 1.7 \bar{\sigma}(k^- p \rightarrow \Lambda \eta') = 0.9 \bar{\sigma}(k^- p \rightarrow \Lambda \pi^0) + 1.1 \bar{\sigma}(\pi^- p \rightarrow \Lambda k^0) \quad (4.17)$$

Taking experimental values for the $\bar{\sigma}$'s found by Aguilar-Benitez^(59,99) et al

$$\begin{aligned} \bar{\sigma}(k^- p \rightarrow \Lambda \eta) &= 236 \pm 55 \mu\text{b}/\text{GeV}^2 \\ \bar{\sigma}(k^- p \rightarrow \Lambda \eta') &= 469 \pm 73 \mu\text{b}/\text{GeV}^2 \\ \bar{\sigma}(k^- p \rightarrow \Lambda \pi^0) &= 576 \pm 52 \mu\text{b}/\text{GeV}^2 \\ \bar{\sigma}(\pi^- p \rightarrow \Lambda k^0) &= 545 \pm 28 \mu\text{b}/\text{GeV}^2 \end{aligned} \quad (4.18)$$

these modifications are seen to be just those required to produce agreement between the left-hand side (l.h.s) and right-hand side (r.h.s) of (4.17). The results can be summarised as follows,

(a) Conventional sum rule (1.32) : l.h.s. = 705, r.h.s. = 1121

(b) Modified sum rule (4.17) : l.h.s. = 1033, r.h.s. = 1129.

The magnitude of the l.h.s. of the sum rule is increased by the factor 1.7 which multiplies $\bar{\sigma}(k^- p \rightarrow \Lambda \eta')$, while the r.h.s. remains relatively unchanged. The inclusion of symmetry breaking in the annihilation and hyperfine splitting strengths changes the sum rule further, again increasing the r.h.s., to give (for the $\rho = 2.8$ fit)

$$\bar{\sigma}(k^- p \rightarrow \Lambda \eta) + 1.9 \bar{\sigma}(k^- p \rightarrow \Lambda \eta') = 0.9 \bar{\sigma}(k^- p \rightarrow \Lambda \pi^0) + 1.1 \bar{\sigma}(\pi^- p \rightarrow \Lambda k^0) \quad (4.19)$$

The result is a further improvement, with l.h.s. = 1127 $\mu\text{b}/\text{GeV}^2$ and r.h.s. = 1118 $\mu\text{b}/\text{GeV}^2$.

Other sum rules have not been analysed so closely and at present experimental data is unable to distinguish between the results of the conventional ground-state and radial mixing schemes. Additional relationships between isoscalar production amplitudes are amenable to investigation, however, the ratio $\bar{\sigma}(\pi^- p \rightarrow \eta' n) / \bar{\sigma}(\pi^- p \rightarrow \eta n)$ being one such example. The magnitude of this quantity and its relationship to the radiative ratio ρ have been analysed in detail in section 4.2, where, for $\rho = 2.8$

$$\frac{\bar{\sigma}(\pi^- p \rightarrow \eta' n)}{\bar{\sigma}(\pi^- p \rightarrow \eta n)} = 0.59 \quad (4.20)$$

Calculations of similar ratios for η' to η production amplitudes in other charge exchange processes follow an identical pattern to (4.20) allowing a universal constant for all processes to be defined⁽¹⁰⁰⁾

$$\frac{\bar{\sigma}(M + X \rightarrow \eta' X')}{\bar{\sigma}(M + X \rightarrow \eta X')} = K_p \quad (4.21)$$

where M is the incident meson and X and X' are initial and final state baryons which partake in the reaction. This process independent relation is only true when M , X and X' do not contain strange quarks, the values of the individual amplitudes being determined by the overlap between M and the non-strange components of the η and η' wavefunctions. The model determination of (4.21) is chosen from the $\rho = 2.8$ fit to be

$$K_p = 0.59$$

Experimental values of K_p are available for a variety of processes, the most significant result being that for $\bar{\sigma}(\pi^- p \rightarrow \eta' n) / \bar{\sigma}(\pi^- p \rightarrow \eta n)$ due to Stanton et al⁽⁹⁴⁾, who find this ratio to be constant at $K_p = 0.65 \pm 0.13$ over the

π^- momentum range $P_L = 3.8 - 200$ GeV/c. Other experimental results are ⁽¹⁰⁰⁾,

$$\frac{\bar{\sigma}(\pi^+ p \rightarrow \eta' \Delta^{++})}{\bar{\sigma}(\pi^+ p \rightarrow \eta \Delta^{++})} = \begin{array}{l} 0.40 \pm 0.18^{(101)}, P_L = 3.65 \text{ GeV/c} \\ 0.24 \pm 0.11^{(102)}, P_L = 5.45 \text{ GeV/c} \\ 0.70 \pm 0.40^{(103)}, P_L = 8.0 \text{ GeV/c} \end{array}$$

$$\frac{\bar{\sigma}(\pi^- p \rightarrow \eta' \Delta^0)}{\bar{\sigma}(\pi^- p \rightarrow \eta \Delta^0)} = 0.25 \pm 0.025^{(104)}, P_L = 7.1 \text{ GeV/c}$$

$$\frac{\bar{\sigma}(\pi^+ n \rightarrow \eta' p)}{\bar{\sigma}(\pi^+ n \rightarrow \eta p)} = \begin{array}{l} 0.27 \pm 0.06^{(105)}, P_L = 1.56 - 2.10 \text{ GeV/c} \\ 0.56 \pm 0.28^{(105)}, P_L = 2.10 - 2.22 \text{ GeV/c} \end{array}$$

Again, agreement with the model prediction is reasonable in most cases, however, higher energy determinations of these quantities would provide a more reliable test of (4.21).

Analogous ratios have been calculated for vector meson production processes, where the ratio of ϕ to ω production amplitudes also defines a universal constant,

$$K_V \equiv \frac{\bar{\sigma}(V + X \rightarrow \phi + X')}{\bar{\sigma}(V + X \rightarrow \omega + X')} \quad (4.22)$$

where V is the incident vector meson and X and X' the initial and final state baryons. The model evaluation of this quantity is again determined by the overlap of the non-strange components of the initial and final state meson wavefunctions but unlike K_p , K_V is virtually independent of ρ . It is, however, very sensitive to the magnitude of the vector annihilation strengths and, as pointed out by Okubu ⁽¹⁰⁰⁾ provides a useful measure of OZI rule violations. Its value is predicted as

$$K_V = 7.4 \times 10^{-4}$$

an order of magnitude smaller than most present experimental results,

$$\frac{\bar{\sigma}(\pi^- p \rightarrow \phi n)}{\bar{\sigma}(\pi^- p \rightarrow \omega n)} = 0.0035^{(106)} \pm 0.0015$$

$$\begin{aligned} \frac{\bar{\sigma}(\pi^+ n \rightarrow \phi p)}{\bar{\sigma}(\pi^+ n \rightarrow \omega p)} &= 0.021^{(107)} \pm 0.011, \quad P_L = 1.54 - 2.6 \text{ GeV/c} \\ &< 0.02^{(108)}, \quad P_L = 5.1 \text{ GeV/c} \\ &< 0.06^{(109)}, \quad P_L = 5.4 \text{ GeV/c} \end{aligned}$$

$$\begin{aligned} \frac{\bar{\sigma}(\pi^+ p \rightarrow \phi \Delta^{++})}{\bar{\sigma}(\pi^+ p \rightarrow \omega \Delta^{++})} &< 0.0033^{(110)}, \quad P_L = 3.7 \text{ GeV/c} \\ &\approx 0.024^{(111)}, \quad P_L = 8.0 \text{ GeV/c} \end{aligned}$$

4.3.2 Strong Decay Processes

The two body final state hadronic decay processes of both ground-state and the first radially excited state vector mesons are investigated with a view to determining relationships between the decay amplitudes of the excited states. A naive procedure is adopted in which the quark model additivity assumption is used to decompose the meson decay amplitudes in terms of a sum of quark amplitudes describing strong $q\bar{q}$ production subprocesses. As an example, consider $\rho \rightarrow 2\pi$ decay which can proceed via strong $u\bar{u}$ or $d\bar{d}$ production as shown in Fig. 4.4. The amplitude for the decay

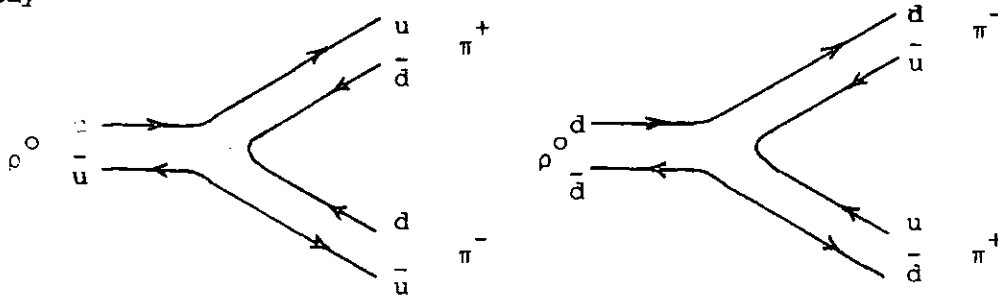


Fig 4.4 : Possible quark sub-processes describing $\rho \rightarrow 2\pi$

is given by :

$$\langle \rho^0 | \pi^+ \pi^- \rangle = \frac{1}{\sqrt{2}} \left[\langle u\bar{u} | (u\bar{d})(\bar{d}u) \rangle - \langle d\bar{d} | (u\bar{d})(\bar{d}u) \rangle \right] \quad (4.23)$$

where, for simplicity the particle wavefunctions

$$\rho^0 = \frac{1}{\sqrt{2}} (u\bar{u} - d\bar{d})$$

$$\pi^+ = u\bar{d} \tag{4.24}$$

$$\pi^- = d\bar{u}$$

have been assumed and $\langle u\bar{u} | (u\bar{d})(d\bar{u}) \rangle$ and $\langle d\bar{d} | (u\bar{d})(d\bar{u}) \rangle$ represent amplitudes describing the strong production of $d\bar{d}$ and $u\bar{u}$ quark combinations respectively. In the radial mixing model the coefficients accompanying these amplitudes will take on different values but it is assumed that the amplitudes themselves will remain unchanged. This property is exploited by first calculating relations amongst the amplitudes using meson vertex and SU(3) selection rules and then using these relations in the radial mixing approach. In this manner a quantitative estimate of the effect of radial mixing upon vector meson decay rates can be made.

The procedure adopted in the following analysis will be to firstly test this method of calculation by its application to the known decay couplings $g_{\rho\pi\pi}$, $g_{\phi k\bar{k}}$ and $g_{k^*k\pi}$ and then, accepting its validity calculate relations between (i) $V' \rightarrow PP$ couplings and (ii) $V' \rightarrow VP$ couplings. It is unknown at present how the amplitudes for the processes (i) and (ii) are related so each case must be treated separately.

(i) $V \rightarrow PP$

The relations required between quark pair creation amplitudes which will allow quantitative predictions of $V \rightarrow PP$ meson couplings are obtained by examining the properties of SU(3) wavefunctions, denoted in

the usual manner by,

$$\begin{array}{cccc}
 \pi^+ & & \pi^0 & & \pi^- \\
 = u\bar{d} & & = \frac{1}{\sqrt{2}}(u\bar{u}-d\bar{d}) & & = d\bar{u} \\
 \rho^+ & & \rho^0 & & \rho^- \\
 \\
 K^+ & & K^0 & & \bar{K}^0 & & K^- \\
 = u\bar{s} & & = d\bar{s} & & = s\bar{d} & & = s\bar{u} \\
 K^{*+} & & K^{*0} & & \bar{K}^{*0} & & K^{*-}
 \end{array} \quad (4.25)$$

$$\begin{array}{cc}
 \eta_8 & \eta_0 \\
 = -\frac{1}{\sqrt{6}}(u\bar{u}+d\bar{d}-2s\bar{s}) & = \frac{1}{\sqrt{3}}(u\bar{u}+d\bar{d}-2s\bar{s}) \\
 \omega_8 & \omega_0
 \end{array}$$

With this notation the G-parity violating coupling $g_{\omega\pi^+\pi^-}$ gives

$$g_{\omega\pi^+\pi^-} = 0 \text{ implies } \langle u\bar{u} | (u\bar{d})(d\bar{u}) \rangle = - \langle d\bar{d} | (u\bar{d})(d\bar{u}) \rangle \quad (4.26)$$

Similar relations are obtained from other couplings, in particular

$$g_{\omega\pi^0\pi^0} = g_{\omega\pi^0\eta_8} = 0 \text{ implies}$$

$$\langle u\bar{u} | (u\bar{u})(u\bar{u}) \rangle = \langle d\bar{d} | (d\bar{d})(d\bar{d}) \rangle = 0 \quad (4.27)$$

Amplitudes involving the production of $s\bar{s}$ quark pairs can be investigated by noting that the U-spin (and V-spin) singlet state ω_0 cannot decay⁽¹¹²⁾ into $k^0\bar{k}^0$ or k^+k^- ,

$$\begin{array}{l}
 g_{\omega_0 k^+k^-} = 0 \text{ implies } \langle u\bar{u} | (u\bar{s})(s\bar{u}) \rangle = - \langle s\bar{s} | (u\bar{s})(s\bar{u}) \rangle \\
 g_{\omega_0 k^0\bar{k}^0} = 0 \text{ implies } \langle d\bar{d} | (d\bar{s})(s\bar{d}) \rangle = - \langle s\bar{s} | (d\bar{s})(s\bar{d}) \rangle
 \end{array} \quad (4.28)$$

Isospin allows these to be connected through $g_{\omega_8 k^+ k^-} = -g_{\omega_8 k^0 \bar{k}^0}$ giving

$$\langle s\bar{s} | (u\bar{s})(s\bar{u}) \rangle = - \langle s\bar{s} | (d\bar{s})(s\bar{d}) \rangle \quad (4.29)$$

The amplitudes of (4.26) involving just u and d quarks are related to those of (4.28) involving s quarks through symmetry properties, thus the SU(3) results⁽¹¹³⁾

$$\begin{aligned} \langle k^{*0} | k^0 \pi^0 \rangle &= -\frac{1}{\sqrt{2}} \langle \rho^0 | \pi^+ \pi^- \rangle : \langle \bar{k}^{*0} | k^- \pi^+ \rangle = -\frac{1}{\sqrt{2}} \langle \rho^0 | \pi^+ \pi^- \rangle \\ \langle \rho^0 | \pi^+ \pi^- \rangle &= 2 \langle \frac{1}{2} \rho^0 + \frac{\sqrt{3}}{2} \omega_8 | k^+ k^- \rangle \end{aligned}$$

give

$$\begin{aligned} \langle d\bar{s} | (d\bar{s})(d\bar{d}) \rangle &= \langle u\bar{u} | (u\bar{d})(d\bar{u}) \rangle \\ \langle s\bar{d} | (s\bar{u})(u\bar{d}) \rangle &= -\langle u\bar{u} | (u\bar{d})(d\bar{u}) \rangle \end{aligned} \quad (4.30)$$

and

$$\langle d\bar{d} | (u\bar{d})(d\bar{u}) \rangle = -\langle s\bar{s} | (u\bar{s})(s\bar{u}) \rangle$$

respectively. Also, the isospin relations

$$\langle k^{*0} | k^+ \pi^- \rangle = -\sqrt{2} \langle k^{*0} | k^0 \pi^0 \rangle = -\langle k^{**} | k^0 \pi^+ \rangle$$

$$\text{imply } \langle d\bar{s} | (d\bar{s})(d\bar{d}) \rangle = \langle d\bar{s} | (u\bar{s})(d\bar{u}) \rangle = -\langle u\bar{s} | (d\bar{s})(u\bar{d}) \rangle \quad (4.31)$$

Denoting $\langle d\bar{d} | (u\bar{d})(d\bar{u}) \rangle = A$ the assignments in Table 4.8 can be made.

$\langle u\bar{u} (u\bar{d})(d\bar{u}) \rangle = -A$	$\langle d\bar{d} (u\bar{d})(d\bar{u}) \rangle = A$
$\langle s\bar{s} (u\bar{s})(s\bar{u}) \rangle = -A$	$\langle u\bar{u} (u\bar{s})(s\bar{u}) \rangle = A$
$\langle s\bar{s} (d\bar{s})(s\bar{d}) \rangle = A$	$\langle d\bar{d} (d\bar{s})(s\bar{d}) \rangle = -A$
$\langle d\bar{s} (d\bar{s})(d\bar{d}) \rangle = -A$	$\langle s\bar{d} (s\bar{u})(u\bar{d}) \rangle = A$
$\langle d\bar{s} (u\bar{s})(d\bar{u}) \rangle = -A$	$\langle u\bar{s} (d\bar{s})(u\bar{d}) \rangle = A$

TABLE 4.8 : Quark production amplitudes for $V \rightarrow PP$ processes.

That the results of Table 4.8 are correct can be checked using the SU(3) predictions^(112,113)

$$\langle k^{*0} | k^+ \pi^- \rangle = \frac{1}{\sqrt{2}} \langle \rho^0 | \pi^+ \pi^- \rangle \quad ; \quad |\langle k^{*0} | k^+ \pi^- \rangle|^2 + |\langle k^{*0} | k^0 \pi^0 \rangle|^2 = \frac{3}{4} |\langle \rho^0 | \pi^+ \pi^- \rangle|^2$$

$$\sqrt{3} \langle \rho^0 | k^0 \bar{k}^0 \rangle = \langle \omega_8 | k^0 \bar{k}^0 \rangle \quad ; \quad \langle \omega_8 | k^+ k^- \rangle = -\langle \omega_8 | k^0 \bar{k}^0 \rangle \quad (4.32)$$

$$\langle \omega_8 | k^+ k^- \rangle = \frac{\sqrt{3}}{2} \langle \rho^0 | \pi^+ \pi^- \rangle$$

which are all reproduced by these amplitudes.

In order to find connections between the couplings of physical vector mesons it is necessary to assume that all the symmetry breaking involved in transforming from an SU(3) basis to the physical basis is manifest in the coefficients appearing in the particle wave functions and that the $q\bar{q}$ production amplitudes as expressed in Table 4.8 remain unchanged. To what extent this assumption is correct can be gauged by examining predictions for the vector to pseudoscalar decay widths. With the wavefunction notation of (4.9) and (4.11) the allowed $V \rightarrow PP$ couplings can be expressed as

$$g_{\rho \pi^+ \pi^-} = -2 \sum_i \alpha_i^{\rho^0} (a_i^{\pi^+})^2 A$$

$$g_{\phi k^+ k^-} = - \sum_i \left[\gamma_i^\phi - \alpha_i^\phi \right] \left\{ g_i^{k^+} \right\}^2 A \quad (4.33)$$

$$\bar{g}_{k^{*+} k^0 \pi^+} = \sum_i f_i^{k^{*+}} g_i^{k^0} a_i^{\pi^+} A = -\sqrt{2} g_{k^{*+} k^+ \pi^0}$$

The radial mixing model wavefunctions for the $\rho = 2.8$ fit (Appendix 3) give the numerical results

$$\begin{aligned}
 g_{\rho\pi^+\pi^-} &= -1.16 A \\
 g_{\phi k^+k^-} &= -0.87 A \\
 g_{k^{*+}k^0\pi^+} &= 0.87 A
 \end{aligned}
 \tag{4.34}$$

predicting couplings in the ratio

$$g_{\rho\pi^+\pi^-}^2 : g_{\phi k^+k^-}^2 : g_{k^{*+}k^0\pi^+}^2 = 3.6 : 2.0 : 2.0
 \tag{4.35}$$

In a ground-state, ideal mixing model these ratios are 4.0 : 2.0 : 2.0.

The decay width for $V \rightarrow PP$ processes is given by⁽¹¹⁴⁾

$$\Gamma(V \rightarrow P_1 P_2) = \frac{2}{3} \frac{g_{VP_1 P_2}^2}{4\pi} \cdot \frac{k^3}{M_V^2}
 \tag{4.36}$$

where K , the centre of mass momentum of P is

$$k^2 = \frac{\left[M_V^2 - (M_1 + M_2)^2 \right] \left[M_V^2 - (M_1 - M_2)^2 \right]}{4M_V^2}
 \tag{4.37}$$

with M_1 and M_2 the masses of P_1 and P_2 . Predictions for the allowed two-body decay widths of the ρ , ϕ and k^* can now be made in terms of the as yet unknown amplitude,

$$\begin{aligned}
 \Gamma(\rho \rightarrow 2\pi) &= 5.54 A^2 \\
 \Gamma(\phi \rightarrow k^+k^-) &= 0.076 A^2 \\
 \Gamma(k^{*+} \rightarrow k^0\pi^+) &= 1.20 A^2
 \end{aligned}
 \tag{4.38}$$

Determining A^2 from the ρ width, $\Gamma_{\text{tot}}(\rho) = 158 \pm 5 \text{ MeV}^{(61)}$, to be

$$A^2 = 28.5 \quad (4.39)$$

provides the numerical results

$$\begin{aligned} \Gamma(\phi \rightarrow k^+ k^-) &= 2.17 \text{ MeV} \\ \Gamma(k^{*+} \rightarrow k^0 \pi^+) &= 34.20 \text{ MeV} \end{aligned} \quad (4.40)$$

Experiment ⁽⁶¹⁾ gives $\Gamma(\phi \rightarrow k^+ k^-) \approx 2.0 \text{ MeV}$ and $\Gamma(k^{*+} \rightarrow k \pi) \approx \Gamma_{\text{tot}}(k^{*+}) = 50.3 \text{ MeV}$.

For the processes considered here this latter value is constructed from the sum

$$\Gamma(k^{*+} \rightarrow k^0 \pi^+) + \Gamma(k^{*+} \rightarrow k^+ \pi^0) = \frac{3}{2} \Gamma(k^{*+} \rightarrow k^0 \pi^+) = 51.3 \text{ MeV} \quad (4.41)$$

in this model. In a ground-state, ideal mixing model the results would have been

$$\begin{aligned} \Gamma(\phi \rightarrow k^+ k^-) &= 1.95 \text{ MeV} \\ \Gamma(k^{*+} \rightarrow k^0 \pi^+) + \Gamma(k^{*+} \rightarrow k^+ \pi^0) &= 46.2 \text{ MeV} \end{aligned} \quad (4.42)$$

These predictions are sufficiently close to experimental values to justify a further investigation of the decay of radial states, using the same method.

The two body decays $\rho' \rightarrow 2\pi$, $\phi' \rightarrow k^+ k^-$ and $k^{*+'} \rightarrow k^0 \pi^+$ are treated in just the same manner as their ground-state counterparts to give

$$\begin{aligned} g_{\rho \pi \pi} &= -2 \sum_i \alpha_i^{\rho'} (g_i^{\pi^+})^2 A \\ g_{\phi k^+ k^-} &= - \sum_i \left[\gamma_i^{\phi'} - \alpha_i^{\phi'} \right] \left\{ g_i^{k^+} \right\}^2 A \\ g_{k^{*+'} k^0 \pi^+} &= \sum_i f_i^{k^{*+'}} g_i^{k^0} g_i^{\pi^+} A \end{aligned} \quad (4.43)$$

Also,

$$g_{\omega' k \bar{k}} = \sum_i \left[\alpha_i^{\omega'} - \gamma_i^{\omega'} \right] (a_i^k)^2 A$$

Again, the $\rho = 2.8$ results give numerical values

$$\begin{aligned}
 g_{\rho \pi\pi} &= -0.27 A \\
 g_{\phi' k\bar{k}} &= -0.13 A & g_{\omega' k\bar{k}} &= 0.11 A \\
 g_{k^{*+} k^0 \pi^+} &= 0.15 A
 \end{aligned} \tag{4.44}$$

which, with the predicted masses $M_{\rho'} = 1.33$ GeV, $M_{\phi'} = 1.59$ GeV, $M_{k^{*+}} = 1.45$ GeV give the ratio of decay widths

$$\begin{aligned}
 \Gamma(\rho' \rightarrow \pi\pi) : \Gamma(\phi' \rightarrow k\bar{k}) : \Gamma(k^{*+} \rightarrow k^0 \pi^+) : \Gamma(\omega' \rightarrow k\bar{k}) \\
 = 6.6 : 1 : 1.5 : 0.4
 \end{aligned} \tag{4.45}$$

(ii) V → VP

The approach to $V \rightarrow VP$ decay widths follows that of the previous $V \rightarrow PP$ treatment. Amplitudes for quark subprocesses are first related using G-parity and SU(3) results. The G-parity violating couplings $g_{\rho \rho^+ \pi^-}$ and $g_{\omega\omega\pi}$ give

$$\langle u\bar{u} | (u\bar{d}) (d\bar{u}) \rangle = \langle d\bar{d} | (u\bar{d}) (d\bar{u}) \rangle \tag{4.46}$$

$$\text{and } \langle u\bar{u} | (u\bar{u}) (u\bar{u}) \rangle = \langle d\bar{d} | (d\bar{d}) (d\bar{d}) \rangle$$

respectively, while the required SU(3) result

$$\langle \omega_8 | \rho^+ \pi^- \rangle = 2 \langle \omega_8 | k^{*+} k^- \rangle \tag{4.47}$$

relates the $u\bar{u}$, $d\bar{d}$ and $s\bar{s}$ production amplitudes

$$\langle u\bar{u} | (u\bar{s}) (s\bar{u}) \rangle = \langle s\bar{s} | (u\bar{s}) (s\bar{u}) \rangle = -\langle u\bar{u} | (u\bar{d}) (d\bar{u}) \rangle \tag{4.48}$$

The final connection is given by isospin where $\langle \omega_8 | \rho^+ \pi^- \rangle = - \langle \omega_8 | \rho^0 \pi^0 \rangle$ results in

$$\langle u\bar{u} | (u\bar{d}) (d\bar{u}) \rangle = - \langle u\bar{u} | (u\bar{u}) (u\bar{u}) \rangle \quad (4.49)$$

As before these amplitudes can be expressed in terms of a common amplitude A_V to give the assignments of Table 4.9. These can be checked with the SU(3) results

$$\langle \rho | k^{*+} k^- \rangle = \sqrt{3} \langle \omega_8 | k^{*+} k^- \rangle \quad (4.50)$$

and $\langle \omega_0 | \rho^+ \pi^- \rangle = - \langle \omega_0 | k^{*+} k^- \rangle$

which are reproduced in this notation.

$\langle u\bar{u} (u\bar{d}) (d\bar{u}) \rangle = A_V$	$\langle d\bar{d} (u\bar{d}) (d\bar{u}) \rangle = A_V$
$\langle u\bar{u} (u\bar{u}) (u\bar{u}) \rangle = A_V$	$\langle d\bar{d} (d\bar{d}) (d\bar{d}) \rangle = - A_V$
$\langle u\bar{u} (u\bar{s}) (s\bar{u}) \rangle = - A_V$	$\langle s\bar{s} (u\bar{s}) (s\bar{u}) \rangle = - A_V$

TABLE 4.9 : Quark production amplitudes for $V \rightarrow VP$ processes.

Assuming, as before, that when the transition is made to the basis of physical states these amplitudes remain unchanged allows relations to be derived between the decay widths for $\rho' \rightarrow \omega \pi^0$, $\omega' \rightarrow \rho^+ \pi^-$ and $\phi' \rightarrow k^* k$. These widths are calculated from the $V' \rightarrow VP$ couplings using

$$\Gamma(V' \rightarrow VP) = \frac{k^3}{12\pi} g_{V'VP}^2 \quad (4.51)$$

with the centre of mass momentum

$$k^2 = \frac{\left[M_{V'}^2 - (M_V + M_P)^2 \right] \left[M_{V'}^2 - (M_V - M_P)^2 \right]}{4 M_{V'}^2} \quad (4.52)$$

With the predicted masses $M_{\rho'} = 1.33 \text{ GeV}$, $M_{\omega'} = 1.34 \text{ GeV}$, $M_{\phi'} = 1.59 \text{ GeV}$ and following the procedure developed in (i) the decay widths are found to be in the ratio

$$\Gamma(\rho' \rightarrow \omega\pi) : \Gamma(\omega' \rightarrow \rho^+\pi^-) : \Gamma(\phi' \rightarrow k^{*+}k^-) = 2.6 : 5.0 : 1.0 \quad (4.53)$$

CHAPTER 5ISOSPIN VIOLATION - THE CONSTITUENT QUARKMODEL APPROACH5.1 INTRODUCTION

The notion of isospin has been used extensively in the theory of nuclear interactions, where it was pointed out by Cassen and Condon⁽¹¹⁵⁾ in 1936 that the ideas of charge independence and charge symmetry (the equality of proton-proton and neutron-neutron interactions) could be neatly encapsulated within the $SU(2)$ algebra of isospin. The idea is simply expressed by saying the strong interactions of the hadrons are invariant with respect to the $SU(2)$ isospin transformations, and so the masses of hadrons belonging to the same isospin multiplet would be identical if all interactions other than the strong interaction could be switched off. Any splitting amongst the masses is then associated with the effects of the electromagnetic interactions which are not invariant under $SU(2)$ transformations.

The principles associated with isospin are repeated at the next level of hadronic structure, that is, at the quark level. The presently known quarks u, d, s, c, b are grouped into isospin multiplets such that (u,d) form a doublet and all the other quarks are isospin singlets. If isospin symmetry is exact the u and d quarks will have equal masses and will behave identically in their strong interactions.

The idea that isospin is a good symmetry of the strong interactions has been challenged by many authors⁽¹¹⁶⁻¹²³⁾ in recent years. Such a symmetry violation would be manifest in the difference expected between the u and d quark masses, the magnitude of this difference representing directly the magnitude of the violation. In section 5.2, the definitions of the

term "quark mass" are examined in terms of the current algebra and constituent quark pictures of hadronic structure and their possible connection is outlined. This is followed by an account in 5.3 of present quantitative estimates of the isospin violating mass difference $\Delta \equiv m_d - m_u$ which in 5.4 is introduced to the linear radial mixing model where its magnitude is confirmed by making a comparison of the model prediction for pseudoscalar isomultiplet mass differences with experiment. This determination allows a prediction for the isospin violating ratio $\Gamma(\psi' \rightarrow \pi^0 \psi) / \Gamma(\psi' \rightarrow \eta \psi)$ to be made.

5.2 QUARK MASSES

Of the many different attempts made to describe hadronic structure those involving the constituent quark model and current algebra techniques are of interest here. Before the advent of QCD as a viable theory of the strong interactions these two approaches produced mass relations among the quarks which were quite incompatible. The PCAC techniques of current algebra can be used to predict the quark mass ratio⁽¹²¹⁻¹²³⁾

$$\left\{ \frac{m_u + m_d}{2m_s} \right\}_{\text{curr.}} \approx \frac{M_\pi^2}{2M_K^2} \approx 0.04 \quad (5.1)$$

however, constituent quark masses, as determined by the radial mixing model, for example, give the quite different value of

$$\left\{ \frac{m_u + m_d}{2m_s} \right\}_{\text{constit.}} \approx 0.7 \quad (5.2)$$

The incompatibility of these pictures led to the distinction between current and constituent masses.

Conventionally a particle mass is defined by a pole in the particle propagator, however, there is a problem when dealing with quarks, for they may be confined, in which case their masses will not be directly measurable by experiment and must be inferred by using an indirect approach, for example, by examining the properties of bound states and their interactions. The mass determined in such a manner will be dependent upon the model used for the analysis.

The constituent quark mass is difficult to define precisely⁽¹²¹⁾ for this very reason ; it depends upon the dynamical details of the models in which it is used. It can be taken, in an approximate sense, as the mass of a quark as it makes its appearance in a hadron in a free quark model, then

$$\begin{aligned}
 m_u^{\text{constit.}} &\approx m_d^{\text{constit.}} \approx \frac{1}{2} M_\rho \approx \frac{1}{3} M_p \approx 330 \text{ MeV} \\
 m_s^{\text{constit.}} &\approx \frac{1}{2} M_\phi \approx 510 \text{ MeV} \\
 m_c^{\text{constit.}} &\approx \frac{1}{2} M_\psi \approx 1.55 \text{ GeV} \\
 m_b^{\text{constit.}} &\approx \frac{1}{2} M_T \approx 4.7 \text{ GeV}
 \end{aligned}
 \tag{5.3}$$

In contrast current quark masses can be given a precise definition in terms of the divergences of the vector and axial vector currents⁽³³⁾,

$$\begin{aligned}
 \partial_\mu^\mu V_\mu^\alpha(x) &= i\bar{q}(x) \left[M, \frac{1}{2} \lambda^\alpha \right] q(x) \\
 \partial_\mu^\mu A_\mu^\alpha(x) &= i\bar{q}(x) \left\{ M, \frac{1}{2} \lambda^\alpha \right\} \gamma_5 q(x)
 \end{aligned}
 \tag{5.4}$$

where

$$q(x) = \begin{pmatrix} u(x) \\ d(x) \\ s(x) \end{pmatrix}$$

and M is the quark mass matrix

$$M = \begin{pmatrix} m_u & 0 & 0 \\ 0 & m_d & 0 \\ 0 & 0 & m_s \end{pmatrix}$$

In order to examine the differences and any connection between these definitions a framework is required in which to discuss them ; such a framework is provided by QCD. The quark mass term which appears in the QCD Lagrangian(1.37) is the bare current quark mass and is the only term which explicitly breaks the chiral $SU(n) \times SU(n)$ symmetry (with n flavours), while still maintaining renormalisability⁽¹²⁴⁾. In any renormalisable theory the mass of the quark depends upon the energy at which it is defined. In perturbative QCD this variation with energy is described as a function of Q^2 (momentum transfer) by⁽¹²⁵⁾

$$\bar{m}_i(Q^2) = Z m_i^0 \quad (5.5)$$

where m_i^0 is the bare mass which appears in (1.37) and Z^{-1} is the factor which renormalises $\bar{q}q$ in the massless theory⁽¹²⁶⁾. When treated perturbatively in this manner the masses take on the role of additional effective coupling constants which appear in the renormalisation group equation, giving, to first order⁽¹²⁶⁾

$$\frac{\partial \bar{m}}{\partial t} = \bar{m} \gamma_m(\bar{g}, \bar{m}/\mu) \quad (5.6)$$

where

$$t \equiv \frac{1}{2} \ln \left\{ \frac{Q^2}{\mu^2} \right\}, \quad \gamma_{m_i} \approx - \frac{g^2}{2\pi} \left[1 + \frac{c m_i^2}{\mu^2} \right]^{-1} \quad (5.7)$$

Also, to first order, the dimensionless coupling is given by

$$g^2 = \frac{48\pi^2}{(33-2n_f) \ln(Q^2/\Lambda^2)} \tag{5.8}$$

for n_f quark flavours, where Λ sets the renormalisation group invariant scale.

The solution of (5.6) depends upon the values taken by g and m_i at the renormalisation point μ . If these boundary conditions are fixed at ⁽¹²⁶⁾

$$m_u(\mu) \approx m_d(\mu) = 0.02 \text{ GeV} ; m_s(\mu) = 0.4 \text{ GeV} ; m_c(\mu) = 1.5 \text{ GeV} \tag{5.9}$$

for $\mu = 3.0 \text{ GeV}$, giving $g^2(\mu)/4\pi = 0.5$ then the solution of (5.6) appears as shown in Fig 5.1 ⁽¹²⁷⁾. Since this result is produced from lowest order perturbation theory, its implications should be treated with caution as $g^2/4\pi$ becomes large.

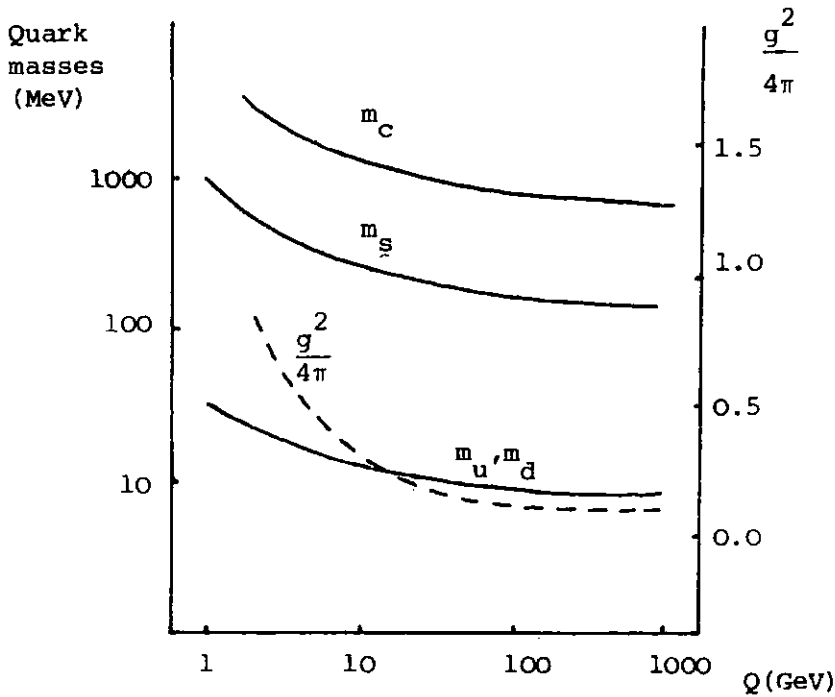


Fig 5.1 : Variation of quark mass with energy.

A further problem arises at low Q^2 . As has been noted, in a massless theory the QCD Lagrangian is invariant under chiral $SU(3) \times SU(3)$ transformations, however, this symmetry appears to be spontaneously broken^(121,128) with $\langle O | \bar{q}q | O \rangle$ taking on non-zero values. The full quark mass then receives a non-perturbative contribution⁽¹²⁹⁾ which is found to be important only for small values of Q^2 . The quark mass, including both the explicit symmetry breaking term given by first order perturbative QCD and the non-perturbative contribution is then⁽¹²⁹⁾

$$m_i(Q^2) = m_{p_i}(Q^2) + m_{NP}(Q^2) \quad (5.10)$$

where $m_{p_i}(Q^2) \sim m_{o_i} (\ln Q^2)^{-12/(33-2n_f)}$ and $m_{NP} \sim \frac{\langle O | \bar{q}q | O \rangle (\ln Q^2)^{-15/(33-2n_f)}}{Q^2}$

with $m_{o_i} \propto m_i$, the explicit mass term appearing in the QCD Lagrangian.

(5.10) represents the full quark mass term which is interpreted loosely⁽¹²⁹⁾ as the constituent quark mass. Accepting (5.10) Politzer⁽¹²⁹⁾ has made rough estimates of the relative sizes of the two terms at finite values of Q^2 .

For the light u and d quarks, the constituent masses should be approximately the same, irrespective of whether $SU(2) \times SU(2)$ is exact or slightly broken by an explicit mass term. Then $m_{NP}(Q^2) \approx 300$ MeV for $Q \approx 700$ MeV. In contrast, for the heavier c quark in the region $Q \approx 3.0$ GeV the non-perturbative contribution is dwarfed by the much larger explicit mass term giving $m_c(Q^2) \approx m_{p_c}(Q^2)$. The s quark lies in between these two extremes, having a small but non-negligible spontaneous contribution. Taking $m_s^{\text{constit.}}$ to be approximately 500 MeV, Politzer finds $m_{p_s} \approx 375$ MeV.

5.3 ISOSPIN VIOLATING MASS DIFFERENCES

The search for evidence of isospin violation has been motivated by the suggestion that isospin is an accidental symmetry^(117,123) in that at the current quark level the bare u and d quark masses are substantially different, while at the constituent level (which provides a reflection of hadron symmetry), upon addition of the non-perturbative contribution, m_u and m_d are approximately equal, leading to an apparent isospin symmetry. The pseudoscalar mass spectrum which, in current algebra, results from the explicit breaking of $SU(3) \times SU(3)$ provides a natural domain in which to search for noticeable effects of an isospin asymmetry. The meson masses are calculated using PCAC techniques to give⁽¹²³⁾

$$M_{\alpha\beta}^2 = \frac{1}{f_\pi^2} \int d^3x d^3y \langle 0 | \left[A_0^\alpha(\vec{x}, 0), \left[A_0^\beta(\vec{y}, 0), H \right] \right] | 0 \rangle \quad (5.11)$$

where the standard definitions

$$A_\mu^\alpha(x) = \bar{q}(x) \gamma_\mu \gamma_5 \frac{1}{2} \lambda^\alpha q(x), \quad \alpha = 1, \dots, 8 \quad (5.12)$$

and

$$\langle 0 | A_\mu^\alpha | \Pi^\beta(p) \rangle = i F_\pi p_\mu \delta_{\alpha\beta} \quad (5.13)$$

have been employed. Assuming that the vacuum expectation values of the bilinear products of quark fields are flavour independent, that is

$$\langle 0 | \bar{u}u | 0 \rangle = \langle 0 | \bar{d}d | 0 \rangle = \langle 0 | \bar{s}s | 0 \rangle \equiv v \quad (5.14)$$

and writing the Hamiltonian, as suggested by QCD, as

$$H = H_0 + m_u \bar{u}u + m_d \bar{d}d + m_s \bar{s}s \quad (5.15)$$

where H_0 is $SU(3) \times SU(3)$ symmetric and the masses provide the symmetry violation, the commutator on the right-hand side of (5.11) is evaluated

to give (Appendix 4)

$$M_{\pi}^2 = -\frac{1}{F_{\pi}^2} (m_u + m_d) V ; \quad M_{K^+}^2 = -\frac{1}{F_{\pi}^2} (m_u + m_s) V ; \quad M_{K^0}^2 = -\frac{1}{F_{\pi}^2} (m_d + m_s) V \quad (5.16)$$

which were first derived by Gell-Mann, Oakes and Renner⁽³⁸⁾.

As they stand these meson (mass)² terms do not include possible electromagnetic contributions. In general⁽¹²⁵⁾

$$\mu_p^2 = M_p^2 + M_Y^2 \quad (5.17)$$

where μ_p represents the physical particle mass and M_Y the electromagnetic mass contribution. These M_Y^2 terms can be eliminated from the problem by appealing to Dashen's theorem⁽¹³⁰⁾, which states that, in the chiral limit

$$M_Y^2(\pi^0) = M_Y^2(K^0) = M_Y^2(\bar{K}^0) = 0 \quad (5.18a)$$

and

$$M_Y^2(\pi^{\pm}) = M_Y^2(K^{\pm}) \quad (5.18b)$$

(5.16) and (5.18) allow the ratios of current quark masses to be evaluated,

$$\frac{m_d}{m_u} = \frac{M_{K^0}^2 - M_{K^+}^2 + M_{\pi^+}^2}{2M_{\pi^0}^2 + M_{K^+}^2 - M_{K^0}^2 - M_{\pi^+}^2} \approx 1.8 \quad (5.19)$$

$$\frac{m_s}{m_d} = \frac{M_{K^0}^2 + M_{K^+}^2 + M_{\pi^+}^2}{M_{K^0}^2 - M_{K^+}^2 + M_{\pi^+}^2} \approx 20 \quad (5.20)$$

(5.19) has also been estimated from experimental data of the baryon mass spectra and $\eta \rightarrow 3\pi$ decay ($m_d/m_u = 2.6$)⁽¹²¹⁾ and $\rho - \omega$ mixing ($m_d/m_u = 2.1$)⁽¹²²⁾. Although there is some discrepancy between these values they do indicate

the isospin symmetry seen at the constituent level of hadron structure is an accidental symmetry and not a reflection of any symmetry at the more fundamental level of current quarks. The apparent symmetry is manifest at the constituent level because the u and d quarks pick up a spontaneous contribution to their masses which, in the energy region where non-strange hadrons are observed, is much larger than the current quark mass.

If the non-perturbative contribution to the constituent quark mass is assumed to be flavour independent then, writing⁽¹¹⁶⁾

$$m_i^{\text{constit.}}(Q^2) = m_i^{\text{curr.}}(Q^2) + m_{\text{NP}}(Q^2) \quad (5.21)$$

the difference $(m_d - m_u)_{\text{constit.}}$ can be estimated by noting

$$\left\{ \frac{m_d - m_u}{m_s - m_d} \right\}_{\text{curr.}} = \left\{ \frac{m_d - m_u}{m_s - m_d} \right\}_{\text{constit.}} = 0.0234 \quad (5.22)$$

using (5.19) and (5.20). Taking constituent quark masses as determined by the radial mixing model gives

$$(m_d - m_u)_{\text{constit.}} \approx 3 \text{ MeV} \quad (5.23)$$

where it has been assumed that the Q^2 dependence of $m_i^{\text{curr.}}(Q^2)$ is independent of i .

5.4 ISOSPIN VIOLATION IN THE RADIAL MIXING MODEL

Observed isospin violations in the spectrum of mesonic states are investigated here in terms of the interactions between their quark constituents in the framework of the radial mixing model developed in Chapter 4. The model is easily extended for this purpose by making the isospin violating additions of

- (i) the strong constituent mass difference $\Delta \equiv m_d - m_u$ and

(ii) electromagnetic Coulombic and hyperfine interaction terms to the Hamiltonian operator. An estimate of the magnitudes of these additions is made by comparing model predictions for the pseudoscalar isomultiplet mass splittings $\pi^+ - \pi^0$, $k^+ - k^0$ and $D^+ - D^0$ with their relatively well determined experimental values. The consequent changes induced in the meson unitary spin wavefunctions are examined by treating (i) and (ii) as perturbations and diagonalising the relevant mass matrices to give isospin violating mixing angles in terms of these additions. The mixing angles allow subsequent evaluation of $\Gamma(\omega \rightarrow 2\pi)$ and the ratio of SU(2) to SU(3) violating processes $\Gamma(\psi' \rightarrow \pi^0 \psi) / \Gamma(\psi' \rightarrow \eta \psi)$.

5.4.1 Isospin Violating Mixing

The linear mass mixing model which was used successfully to describe the mass spectra and decays of vector and pseudoscalar mesons in Chapter 4 is extended by including

$$(i) \quad \Delta = m_d - m_u \text{ and}$$

$$(ii) \quad H_{em} = \alpha_{em} \frac{e_a e_b}{e^2} \left[\frac{1}{r_{ab}} - \frac{8\pi}{3} \frac{\vec{\sigma}_a \cdot \vec{\sigma}_b}{m_a m_b} \delta^3(r_{ab}) \right]$$

$$\equiv e_a e_b \left[a + b \frac{\vec{\sigma}_a \cdot \vec{\sigma}_b}{m_a m_b} \right] \quad (5.24)$$

in the mass matrix

$$\langle q_a, \bar{q}_b, n' | M | q_a, \bar{q}_b, n \rangle = M_{abnn'} \delta_{aa'} \delta_{bb'} + \frac{A_{aa'} \delta_{ab} \delta_{a'b'}}{m_a m_b \sqrt{nn'}}$$

$$\text{with } M_{abnn'} = (m_a + m_b + E_n) \delta_{nn'} + \frac{B_{ab}}{m_a m_b \sqrt{nn'}} \quad (5.25)$$



where e_i are the quark charges, r_{ab} is the inter-quark separation and a and b are parameters characterising the strengths of the electromagnetic Coulomb and hyperfine interactions respectively. The form of the mass matrix (5.25) differs from that of (4.1) by the inclusion of the explicit dependence of B_{ab} and A_{aa} , on quark mass. To allow quantitative predictions the various parameter values obtained in the $\rho = 2.8$ fit, as displayed in Table 4.7, are employed here with the necessary modifications.

The inclusion of (i) and (ii) in (5.25) allows isospin violating isoscalar-isovector mixing between $\pi^0 - \eta, \pi^0 - \eta', \pi^0 - \eta_c$ and $\rho - \omega$ and $\rho - \phi$ to be described. This mixing is produced not only through the straightforward additions of (i) and (ii) but also by the effect of Δ on the hyperfine and annihilation interaction terms⁽¹¹⁶⁾ which are proportional to $1/m_a m_b$. This inverse mass dependence is exploited to give the relevant terms a Δ dependence through the first order substitution $1/m_d = (1 - \Delta/m_u)/m_u$. It is assumed that this is the only substantial effect that isospin violations will have on these interaction terms so that the values of the parameters B_{ab} and A_{aa} , will remain unchanged. The ground-state mass matrix in the qq basis is then

$$\left[\begin{array}{cccc}
 \left\{ \begin{array}{l} 2m_u + 4a + \frac{4b\vec{\sigma}\cdot\vec{\sigma}}{2} \\ \frac{B_{uu}}{2} \vec{\sigma}\cdot\vec{\sigma} + \frac{A_{uu}}{2} \end{array} \right\} & \frac{A_{ud}}{m_u} \left\{ 1 - \frac{\Delta}{m_u} \right\} & \frac{A_{us}}{m_u m_s} & \frac{A_{uc}}{m_u m_c} \\
 \frac{A_{ud}}{m_u} \left\{ 1 - \frac{\Delta}{m_u} \right\} & \left\{ \begin{array}{l} 2m_u + 2\Delta + a + \frac{b\vec{\sigma}\cdot\vec{\sigma}}{2} + \frac{A_{dd}}{2} \left(1 - \frac{2\Delta}{m_u} \right) \\ + \frac{B_{dd}}{2} \left(1 - \frac{2\Delta}{m_u} \right) \end{array} \right\} & \frac{A_{ds}}{m_u m_s} \left\{ 1 - \frac{\Delta}{m_u} \right\} & \frac{A_{dc}}{m_u m_c} \left\{ 1 - \frac{\Delta}{m_u} \right\} \\
 \frac{A_{us}}{m_u m_s} & \frac{A_{ds}}{m_u m_s} \left\{ 1 - \frac{\Delta}{m_u} \right\} & \left\{ \begin{array}{l} 2m_s + a + \frac{b\vec{\sigma}\cdot\vec{\sigma}}{2} \\ + \frac{B_{ss}}{2} \vec{\sigma}\cdot\vec{\sigma} + \frac{A_{ss}}{2} \end{array} \right\} & \frac{A_{sc}}{m_s m_c} \\
 \frac{A_{uc}}{m_u m_c} & \frac{A_{dc}}{m_u m_c} \left\{ 1 - \frac{\Delta}{m_u} \right\} & \frac{A_{sc}}{m_s m_c} & \left\{ \begin{array}{l} 2m_c + 4a + \frac{4b\vec{\sigma}\cdot\vec{\sigma}}{2} \\ + \frac{B_{cc}}{2} \vec{\sigma}\cdot\vec{\sigma} + \frac{A_{cc}}{2} \end{array} \right\}
 \end{array} \right]$$

with $\vec{\sigma} \cdot \vec{\sigma} = -3/4$ for the pseudoscalars and $+1/4$ for the vectors.

In order to find the isospin violating mass mixing elements in the pure isospin basis the product

$$M_{SU(2)} = U M_{qq} U^T \quad (5.27)$$

is formed, where M_{qq} is the mass matrix in the $q\bar{q}$ basis and U is the matrix of eigenvectors obtained from the $\rho = 2.8$ fit in Chapter 4, which would diagonalise M_{qq} if the isospin violating additions (i) and(ii) were absent. The resulting mass matrix in the ground-state is then

$$M_{SU(2)} = \begin{bmatrix} M_{\pi^0} & \delta_{\pi\eta} & \delta_{\pi\eta'} & \delta_{\pi\eta_c} \\ \delta_{\pi\eta} & M_{\eta} & 0 & 0 \\ \delta_{\pi\eta'} & 0 & M_{\eta'} & 0 \\ \delta_{\pi\eta_c} & 0 & 0 & M_{\eta_c} \end{bmatrix} \quad (5.28)$$

where the isospin violating mixing of $\eta-\eta' -\eta_c$ is ignored since its effects on the π^0 wavefunction, which is of primary interest here, are negligible. The off-diagonal mass mixing elements in (5.28) contain terms linear in Δ , a and b which are multiplied by the appropriate wavefunction coefficients a_i^P , b_i^P , c_i^P and d_i^P , in the notation of (4.9). The corresponding mixing elements for the vectors are obtained by making the replacements $\pi^0 \rightarrow \rho^0$, $\eta \rightarrow \omega$, $\eta' \rightarrow \phi$ and $\eta_c \rightarrow \psi$.

The relatively large widths of the vector states, particularly the ρ , are responsible for further contributions to the mixing scheme which are not observed in the pseudoscalar case. Including these effects in the mass matrix

involves rewriting (5.28) as ⁽¹¹⁶⁾

$$\begin{bmatrix} M_{\rho} - \frac{i\Gamma_{\rho}}{2} & \delta_{\rho\omega} & \delta_{\rho\phi} \\ \delta_{\rho\omega} & M_{\omega} - \frac{i\Gamma_{\omega}}{2} & 0 \\ \delta_{\rho\phi} & 0 & M_{\phi} - \frac{i\Gamma_{\phi}}{2} \end{bmatrix} \quad (5.29)$$

which allows the investigation of ρ - ω interference effects. In practice $\delta_{\rho\phi} \approx 0$ and can be safely ignored in future applications.

Vector mixing is further complicated by the presence of electromagnetic annihilation contributions to the mass matrix via the process $\rho \rightarrow \gamma \rightarrow \rho$, $\rho \rightarrow \gamma \rightarrow \omega$ and $\omega \rightarrow \gamma \rightarrow \omega$. Denoting the amplitude for $\rho \rightarrow \gamma$ by

$$A(\rho \rightarrow \gamma) \equiv a_n \sim \langle \rho | J | 0 \rangle \quad (5.30)$$

where J is the electromagnetic current operator responsible for the transition, then by noting that J couples to a $q\bar{q}$ pair proportional to the charge of the quark q ⁽¹³¹⁾ the amplitude for $\omega \rightarrow \gamma$ can be evaluated as

$$A(\omega \rightarrow \gamma) = \frac{\sum_i \alpha_i^{\omega} \left\{ \frac{2}{3} + (-1/3) \right\}}{\sum_i \alpha_i^{\rho} \left\{ \frac{2}{3} - (-1/3) \right\}} a_n \quad (5.31)$$

in the notation of (4.9). Taking α_i^{ρ} and α_i^{ω} values from the $\rho = 2.8$ fit gives

$$A(\omega \rightarrow \gamma) = 0.342 a_n \quad (5.32)$$

Thus the electromagnetic annihilation contribution to the vector mass matrix is

$$M_a = \begin{bmatrix} a_n^2 & 0.342 a_n^2 \\ 0.342 a_n^2 & 0.117 a_n^2 \end{bmatrix} \begin{matrix} \bar{\rho} \\ \bar{\omega} \end{matrix} \quad (5.33)$$

where $\bar{\rho}$ and $\bar{\omega}$ are the pure isospin states.

Eigenvectors in the physical basis, which are obtained by diagonalisation of $M_{SU(2)}$, can be expressed in terms of isovector-isoscalar mixing angles defined by

$$\begin{aligned} |\pi^0\rangle &= |\bar{\pi}^0\rangle + \theta_p |\bar{\eta}\rangle + \phi_p |\bar{\eta}'\rangle + \chi_p |\bar{\eta}_c\rangle \\ |\eta\rangle &= |\bar{\eta}\rangle - \theta_p |\bar{\pi}^0\rangle \\ |\eta'\rangle &= |\bar{\eta}'\rangle - \phi_p |\bar{\pi}^0\rangle \\ |\eta_c\rangle &= |\bar{\eta}_c\rangle - \chi_p |\bar{\pi}^0\rangle \end{aligned} \quad (5.34)$$

where the barred symbols indicate pure isospin eigenstates. Unitary spin wavefunctions for the vectors are constructed in a similar manner. Diagonalisation of $M_{SU(2)}$ with (5.34) produces pseudoscalar mixing angles

$$\theta_p = - \frac{\delta_{\pi\eta}}{M_\eta - M_\pi} ; \quad \phi_p = - \frac{\delta_{\pi\eta'}}{M_{\eta'} - M_\pi} ; \quad \chi_p = - \frac{\delta_{\pi\eta_c}}{M_{\eta_c} - M_\pi} \quad (5.35)$$

and the vector mixing angle of interest here

$$\theta_V = \frac{\delta_{\rho\omega} + 0.342 a_n^2}{M_\rho - M_\omega + 0.883 a_n^2 + 1/2 (\Gamma_\omega - \Gamma_\rho)} \quad (5.36)$$

Substituting particle masses and parameter values gives

$$\begin{aligned}\theta_p &= - (3.02 \times 10^{-3})\Delta + (2.16 \times 10^{-3})a - (2.25 \times 10^{-8})b \\ \phi_p &= (2.48 \times 10^{-4})\Delta - (8.27 \times 10^{-4})a + (3.41 \times 10^{-9})b \quad (5.37) \\ \chi_p &= -(1.21 \times 10^{-5})\Delta - (1.38 \times 10^{-5})a + (1.33 \times 10^{-10})b\end{aligned}$$

The annihilation contribution to θ_V has been calculated by Isgur⁽¹¹⁶⁾, who finds $a_n^2 = 1.4$ MeV giving

$$\theta_V = \left[0.74\Delta - 1.50 a - (2.20 \times 10^{-6})b + 0.479 \right] \times 14.26 \times 10^{-3} e^{i(94)^\circ} \quad (5.38)$$

The predicted ρ - ω phase angle agrees well with experimental values which range from⁽¹⁵⁹⁾ $(85 \pm 15)^\circ$ to⁽¹⁶⁰⁾ $(100 \pm 38)^\circ$.

5.4.2 Isomultiplet Mass Differences

The magnitudes of Δ , a and b can be determined by comparing model predictions for isomultiplet mass differences, for example $\pi^+ - \pi^0$, with their experimental values. Few such mass differences are well determined experimentally. Where sufficient information is available Particle Data Group averages are used,

$$\begin{aligned}M_{\pi^+} - M_{\pi^0} &= 4.604 \pm 0.004 \text{ MeV} & M_{K^+} - M_{K^0} &= -4.01 \pm 0.13 \text{ MeV} \\ M_{\bar{K}^{*+}} - M_{K^{*0}} &= -4.31 \pm 0.62 \text{ MeV} & & (5.39)\end{aligned}$$

The $D^+ - D^0$ and $D^{*+} - D^{*0}$ differences have been determined by Peruzzi et al⁽¹⁶¹⁾ who quote

$$M_{D^+} - M_{D^0} = 5.0 \pm 0.8 \text{ MeV} \quad M_{D^{*+}} - M_{D^{*0}} = 2.6 \pm 1.8 \quad (5.40)$$

Also $M_{\rho^+} - M_{\rho^0} = -2.4 \pm 2.1$ ⁽¹⁶²⁾

Model predictions of these quantities are given by diagonalising the $I \neq 0$ sectors of the mass matrix,

$$\begin{aligned} M_{\pi^+} - M_{\pi^0} &= -\frac{9}{2} a + \frac{3}{4} \frac{9b}{2m_u^2} (a^\pi)^2 \\ M_{K^+} - M_{K^0} &= -\Delta - 3a + \frac{3}{4} \frac{3b}{m_u m_s} (a^K)^2 - \frac{3}{4} \frac{B_{ds}}{m_u m_s} \cdot \frac{\Delta}{m_u} (a^K)^2 \\ M_{D^+} - M_{D^0} &= \Delta - 6a + \frac{3}{4} \frac{6b}{m_u m_c} (a^D)^2 + \frac{3}{4} \frac{B_{cd}}{m_u m_c} \cdot \frac{\Delta}{m_u} (a^D)^2 \end{aligned} \quad (5.41)$$

for the pseudoscalars, and

$$\begin{aligned} M_{\rho^+} - M_{\rho^0} &= -\frac{9}{2} a - \frac{1}{4} \frac{9b}{2m_u^2} (a^\rho)^2 - a_n^2 - 2\theta_V \delta'_{\rho\omega} - \theta_V^2 M_\omega \\ M_{K^{*+}} - M_{K^{*0}} &= -\Delta - 3a - \frac{1}{4} \frac{3b}{m_u m_s} (a^{K^*})^2 + \frac{1}{4} \frac{B_{ds}}{m_u m_s} \cdot \frac{\Delta}{m_u} (a^{K^*})^2 \\ M_{D^{*+}} - M_{D^{*0}} &= \Delta - 6a - \frac{1}{4} \frac{6b}{m_u m_c} (a^{D^*})^2 - \frac{1}{4} \frac{B_{cd}}{m_u m_c} \cdot \frac{\Delta}{m_u} (a^{D^*})^2 \end{aligned} \quad (5.42)$$

for the vectors where $a^P = \sum_{n=1}^4 (a_n^P / \sqrt{n})$, $\delta'_{\rho\omega} = \delta_{\rho\omega} + 0.342 a_n^2$ and the strong contributions to $M_{\pi^+} - M_{\pi^0}$, which are proportional to (mixing angle)² are ignored. By substituting model parameters, Δ , a and b are determined from (5.41) with (5.39) and (5.40) to give

$$\begin{aligned} \Delta &= 2.78 \pm 0.07 \text{ MeV} ; \quad a = -0.047 \pm 0.13 \text{ MeV} \\ b &= (8.32 \pm 1.19) \times 10^4 \text{ MeV}^3 \end{aligned} \quad (5.43)$$

where the errors quoted correspond to the changes induced by the errors on $M_{D^+} - M_{D^0} = 5.0 \pm 0.8$ MeV. Predictions are made for the vector mass differences

$$M_{\rho^+} - M_{\rho^0} = -2.84 \text{ MeV} : M_{k^{*+}} - M_{k^{*0}} = -2.41 \text{ MeV} : M_{D^{*+}} - M_{D^{*0}} = 2.59 \text{ MeV} \quad (5.44)$$

The contributions to these isomultiplet mass differences from each of the isospin violating interactions are displayed in Table 5.1 (in MeV). The strong contribution to $M_{\pi^+} - M_{\pi^0}$ can be estimated using the parameter values in (5.43) to give

Mass Difference	$\pi^+ - \pi^0$	$k^+ - k^0$	$D^+ - D^0$	$\rho^+ - \rho^0$	$k^{*+} - k^{*0}$	$D^{*+} - D^{*0}$
Strong (Δ)	0.04	-6.02	3.80	-1.09	-2.25	2.54
e/M Coulombic (a)	0.21	0.14	0.28	0.21	0.14	0.28
e/M Hyperfine (b)	4.39	1.88	0.92	-0.57	-0.31	-0.22
Other	0	0	0	-1.4	0	0
Total	4.6	-4.0	5.0	-2.84	-2.4	2.6
Experiment	4.6	-4.0	5.0	-2.4	-4.3	2.6

TABLE 5.1 : Strong and electromagnetic contributions to isomultiplet mass differences. All values are quoted in MeV.

$$(M_{\pi^+} - M_{\pi^0})_{\text{strong}} = 2 \left[\theta_p^2 (M_{\pi} - M_{\pi'}) + \phi_p^2 (M_{\pi'} - M_{\pi}) + \chi_p^2 (M_{\pi_c} - M_{\pi}) \right] - \theta_p^2 M_{\pi} - \phi_p^2 M_{\pi'} - \chi_p^2 M_{\pi_c} \quad (5.45)$$

From (5.37) and (5.43) $\theta_p = -0.011$, $\phi_p = 0.001$ and $\chi_p = -0.22 \times 10^{-4}$ thus

$(M_{\pi^+} - M_{\pi^0})_{\text{strong}} = 0.04 \text{ MeV}$, much less than the electromagnetic contributions, justifying its omission in the earlier calculation.

5.4.3 $\omega \rightarrow 2\pi$ Decay

The parameter values obtained in (5.43) allow the magnitude of θ_V and hence $\Gamma(\omega \rightarrow 2\pi)$ to be estimated. Writing the physical ω as

$$|\omega\rangle = |\bar{\omega}\rangle - \theta_V |\bar{\rho}\rangle \quad (5.46)$$

the isospin violating decay width is given by

$$\Gamma(\omega \rightarrow 2\pi) = \left\{ \frac{P_\omega}{P_\rho} \right\}^3 \left\{ \frac{M_\rho}{M_\omega} \right\}^2 \theta_V^2 \Gamma(\rho \rightarrow 2\pi) \quad (5.47)$$

where the pion centre of mass momentum $P_V^2 = (M_V^2 - 4M_\pi^2)/4$ and $\Gamma(\rho \rightarrow 2\pi) = 158 \text{ MeV}$. The Particle Data Group average value⁽⁶¹⁾ for this decay rate is quoted as

$B(\omega \rightarrow 2\pi) = 0.0133 \pm 0.0027$, however results taken from individual experiments vary considerably from a maximum⁽¹³⁵⁾ $B(\omega \rightarrow 2\pi) = 0.04 \pm 0.03$ to a minimum⁽¹³⁶⁾ $B(\omega \rightarrow 2\pi) = 0.01 \pm 0.001$.

The parameter values of (5.43) give $|\theta_V| = 0.034$ and hence $B(\omega \rightarrow 2\pi) = 0.018$ in close agreement with the PDG average.

5.4.4 The Isospin Violating Decay $\psi' \rightarrow \pi^0 \psi$

The $\psi' \rightarrow \pi^0 \psi$ partial width has been observed^(137,138) in two experiments performed by the Mark II and Crystal Ball collaborations. They quote their results as a ratio of this SU(2) violating width to that of the SU(3) violating $\Gamma(\psi' \rightarrow \eta \psi)$ giving $(40 \pm 10) \times 10^{-3}$ and $(60 \pm 20) \times 10^{-3}$ respectively.

A study of the isospin violating process $\psi' \rightarrow \psi \pi^0$ in the constituent quark framework requires a knowledge of the $c\bar{c}$ component in the π^0 wavefunction, which is responsible for the decay, Fig. 5.2. This component arises from both $\pi^0 - \eta_c$ and $\pi^0 - \eta$, $\pi^0 - \eta'$ mixing, since the OZI rule violating

annihilation amplitudes produce significant mixing of $c\bar{c}$ in the η and η' wavefunctions (52,90).

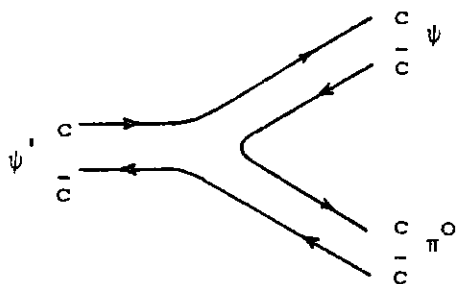


Fig 5.2 : Strong production of a $c\bar{c}$ pair in $\psi' \rightarrow \pi^0 \psi$ decay.

Using the expansion for the π^0 in (5.34) the amplitude for this process is

$$A(\psi' \rightarrow \pi^0 \psi) = A(\psi' \rightarrow \bar{\pi}^0 \psi) + \theta_P A(\psi' \rightarrow \bar{\eta} \psi) + \phi_P A(\psi' \rightarrow \bar{\eta}' \psi) + \chi_P A(\psi' \rightarrow \bar{\eta}_c \psi) \quad (5.48)$$

The quark model allows this to be rewritten in terms of an unknown amplitude involving the quark sub-process which describes the strong production of a $c\bar{c}$ pair, Fig. 5.2[†]. This unknown amplitude is eliminated by dividing (5.48) by the amplitude for the SU(3) violating process $\psi' \rightarrow \eta \psi$ to give

$$\begin{aligned} \frac{A(\psi' \rightarrow \pi^0 \psi)}{A(\psi' \rightarrow \eta \psi)} &\approx \frac{\theta_P A(\psi' \rightarrow \bar{\eta} \psi) + \phi_P A(\psi' \rightarrow \bar{\eta}' \psi) + \chi_P A(\psi' \rightarrow \bar{\eta}_c \psi)}{A(\psi' \rightarrow \bar{\eta} \psi)} \\ &= -0.011 - 2.01 \times 10^{-3} - 0.017 \\ &= -0.030 \end{aligned} \quad (5.49)$$

Contributions corresponding to π^0 mixing with the η, η' and η_c are shown explicitly.

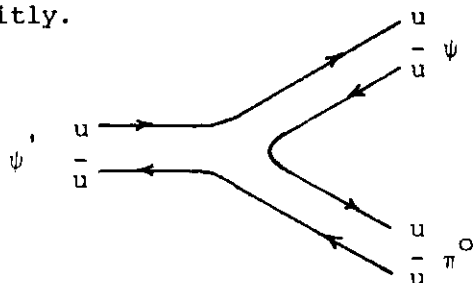


Fig 5.3 : Strong production of a $u\bar{u}$ pair in $\psi' \rightarrow \pi^0 \psi$ decay.

[†] The other possible process leading to this decay, shown in Fig 5.3, is strongly suppressed compared to that in Fig.5.2 due to the very small mixing of uu components into the ψ' and ψ wavefunctions. This is a reflection of the pseudoscalar quark annihilation amplitudes being in general an order of magnitude larger than the vector annihilation amplitudes.

Previous analyses of this ratio have only included the effects of mixing η (117,119) or at best (118,120) η and η' with the π^0 , however, this determination indicates that although the π^0 - η_c mixing angle χ_p is two orders of magnitude smaller than θ_p the relative proportion of $c\bar{c}$ in the η_c and η wavefunctions annuls this suppression leading to contributions from π^0 - η_c and π^0 - η mixing which are roughly of equal importance.

The ratio (5.49) can be re-expressed to indicate the contributions arising from the strong and Coulombic and hyperfine electromagnetic interactions respectively

$$R_A = -0.036 + 3.27 \times 10^{-4} + 0.0062 \quad (5.50)$$

Equation (5.50) indicates that the isospin violating strong interactions are predominantly responsible for the $\psi' \rightarrow \pi^0 \psi$ decay process, contributions to the amplitude from the electromagnetic interactions are much smaller in comparison and of opposite sign thus reducing the absolute magnitude of (5.50). This is just as observed in $\omega \rightarrow 2\pi$ decay where the amplitude is proportional to θ_v . In this case 85% of the amplitude arises from the contribution due to the strong interaction while the remaining 15% results from the effects of the electromagnetic Coulombic, hyperfine and annihilation interactions. Both strong and electromagnetic contributions are of the same sign.

Multiplying (5.50) by the relevant phase space factors yields the required ratio of decay widths

$$R = \frac{\Gamma(\psi' \rightarrow \pi^0 \psi)}{\Gamma(\psi' \rightarrow \eta \psi)} = 18 \times 10^{-3} \quad (5.51)$$

a factor of two or three less than the present experimental determinations. Agreement could be improved by increasing Δ and decreasing a and b in

magnitude, however, such changes would spoil the satisfactory picture of isomultiplet mass differences described in section 5.4.2.

In conclusion, upon addition of the isospin violating contributions (5.24) to the interaction Hamiltonian, this constituent quark model which involves full symmetry breaking amongst its parameters can provide a reasonable description of both isomultiplet mass differences and the branching ratio $B(\omega \rightarrow 2\pi)$. The prediction for R given in (5.51) is smaller than its experimental values determined by the Mark II and Crystal Ball collaborations. However its evaluation raises the interesting problem of the relative importance of contributions from $\pi^0-\eta, \pi^0-\eta'$ and $\pi^0-\eta_c$ mixing. The relative suppression of $c\bar{c}$ components in the η and η' wavefunctions compared with those in the η_c implies that the latter $\pi^0-\eta_c$ mixing contribution is the dominant contribution to R.

The mixing scheme described by (5.34) has the effect of changing the relative importance of the $u\bar{u}$ and $d\bar{d}$ components of the unitary spin wavefunctions. In the ground state the pseudoscalar and vector wavefunctions are

$$\begin{aligned} |\pi^0\rangle &= 0.657 u\bar{u} - 0.647 d\bar{d} + (7.72 \times 10^{-3}) s\bar{s} \\ |\eta\rangle &= 0.420 u\bar{u} + 0.434 d\bar{d} - 0.748 s\bar{s} \\ |\eta'\rangle &= 0.491 u\bar{u} + 0.493 d\bar{d} + 0.509 s\bar{s} \end{aligned} \quad (5.52)$$

$$\begin{aligned} |\rho\rangle &\approx 0.695 \left[(1 - \theta_V) u\bar{u} - (1 + \theta_V) d\bar{d} \right] \\ |\omega\rangle &\approx 0.695 \left[(1 + \theta_V) u\bar{u} + (1 - \theta_V) d\bar{d} \right] \end{aligned} \quad (5.53)$$

Thus for the pseudoscalars the $u\bar{u}$ component of the $I = 0$ state is increased relative to the $d\bar{d}$ component while the reverse is true for the $I = 1$ states. This is just as observed by Isgur et al^(116,117), with the result that their conclusions, for example,

$$\Gamma(\rho^0 \rightarrow \pi^0 \gamma) \approx 1.09 \Gamma(\rho^+ \rightarrow \pi^+ \gamma)$$

(calculated using (5.52) & (5.53)) are reproduced here.

5.4.5 A Note on Isomultiplet Mass Differences

The strong and electromagnetic contributions to isomultiplet mass differences quoted in table 5.1 are the result of a three parameter fit constrained by the $\pi^+ - \pi^0$, $K^+ - K^0$ and $D^+ - D^0$ mass splittings and the form of the Hamiltonian(5.24). The magnitudes of the electric and magnetic contributions obtained in this manner do not agree with those found by other authors^{116,164} whose explicit calculations indicate that the Coulombic component is consistently larger than the hyperfine component. Matching the terms containing a and b in the expressions (5.41) and (5.42) for the isomultiplet mass differences with their calculated values given in refs. 116 and 164 indicates

$$a \approx -0.25 \text{ MeV and } b \approx 1 \times 10^4 \text{ MeV}^3$$

that is, a and b are expected to have substantially different values from those obtained in the simple fit ($a = -0.047 \text{ MeV}$, $b = 8.34 \times 10^4 \text{ MeV}^3$) of section 5.4.2. Accepting $\Delta \approx 3 \text{ MeV}$ these revised values of a and b allow the following predictions

$$M_{\pi^+} - M_{\pi^0} \approx 1.7 \text{ MeV}; M_{K^+} - M_{K^0} \approx -5.6 \text{ MeV}; M_{D^+} - M_{D^0} \approx 5.7 \text{ MeV} \quad (5.54)$$

$$M_{\rho^+} - M_{\rho^0} \approx -2.3 \text{ MeV}; M_{K^{*+}} - M_{K^{*0}} \approx -1.7 \text{ MeV}; M_{D^{*+}} - M_{D^{*0}} \approx 4.7 \text{ MeV}$$

$$B(\omega \rightarrow 2\pi) \approx 0.029 R \approx 27 \times 10^3$$

While the $M_{D^+} - M_{D^0}$ and $M_{\rho^+} - M_{\rho^0}$ predictions are satisfactory $M_{\pi^+} - M_{\pi^0}$ and $M_{K^{*+}} - M_{K^{*0}}$ are too small and $M_{K^+} - M_{K^0}$ and $M_{D^{*+}} - M_{D^{*0}}$ are too large. $B(\omega \rightarrow 2\pi)$ is again predicted with a value close to those obtained experimentally while an improved estimate for R is indicated. The poor predictions for the hadron mass splittings in (5.54) imply that the form of the electromagnetic Hamiltonian given in (5.24) does not represent the whole picture. A relativistic calculation of the pion mass difference performed by Coleman and Schnitzer¹⁶⁵ gives $M_{\pi^+} - M_{\pi^0} \approx 5 \text{ MeV}$. Relativistic effects could also be of considerable importance for the isomultiplet splittings of the higher mass states.

CHAPTER 6

THE CURRENT ALGEBRA APPROACH TO $\rho = \Gamma(\psi \rightarrow \eta' \gamma) / \Gamma(\psi \rightarrow \eta \gamma)$

AND $R = \Gamma(\psi' \rightarrow \pi^0 \psi) / \Gamma(\psi' \rightarrow \eta \psi)$

6.1 INTRODUCTION

The breaking of the SU(2) (isospin), SU(3) and SU(4) unitary symmetries has been analysed in detail in Chapters 2 to 5 in terms of a non-relativistic quark model where the symmetry breaking was introduced explicitly by giving a flavour dependence to the constituent quark mass and interaction terms occurring in meson mass matrices. The pseudoscalar particles were of particular interest where the η - η' mixing pattern provided, through model predictions, a sensitive indicator of SU(3) violating effects, and the construction of the π^0 wavefunction, in particular its $I = 0$ components resulting from π^0 - η , π^0 - η' and π^0 - η_c mixing allowed a measure of isospin violation in hadron processes. With this in mind, a close study was made of the two ratios

$$\rho \equiv \frac{\Gamma(\psi \rightarrow \eta' \gamma)}{\Gamma(\psi \rightarrow \eta \gamma)} \quad R \equiv \frac{\Gamma(\psi' \rightarrow \pi^0 \psi)}{\Gamma(\psi' \rightarrow \eta \psi)}$$

where ρ is particularly sensitive to SU(3) violations and R is determined predominantly by the $(m_d - m_u)$ constit. mass difference.

The magnitudes of these ratios can also be estimated using current algebra techniques⁽³³⁾, applied within the framework of QCD². As noted in Chapter 1 in the limit of zero quark masses ($m_i \rightarrow 0$) the QCD Lagrangian possesses a $U(n_f) \times U(n_f)$ symmetry (ignoring anomalies in the axial divergence) where n_f is the number of flavours in the theory. This symmetry is retained in an approximate sense, when the quarks are allowed to take on non-zero values provided the condition $m_i/\mu \ll 1$ holds where μ is the renormalisation

point. This is certainly true for m_u and m_d , and more approximately so for m_s so the QCD Lagrangian has an approximate $U(3) \times U(3)$ symmetry.

This symmetry is believed to be spontaneously broken, the axial part being realised in a Nambu-Goldstone fashion such that the pseudoscalar mesons appear as Goldstone excitations (in the limit $m_i = 0$) in the particle spectrum. (It has been shown⁽¹³⁹⁾ in the large N_c limit of QCD, where N_c is the number of colours, that the chiral symmetry is indeed spontaneously broken). Thus nine pseudoscalar Goldstone bosons are expected which acquire a mass when m_i assume non-zero values. PCAC (partial conservation of axial current) techniques allow these masses to be evaluated as shown in (5.11),

$$M_{\alpha\beta}^2 F_{\alpha\alpha} F_{\beta\beta} = \langle 0 | \left[Q^a, \left[Q^b, H \right] \right] | 0 \rangle \quad (6.1)$$

where the Hamiltonian operator is given in (5.15) and Q^a are the generators of the broken symmetry. The vacuum to pseudoscalar particle matrix elements of the axial vector currents have been redefined here to allow for possible symmetry breaking in their values,

$$\langle 0 | A_{\mu}^a | P \rangle = i F_{aP} q_{\mu} \quad (6.2)$$

Defining $F_{ij} \equiv F_{\pi} \delta_{ij}$ for $i, j = 1, \dots, 8$ and $F_{00} \equiv F_0$ the results of (5.16) are reproduced together with

$$\begin{aligned} M_{88}^2 F^2 &= -\frac{1}{3} (m_u + m_d + 4 m_s) V \\ M_{80}^2 F_0 F_{\pi} &= -\frac{2}{\sqrt{18}} (m_u + m_d - 2 m_s) V \\ M_{00}^2 F_0^2 &= -\frac{2}{3} (m_u + m_d + m_s) V \end{aligned} \quad (6.3)$$

Although evidence from current algebra suggests that isospin is strongly broken at the current quark level, it is instructive to assume, for the moment, that this symmetry is not violated and analyse the consequences of (5.16) and (6.3). In this way a strong analogy can be drawn between the shortcomings of this procedure and those of the corresponding calculation in the constituent quark framework (Chapter 2). The isoscalar mass elements are rewritten as

$$\begin{aligned}
 M_{88}^2 &= \frac{1}{3} (4M_k^2 - M_\pi^2) \\
 M_{80}^2 &= \frac{2\sqrt{2}}{3} \alpha (M_k^2 - M_\pi^2) \\
 M_{\infty}^2 &= \frac{2}{3} \alpha^2 (M_k^2 + M_{\pi/2}^2)
 \end{aligned} \tag{6.4}$$

where $\alpha \equiv F_\pi/F_0$. The eigenvalues of this mass matrix are given by⁽¹⁴⁰⁾

$$M_1^2 = \frac{4}{3} M_k^2 \left(1 + \frac{\alpha^2}{2}\right) + O(M_\pi^2) : M_2^2 = \frac{3 M_\pi^2}{(1 + \alpha^2/2)} + O\left\{\frac{M_\pi^4}{M_k^4}\right\} \tag{6.5}$$

In the limit $\alpha \rightarrow 0$, $M_1^2 \rightarrow 4/3 M_k^2$, the Gell-Mann/Okubu value, allowing M_1 to be associated with the physical η , however a problem arises with the interpretation of M_2 which has mass

$$M_2 \leq \sqrt{3} M_\pi \tag{6.6}$$

(The Weinberg bound⁽¹⁴⁰⁾) since no such light particle is observed in the meson spectrum. This mass puzzle, why the particle associated with the U(1) axial current is predicted to have a low mass as given in (6.6) when it is expected to be of the order of the $\eta'(958)$ mass is the origin of the U(1) problems^(125,141).

The deficiencies encountered in this approach are precisely those of the conventional constituent quark mixing model described in section 2.2. Indeed, the results encountered there can be reproduced here by setting $F_0 = F_\pi$, the eigenvalues of the mass matrix now correspond to those expected in the ideal mixing case,

$$M_1^2 = 2M_K^2 - M_\pi^2 \quad \text{and} \quad M_2 = M_\pi^2 \quad (6.7)$$

If isospin conservation is not assumed and m_u and m_d are allowed to take different values, as indicated by current algebra, diagonalisation of the mass matrix yields physical eigenstates which are the pure quark combinations ⁽¹²³⁾ $u\bar{u}$, $d\bar{d}$ and $s\bar{s}$ with masses

$$\frac{2 m_u}{F_\pi^2} V \quad : \quad \frac{2 m_d}{F_\pi^2} V \quad : \quad \frac{2 m_s}{F_\pi^2} V \quad (6.8)$$

Thus, not only is an unwanted light isoscalar particle predicted but also observable isospin violations of the order

$$\frac{M_{\pi^+}^2 - M_{\pi^0}^2}{M_{\pi^+}^2 + M_{\pi^0}^2} \sim \frac{m_d - m_u}{m_d + m_u} \approx 0.3 \quad (6.9)$$

both of which are not manifest in the spectrum of states.

It is believed ⁽¹⁴¹⁾ that these connected "U(1)" problems will find a solution via the inclusion of the anomalous divergence in the U(1) axial current. The triangle anomaly, Fig 1.6, allows two distinct currents to be associated with the U(1) axial symmetry. The Noether current, conserved in the limit $m_1 \rightarrow 0$ can only be defined in a gauge dependent way ⁽¹⁴²⁾, however a gauge invariant current can be constructed which contains the anomaly contribution in its divergence and thus has the property

$$\partial_\mu A_0^\mu \neq 0$$

even in the $m_i \rightarrow 0$ limit. The U(1) Goldstone boson discussed above is associated with the former current while the physical particle observed in the meson spectrum is associated with the latter.

The calculation of the mass of the particle related to the U(1) axial current involves the integral⁽¹²⁵⁾ over $F_a^{\mu\nu} \tilde{F}_{\mu\nu}^a$ where $\tilde{F}_{\mu\nu}^a$ is the dual of the field strength tensor

$$\tilde{F}_{\mu\nu}^a = \frac{1}{2} \epsilon_{\mu\nu\sigma\lambda} F_{\sigma\lambda}^a \quad (6.10)$$

Before 1976 it was believed that such integrals would vanish with the result that a Goldstone excitation would also appear associated with the gauge invariant current. The advent of instantons⁽¹⁴³⁾ however, changed this conclusion⁽¹⁴⁴⁾. They implied that the integral over $\tilde{F}F$ could take on non-zero values with the result that the U(1) pseudoscalar state acquired a mass contribution connected with the triangle anomaly which was independent of quark mass, thus eliminating the problem of the light pseudoscalar. The effective symmetry of the QCD Lagrangian was thus reduced from U(3) x U(3) to SU(3) x SU(3) x U_B(1) where U_B(1) represents baryon number conservation. (Note however, that Witten⁽¹⁴⁵⁾ has proposed that the U(1) pseudoscalar particle can be treated as a Goldstone boson in the limit $N_c \rightarrow \infty$).

The anomaly contribution to the mass of the SU(3) singlet state is analogous to that provided by the annihilation of $q\bar{q}$ pairs in the constituent quark framework. The π^0 , η and η' acquire mass contributions associated with the anomaly via mixing induced by SU(2) and SU(3) violations, which in turn imply deviations from the ideal mixing schemes discussed above. Physical eigenstates are then no longer pure quark combinations and isospin violations are reduced to

$$\frac{M_{K^0}^2 - M_{K^+}^2}{M_{K^0}^2 + M_{K^+}^2} \sim \frac{m_d - m_u}{m_s} \quad (6.11)$$

which is of the order of magnitude observed in hadron processes.

6.2 CURRENT AND DIVERGENCE DEFINITIONS

Using the notation of Chapter 1 the QCD Lagrangian is

$$\mathcal{L}_{\text{QCD}}(x) = -\frac{1}{4} F_{\mu\nu}^a(x) F_a^{\mu\nu}(x) + i \sum_{j=1}^n \bar{q}_j^\alpha(x) \gamma_\mu (D_\mu)_{\alpha\beta} q_j^\beta(x) - \sum_{j=1}^n m_j \bar{q}_j^\alpha(x) q_{\alpha j}(x) \quad (6.12)$$

where, for three flavours $q(x)$ is formed from a triplet of quark fields

$$q = \begin{pmatrix} u \\ d \\ s \end{pmatrix} \quad (6.13)$$

The SU(3) axial currents are defined in the usual manner by

$$A_\mu^\alpha(x) = \bar{q}(x) \gamma_\mu \gamma_5 \frac{1}{2} \lambda^\alpha q(x) \quad (6.14)$$

where α runs from 1 to 8. The definition of the U(1) axial current is complicated by the presence of the anomaly associated with the triangle diagram, Fig 1.6. Problems with the renormalisation of the amplitude associated with the diagram imply that the U(1) axial symmetry current, \tilde{A}_μ^0 , is not gauge invariant⁽¹⁴²⁾,

$$\tilde{A}_\mu^0 = \text{gauge dependent} \quad (6.15)$$

$$\partial_\mu \tilde{A}_0^\mu = 0 \text{ for } m_i = 0$$

The amplitude can, however, be renormalised in a gauge invariant manner to give a different operator, A_μ^0 , with the property

$$\partial_\mu A_0^\mu = \frac{2n_f}{\sqrt{6}} \frac{g^2}{32\pi^2} F_a^{\mu\nu} \tilde{F}_{\mu\nu}^a \quad (6.16)$$

These two operators are related by

$$A_{\mu}^{\circ} = \tilde{A}_{\mu}^{\circ} + \frac{2n_f}{\sqrt{6}} k_{\mu} \quad (6.17)$$

$$\text{where } (142) k^{\mu} = \frac{g^2}{32\pi^2} \epsilon^{\mu\alpha\beta\gamma} A_{\alpha}^a (F_{\beta\gamma}^a - \frac{1}{3} g f^{abc} A_{\beta}^a A_{\gamma}^c) \quad (6.18)$$

$$\text{and } \partial_{\mu} k^{\mu} = \frac{g^2}{32\pi^2} F_a^{\mu\nu} \tilde{F}_{\mu\nu}^a \quad (6.19)$$

k^{μ} is a gauge dependent vector associated with the triangle anomaly,

The divergences of the SU(3) axial Noether currents are

$$\partial_{\mu} A_{\alpha}^{\mu}(x) = i\bar{q}(x) \left\{ M, \frac{1}{2} \lambda^{\alpha} \right\} \gamma_5 q(x) \quad (6.20)$$

where M is the quark mass matrix and $\alpha = 1, \dots, 8$. These are conserved in the limit $m_q \rightarrow 0$. The divergence of the U(1) axial current is similarly defined

$$\partial_{\mu} \hat{A}_{\alpha}^{\mu}(x) = i\bar{q}(x) \left\{ M, \frac{1}{2} \lambda^{\circ} \right\} \gamma_5 q(x) \quad (6.21)$$

where λ^{α} is replaced by $\lambda^{\circ} = \sqrt{\frac{2}{3}} I$ with I the unit matrix. The divergence of A_{μ}° is then given by (6.17), (6.19) and (6.21).

In order to investigate the current algebra predictions for ρ and R it will be necessary to evaluate the matrix elements of the divergences $\partial_{\mu} A_{\alpha}^{\mu}$ between the vacuum and pseudoscalar states which arise in the SU(3) and U(1) axial Ward Identities⁽¹²⁵⁾. For this purpose the usual definition (6.2) is employed. Taking the divergence of (6.2) yields the required quantity,

$$\langle 0 | \partial_{\mu} A_{\alpha}^{\mu} | P \rangle = F_{\alpha p} M_p^2 \quad (6.22)$$

and similarly

$$\langle 0 | \partial_\mu \tilde{A}_0^\mu | P \rangle = \tilde{F}_{op} M_p^2 \quad (6.23)$$

$$\begin{aligned} \text{Then } \langle 0 | \tilde{A}_0^\mu | P \rangle &\equiv i q^\mu \tilde{F}_{op} \\ &= \langle 0 | A_0^\mu - \frac{2n_f}{\sqrt{6}} k^\mu | P \rangle \\ &\equiv i q^\mu (F_{op} - A_p) \end{aligned} \quad (6.24)$$

$$\text{with } \langle 0 | \frac{2n_f}{\sqrt{6}} k^\mu | P \rangle = i q^\mu A_p \quad (6.25)$$

The notation adopted here is taken from similar treatments by Goldberg⁽¹⁴⁶⁾ and Williams and van Herwijnen⁽¹⁴⁷⁾. The two U(1) decay constants are seen to be related via the matrix element defined by A_p .

In future applications A_p will be associated with the gluon content of the $I_3 = 0$ pseudoscalar states which is responsible for deviations from ideal mixing and hence for OZI violating decays. Its effect is similar to that of the annihilation interaction encountered earlier in pseudoscalar mixing schemes. To calculate the widths of the processes of interest, $\psi \rightarrow P\gamma$ and $\psi' \rightarrow P\psi$ it is assumed that the decays proceed by the radiation of the pseudoscalar by the heavy quark state via two intermediate gluons⁽¹⁴⁸⁾, $V_1 \rightarrow V_2 + GG$ where V_1 and V_2 are the $c\bar{c}$ vector states. The intermediate gluon state subsequently decays into the required pseudoscalar. A ratio of similar decays is thus given by

$$\begin{aligned} \frac{A(V_1 \rightarrow V_2 P_1)}{A(V_1 \rightarrow V_2 P_2)} &= \frac{A(V_1 \rightarrow V_2 GG)}{A(V_1 \rightarrow V_2 GG)} \cdot \frac{A(GG \rightarrow P_1)}{A(GG \rightarrow P_2)} \\ &= \frac{\langle 0 | O_g | P_1 \rangle}{\langle 0 | O_g | P_2 \rangle} \end{aligned} \quad (6.26)$$

where O_g is some operator ⁽¹⁴⁹⁾ which causes the transition $GG \rightarrow P$.

In order to make predictions for such physical processes numerical values must be obtained for the pseudoscalar decay constants $F_{\alpha p}$ and A_p . These will be calculated in section 6.4, however three relations between these quantities can be found immediately by noting that

- (a) $F_{0\eta}, F_{0\eta'}, F_{8\eta}, F_{8\eta'}$ describe the mixing between $\alpha = 8$ and $\alpha = 0$ components of $\partial_\mu A_\alpha^\mu$ to produce the physical operators $\partial_\mu A_\eta^\mu$ and $\partial_\mu A_{\eta'}^\mu$, and
- (b) $F_{8\pi}, F_{0\pi}, F_{3\eta}, F_{3\eta'}$ similarly define isospin violating mixing between the $\alpha = 3, 8$ and 0 components of $\partial_\mu A_\alpha^\mu$ which comprise the physical operators $\partial_\mu A_\pi^\mu, \partial_\mu A_\eta^\mu$ and $\partial_\mu A_{\eta'}^\mu$.

The singlet and octet divergences can be related to the physical divergences by defining the physical particle interpolating fields ϕ_p as ⁽¹⁴⁶⁾

$$\begin{bmatrix} \partial_\mu A_3^\mu \\ \partial_\mu A_8^\mu \\ \partial_\mu A_0^\mu \end{bmatrix} = \begin{bmatrix} F_\pi M_\pi^2 & F_{3\eta} M_\eta^2 & F_{3\eta'} M_{\eta'}^2 \\ F_{8\pi} M_\pi^2 & F_{8\eta} M_\eta^2 & F_{8\eta'} M_{\eta'}^2 \\ F_{0\pi} M_\pi^2 & F_{0\eta} M_\eta^2 & F_{0\eta'} M_{\eta'}^2 \end{bmatrix} \begin{bmatrix} \phi_{\pi 0} \\ \phi_\eta \\ \phi_{\eta'} \end{bmatrix} \quad (6.27)$$

$$\text{and} \quad \langle 0 | \partial_\mu A_p^\mu | P \rangle \equiv F_p M_p^2 \langle 0 | \phi_p | P \rangle \quad (6.28)$$

where the interpolating field is normalised such that

$$\langle 0 | \phi_p | P \rangle = 1$$

(6.27) can thus be rewritten as

$$\begin{bmatrix} \partial_\mu A_3^\mu \\ \partial_\mu A_8^\mu \\ \partial_\mu A_0^\mu \end{bmatrix} = \begin{bmatrix} 1 & F_{3\eta}/F_\eta & F_{3\eta'}/F_{\eta'} \\ F_{8\pi}/F_\pi & F_{8\eta}/F_\eta & F_{8\eta'}/F_{\eta'} \\ F_{0\pi}/F_\pi & F_{0\eta}/F_\eta & F_{0\eta'}/F_{\eta'} \end{bmatrix} \begin{bmatrix} \partial_\mu A_\pi^\mu \\ \partial_\mu A_\eta^\mu \\ \partial_\mu A_{\eta'}^\mu \end{bmatrix} \quad (6.30)$$

where the physical divergences are just linear combinations of $\partial_\mu A_3^\mu$, $\partial_\mu A_8^\mu$ and $\partial_\mu A_0^\mu$. The 3x3 matrix on the right-hand side of (6.30) is similar in appearance to the rotation matrix encountered previously in mixing problems. Assuming (6.30) can be expressed^(34,150,151) as

$$\begin{bmatrix} \partial_\mu A_3^\mu \\ \partial_\mu A_8^\mu \\ \partial_\mu A_0^\mu \end{bmatrix} = \begin{bmatrix} 1 & & -\lambda_{\pi\eta} & -\lambda_{\pi\eta'} \\ (\lambda_{\pi\eta} \cos\theta - \lambda_{\pi\eta'} \sin\theta) & \cos\theta & & \\ (\lambda_{\pi\eta} \sin\theta + \lambda_{\pi\eta'} \cos\theta) & \sin\theta & \cos\theta & \end{bmatrix} \begin{bmatrix} \partial_\mu A_\pi^\mu \\ \partial_\mu A_\eta^\mu \\ \partial_\mu A_{\eta'}^\mu \end{bmatrix} \quad (6.31)$$

where $\lambda_{\pi\eta}$, $\lambda_{\pi\eta'}$, and θ are the isospin violating π - η , π - η' and octet-singlet mixing angles, the following identifications can be made,

$$\begin{aligned} F_{3\eta} &= -\lambda_{\pi\eta} F_\eta & F_{3\eta'} &= -\lambda_{\pi\eta'} F_{\eta'} \\ F_{8\pi} &= (\lambda_{\pi\eta} \cos\theta - \lambda_{\pi\eta'} \sin\theta) F_\pi & F_{0\pi} &= (\lambda_{\pi\eta} \sin\theta + \lambda_{\pi\eta'} \cos\theta) F_\pi \\ F_{8\eta} &= \cos\theta F_\eta & F_{8\eta'} &= -\sin\theta F_{\eta'} \\ F_{0\eta} &= \sin\theta F_\eta & F_{0\eta'} &= \cos\theta F_{\eta'} \end{aligned} \quad (6.32)$$

The original eight $F_{\alpha\beta}$ have been reduced to the five unknowns $\lambda_{\pi\eta}$, $\lambda_{\pi\eta'}$, θ , F_η and $F_{\eta'}$. Three relations follow from (6.32),

$$\frac{F_{0\eta}}{F_{8\eta}} = - \frac{F_{8\eta'}}{F_{0\eta'}} \quad (6.33)$$

$$F_{8\pi} = \left\{ \frac{F_{3\eta} F_{8\eta}}{F_\eta^2} + \frac{F_{3\eta'} F_{8\eta'}}{F_{\eta'}^2} \right\} F_\pi \quad (6.34)$$

$$F_{0\pi} = \left\{ \frac{F_{3\eta} F_{0\eta}}{F_\eta^2} + \frac{F_{3\eta'} F_{0\eta'}}{F_{\eta'}^2} \right\} F_\pi \quad (6.35)$$

where $F_{\eta}^2 = F_{0\eta}^2 + F_{8\eta}^2$ and $F_{\eta'}^2 = F_{0\eta'}^2 + F_{8\eta'}^2$. (6.32) to (6.35) will be combined with further relations involving the $F_{\alpha p}$ obtained from SU(3) and U(1) axial Ward identities, to determine their numerical value.

6.3 AXIAL VECTOR WARD IDENTITIES

In many applications of current algebra physical implications of the theory are extracted by considering matrix elements such as (33,152)

$$M_{\mu}^{\alpha\beta} = \lim_{q \rightarrow 0} \int d^4x e^{-iq \cdot x} \langle 0 | T \left\{ A_{\mu}^{\alpha}(x) \partial^{\nu} A_{\nu}^{\beta}(0) \right\} | 0 \rangle \quad (6.36)$$

where $A_{\mu}^{\alpha}(x)$ is a current operator and T indicates the time ordering operation.

For this particular analysis the following contraction is required

$$\int d^4x \partial^{\mu} \langle 0 | T \left\{ A_{\mu}^{\alpha}(x) \partial^{\nu} A_{\nu}^{\beta}(0) \right\} | 0 \rangle \quad (6.37)$$

(6.37) is evaluated to give the SU(3) and U(1) axial Ward identities,

$$\begin{aligned} & \int d^4x \partial^{\mu} \langle 0 | T \left\{ A_{\mu}^{\alpha}(x) \partial^{\nu} A_{\nu}^{\beta}(0) \right\} | 0 \rangle \\ &= \int d^4x \langle 0 | T \left\{ \partial^{\mu} A_{\mu}^{\alpha}(x) \partial^{\nu} A_{\nu}^{\beta}(0) \right\} | 0 \rangle + \langle 0 | \left[Q_5^{\alpha}, \partial^{\nu} A_{\nu}^{\beta}(0) \right] | 0 \rangle \end{aligned} \quad (6.38)$$

for $\alpha, \beta = 1, \dots, 8$ and

$$\begin{aligned} & \int d^4x \partial^{\mu} \langle 0 | T \left\{ \tilde{A}_{\mu}^{\alpha}(x) \partial^{\nu} \tilde{A}_{\nu}^{\beta}(0) \right\} | 0 \rangle \\ &= \int d^4x \langle 0 | T \left\{ \partial^{\mu} \tilde{A}_{\mu}^{\alpha}(x) \partial^{\nu} \tilde{A}_{\nu}^{\beta}(0) \right\} | 0 \rangle + \langle 0 | \left[\tilde{Q}_5^{\alpha}, \partial^{\nu} \tilde{A}_{\nu}^{\beta}(0) \right] | 0 \rangle \end{aligned} \quad (6.39)$$

where the gauge dependent symmetry current appears in the latter identity.

(6.39) can be rewritten in terms of the gauge invariant operator $A_\mu^0(x)$ (125,141)

$$\begin{aligned} & \left\{ d^4x \partial^\mu \langle 0 | T \left\{ A_\mu^0(x) \partial^\nu \tilde{A}_\nu^0(o) \right\} | 0 \rangle \right. \\ & + \langle 0 | \left[\tilde{Q}_5^0, \partial^\nu \tilde{A}_\nu^0(o) \right] | 0 \rangle + \frac{2n_f}{\sqrt{6}} \frac{g^2}{32\pi^2} \left. \left\{ d^4x \langle 0 | T \left\{ F_a^{\mu\nu} \tilde{F}_{\mu\nu}^a(x) \partial^\nu A_\nu^0(o) \right\} | 0 \rangle \right\} \right. \\ & = \left. \left\{ d^4x \langle 0 | T \left\{ \partial_\mu A_\mu^0(x) \partial_\nu \tilde{A}_\nu^0(o) \right\} | 0 \rangle + \langle 0 | \left[\tilde{Q}_5^0, \partial^\nu \tilde{A}_\nu^0(o) \right] | 0 \rangle \right\} \right. \quad (6.40) \end{aligned}$$

where the substitution $\tilde{A}_\mu^0(x) = A_\mu^0(x) - \frac{2n_f}{\sqrt{6}} k_\mu$ has been used. This re-arrangement involves a definition of the time ordering operation applied to $F_a^{\mu\nu} \tilde{F}_{a\mu\nu}$

$$\frac{g^2}{32\pi^2} \langle 0 | T \left\{ F_a^{\mu\nu} \tilde{F}_{\mu\nu}^a(x) \partial^\nu \tilde{A}_\nu^0(o) \right\} | 0 \rangle = \partial^\mu \langle 0 | T \left\{ k_\mu(x) \partial^\nu A_\nu^0(o) \right\} | 0 \rangle \quad (6.41)$$

a point discussed in detail by Crewther, reference 141.

When the chiral symmetry of the QCD Lagrangian is explicitly broken by the introduction of quark mass terms the pseudoscalar Goldstone bosons which couple to the physical currents contained in the left-hand side of (6.38) and (6.40) acquire a mass, so the terms containing these currents vanish (125,153)

$$\left\{ d^4x \partial^\mu \langle 0 | T \left\{ A_\mu^\alpha(x) \partial^\nu A_\nu^\beta(o) \right\} | 0 \rangle \right. = \left. \left\{ d^4x \partial^\mu \langle 0 | T \left\{ A_\mu^0(x) \partial^\nu \tilde{A}_\nu^0(o) \right\} | 0 \rangle \right\} = 0 \quad (6.42)$$

yielding

$$\left\{ d^4x \langle 0 | T \left\{ \partial_\mu A_\mu^\alpha(x) \partial^\nu A_\nu^\beta(o) \right\} | 0 \rangle \right. = - \left. \langle 0 | \left[\tilde{Q}_5^\alpha, \partial^\nu A_\nu^\beta(o) \right] | 0 \rangle \quad (6.43a)$$

$$\text{and} \quad \int d^4x \langle 0 | T \left\{ \partial^\mu A_\mu^0(x) \partial^\nu \tilde{A}_\nu^0(0) \right\} | 0 \rangle = - \langle 0 | \left[\tilde{Q}_5^0, \partial^\nu \tilde{A}_\nu^0(0) \right] | 0 \rangle \quad (6.43b)$$

In precisely the same manner the "mixed" Ward identity can be derived

$$\int d^4x \langle 0 | T \left\{ \partial^\mu A_\mu^\alpha(x) \partial^\nu A_\nu^\beta(0) \right\} | 0 \rangle = - \langle 0 | \left[\tilde{Q}_5^\alpha, \partial^\nu A_\nu^\beta(0) \right] | 0 \rangle \quad (6.43c)$$

These three equations can be re-expressed in a general form,

$$\int d^4x \langle 0 | T \left\{ \partial^\mu A_\mu^\alpha(x) \partial^\nu A_\nu^\beta(0) \right\} | 0 \rangle = - \langle 0 | \left[\tilde{Q}_5^\alpha, \partial^\nu A_\nu^\beta(0) \right] | 0 \rangle \quad (6.44)$$

with α and β now taking on values $\alpha, \beta = 0, 1, \dots, 8$, with the two important conditions

(i) when $\alpha = 0$, \tilde{Q}_5^α is replaced by \tilde{Q}_5^0 and

(ii) when $\beta = 0$, $\partial^\nu A_\nu^\beta(0)$ is replaced by $\partial^\nu \tilde{A}_\nu^0(0)$.

The equations involving the required pseudoscalar decay constants are obtained from (6.44) by assuming that the vacuum expectation value on the left-hand side is dominated by single particle pseudoscalar intermediate states^(33,125,154). Using the definitions (6.2) and (6.23) and denoting the intermediate states by P this is evaluated to give

$$\int d^4x \langle 0 | T \left\{ \partial^\mu A_\mu^\alpha(x) \partial^\nu A_\nu^\beta(0) \right\} | 0 \rangle = - i \sum_P M_P^2 F_{\alpha P} F_{\beta P} \quad (6.45)$$

$$\text{and} \quad i \sum_P M_P^2 F_{\alpha P} F_{\beta P} = \langle 0 | \left[\tilde{Q}_5^\alpha, \partial^\nu A_\nu^\beta(0) \right] | 0 \rangle \quad (6.46)$$

The sum over P contained in (6.46) occurs because of the SU(2) (isospin) and SU(3) violation observed in the particle spectrum. The SU(3) violating mixing of octet and singlet A_μ^0 and A_μ^8 to produce the physical η and η'

operators implies that $\partial^\mu A_\mu^8$, for example, will connect both the η and η' pseudoscalar states with the vacuum. Isospin violations produce similar connections. As an example consider the mixed identity with $\alpha = 0, \beta = 8$

$$i (M_\pi^2 F_{0\pi} F_{8\pi} + M_\eta^2 F_{0\eta} F_{8\eta} + M_{\eta'}^2 F_{0\eta'} F_{8\eta'}) = \langle 0 | \left[\tilde{Q}_5^0, \partial^\nu A_\nu^8(0) \right] | 0 \rangle$$

where $\partial^\mu A_\mu^8$ and $\partial^\mu A_\mu^0$ connect η, η' and π^0 states with the vacuum. The contributions from the isospin violating $F_{0\pi}$ and $F_{8\pi}$ are much smaller than those obtained from the SU(3) violating $F_{8\eta}, F_{8\eta'}, F_{0\eta}$ and $F_{0\eta'}$, and in future applications such terms will be dropped.

The only problem which remains is to evaluate the commutator contained on the right-hand side of (6.46). This is performed in the standard way by noting⁽³³⁾

$$\partial^\nu A_\nu^\beta(0) = i \left[H_{SB}, Q_5^\beta \right] \quad (6.47)$$

and substituting the relevant expression for the symmetry breaking Hamiltonian H_{SB} . In order to keep the number of unknowns in the problem to a minimum, H_{SB} is written as before

$$H_{SB} = m_u \bar{u}u + m_d \bar{d}d + m_s \bar{s}s \quad (6.48)$$

and the commutator evaluated in terms of the three renormalisation invariant quantities⁽¹²⁵⁾ $m_q \langle 0 | \bar{q}q | 0 \rangle$ with $q = u, d, s$. In the general case the commutator is given by

$$\left[Q_5^\alpha, \partial^\nu A_\nu^\beta(0) \right] = -\frac{i\bar{q}}{4} \left[(\lambda^\beta M \lambda^\alpha + \lambda^\beta \lambda^\alpha M) \delta_{\beta\alpha} + (\lambda^\alpha M \lambda^\beta + M \lambda^\alpha \lambda^\beta) \delta_{\alpha\beta} \right] q \quad (6.49)$$

where (6.20), (6.47) and (6.48) have been employed and repeated use made

of the quark field anti-commutation relations

$$\left\{ q_i(\vec{x}, t), q_j(\vec{y}, t) \right\} = \left\{ q_i^\dagger(\vec{x}, t), q_j^\dagger(\vec{y}, t) \right\} = 0$$

$$\left\{ q_i^\dagger(\vec{x}, t), q_j(\vec{y}, t) \right\} = \delta_{ij} \delta^3(\vec{x} - \vec{y}) \quad (6.50)$$

In this notation $\delta_{\alpha\beta}$ implies that the corresponding elements in the column and row vectors obtained from $\lambda^\alpha q$ and $\bar{q} \lambda^\beta$ must contain quarks or anti-quarks of the same flavour.

Substituting the relevant SU(3) Gell-Mann matrices in (6.49) evaluates the right-hand side of (6.46) yielding the following equations for the pseudoscalar decay constants,

$$M_\pi^2 F_\pi^2 = -(m_u \langle \bar{u}u \rangle_0 + m_d \langle \bar{d}d \rangle_0)$$

$$M_{k^+}^2 F_k^2 = -(m_u \langle \bar{u}u \rangle_0 + m_s \langle \bar{s}s \rangle_0) \quad (6.51)$$

$$M_{k^0}^2 F_k^2 = -(m_d \langle \bar{d}d \rangle_0 + m_s \langle \bar{s}s \rangle_0)$$

$$M_\pi^2 F_{8\pi}^2 + M_\eta^2 F_{8\eta}^2 + M_{\eta'}^2 F_{8\eta'}^2 = -1/3 (m_u \langle \bar{u}u \rangle_0 + m_d \langle \bar{d}d \rangle_0 + 4m_s \langle \bar{s}s \rangle_0)$$

$$M_\pi^2 F_{8\pi}^2 \tilde{F}_{0\pi} + M_\eta^2 F_{8\eta}^2 \tilde{F}_{0\eta} + M_{\eta'}^2 F_{8\eta'}^2 \tilde{F}_{0\eta'} = -\frac{2}{\sqrt{18}} (m_u \langle \bar{u}u \rangle_0 + m_d \langle \bar{d}d \rangle_0 - 2m_s \langle \bar{s}s \rangle_0) \quad (6.52)$$

$$M_\pi^2 F_{0\pi} F_{8\pi} + M_\eta^2 F_{0\eta} F_{8\eta} + M_{\eta'}^2 F_{0\eta'} F_{8\eta'} = -\frac{2}{\sqrt{18}} (m_u \langle \bar{u}u \rangle_0 + m_d \langle \bar{d}d \rangle_0 - 2m_s \langle \bar{s}s \rangle_0)$$

$$M_\pi^2 F_{0\pi} \tilde{F}_{0\pi} + M_\eta^2 F_{0\eta} \tilde{F}_{0\eta} + M_{\eta'}^2 F_{0\eta'} \tilde{F}_{0\eta'} = -\frac{2}{3} (m_u \langle \bar{u}u \rangle_0 + m_d \langle \bar{d}d \rangle_0 + m_s \langle \bar{s}s \rangle_0)$$

$$M_\pi^2 F_{3\pi} F_{8\pi} + M_\eta^2 F_{3\eta} F_{8\eta} + M_{\eta'}^2 F_{3\eta'} F_{8\eta'} = -\frac{1}{\sqrt{3}} (m_u \langle \bar{u}u \rangle_0 - m_d \langle \bar{d}d \rangle_0)$$

$$M_\pi^2 F_{\pi\pi} \tilde{F}_{0\pi} + M_\eta^2 F_{3\eta} \tilde{F}_{0\eta} + M_{\eta'}^2 F_{3\eta'} \tilde{F}_{0\eta'} = -\frac{2}{\sqrt{6}} (m_u \langle \bar{u}u \rangle_0 - m_d \langle \bar{d}d \rangle_0) \quad (6.53)$$

$$M_\pi^2 F_{0\pi} F_\pi + M_\eta^2 F_{0\eta} F_{3\eta} + M_{\eta'}^2 F_{0\eta'} F_{3\eta'} = -\frac{2}{\sqrt{6}} (m_u \langle \bar{u}u \rangle_0 - m_d \langle \bar{d}d \rangle_0)$$

where $\langle \dots \rangle_0$ denotes a vacuum expectation value. Equations (6.51) in which isospin violations in F_π and F_k are neglected, are used in (6.52) to replace the $m_q \langle \bar{q}q \rangle_0$ terms with experimentally determined values M_π , M_k , $F_\pi (= 0.093 \text{ GeV})$ and $F_k (= 0.114 \text{ GeV})$. The four equations in (6.52) are dominated by the products containing the SU(3) violating $F_{8\eta}$, $F_{8\eta}'$, $F_{0\eta}$, $F_{0\eta}'$, $\tilde{F}_{0\eta}$ and $\tilde{F}_{0\eta}'$ decay constants, the contributions from the isospin violating F_{0p} are negligible in comparison, their magnitudes being determined by (6.53).

An analysis of these equations can be conveniently segregated into two parts comprising (i) the solution of the SU(3) violating equations of (6.52) to give A_η and A_η' from which ρ can be calculated and (ii) the solution of the isospin violating equations (6.53) to give A_π and hence the ratio R.

6.4 SOLUTION OF THE SU(3) VIOLATING EQUATIONS

In order to calculate the ratios ρ and R a suitable form for the interpolating operator of (6.26) must be chosen. This is given by ^(146,148,149)

$$O_g = \frac{2n_f}{\sqrt{6}} \cdot \frac{g^2}{32\pi^2} F_a^{\mu\nu} \tilde{F}_{\mu\nu}^a \quad (6.54)$$

where the vacuum to pseudoscalar matrix elements are, from (6.25)

$$\langle 0 | \frac{2n_f}{\sqrt{6}} \cdot \frac{g^2}{32\pi^2} F_a^{\mu\nu} \tilde{F}_{\mu\nu}^a | P \rangle = M_{P P}^2 A_{P P} \quad (6.55)$$

Thus the ratio of decay widths

$$\frac{\Gamma(V_1 \rightarrow V_2 P_1)}{\Gamma(V_1 \rightarrow V_2 P_2)} = \left\{ \frac{P_1}{P_2} \right\}^3 \left\{ \frac{M_{P_1 P_1}^2 A_{P_1 P_1}}{M_{P_2 P_2}^2 A_{P_2 P_2}} \right\}^2 \quad (6.56)$$

where the relevant phase space factors are included (P_i represent the centre of mass momenta appropriate to the process).

Equations (6.52) can be rewritten using (6.51) by following the same procedure adopted in Chapter 2. These previous analyses in the constituent quark framework uncovered the inability of the models considered to adequately describe the meson states constructed from quarks of different flavours (K, D, etc.). Should a similar problem be present in this treatment the uncertainties expressed in Chapter 2 would also arise here, however, within the framework adopted their extent is, at present, unknown. Accepting this possible deficiency (6.52) become,

$$\begin{aligned}
 M_{\eta}^2 F_{8\eta}^2 + M_{\eta'}^2 F_{8\eta'}^2 &= \frac{1}{3} \left[2 F_k^2 (M_{k^0}^2 + M_{k^+}^2) - M_{\pi}^2 F_{\pi}^2 \right] \\
 M_{\eta}^2 F_{8\eta}^2 \tilde{F}_{\eta} + M_{\eta'}^2 F_{8\eta'}^2 \tilde{F}_{\eta'} &= -\frac{2}{\sqrt{18}} \left[F_k^2 (M_{k^0}^2 + M_{k^+}^2) - 2M_{\pi}^2 F_{\pi}^2 \right] \\
 M_{\eta}^2 F_{\eta}^2 F_{8\eta} + M_{\eta'}^2 F_{\eta'}^2 F_{8\eta'} &= -\frac{2}{\sqrt{18}} \left[F_k^2 (M_{k^0}^2 + M_{k^+}^2) - 2M_{\pi}^2 F_{\pi}^2 \right] \\
 M_{\eta}^2 F_{\eta}^2 \tilde{F}_{\eta} + M_{\eta'}^2 F_{\eta'}^2 \tilde{F}_{\eta'} &= \frac{1}{3} \left[F_k^2 (M_{k^0}^2 + M_{k^+}^2) + M_{\pi}^2 F_{\pi}^2 \right]
 \end{aligned} \tag{6.57}$$

These four equations contain six unknown decay constants. Of the two further constraints required for a complete solution, one is provided by (6.33), as dictated by the mixing scheme of (6.31), the other is obtained from Goldberg's result⁽¹⁴⁶⁾ for the ratio of $\eta \rightarrow 2\gamma$ to $\pi^0 \rightarrow 2\gamma$ decay widths.

The matrix element relevant to the radiative decay $P \rightarrow 2\gamma$ of a pseudo-scalar meson P is given by⁽¹¹⁴⁾

$$M = A_{P \rightarrow 2\gamma} \epsilon_{\alpha\beta\gamma\delta} P_1^\alpha \epsilon_1^{*\beta} P_2^\gamma \epsilon_2^{*\delta} \tag{6.58}$$

where P_i and ϵ_i are the momenta and polarisations respectively of the two final state photons. This yields a decay width

$$\Gamma(P \rightarrow 2\gamma) = \frac{M^2}{8} \cdot \frac{A_{P \rightarrow 2\gamma}}{4\pi} \tag{6.59}$$

Experimental values for such widths are

(i) $\pi^0 \rightarrow 2\gamma$; The particle data group tables⁽⁶¹⁾ give $\Gamma(\pi^0 \rightarrow 2\gamma) = 7.5 \pm 0.5$ eV,

(ii) $\eta \rightarrow 2\gamma$; Two values are reproduced in the particle data group tables⁽⁶¹⁾

$$(a) \Gamma(\eta \rightarrow 2\gamma) = 1.00 \pm 0.22 \text{ KeV}^{(155)} \quad (b) \Gamma(\eta \rightarrow 2\gamma) = 0.324 \pm 0.046^{(156)} \quad (6.60)$$

however, the latter result is quoted as an average.

Goldberg⁽¹⁴⁶⁾ has calculated the ratio of amplitude for $\eta' \rightarrow 2\gamma$, $\eta \rightarrow 2\gamma$ and $\pi^0 \rightarrow 2\gamma$ using low energy theorems to give

$$A_{\eta' \rightarrow 2\gamma} : A_{\eta \rightarrow 2\gamma} : A_{\pi^0 \rightarrow 2\gamma} = (F_{8\eta} S_3 - F_{0\eta} S_8) : (F_{0\eta'} S_8 - F_{8\eta'} S_3) : (F_{8\eta} F_{0\eta'} - F_{0\eta} F_{8\eta'}) \frac{S_3}{F_\pi} \quad (6.61)$$

where $(S_3, S_8, S_0) = \frac{\sqrt{3}}{18} (\sqrt{3}, 1, 2\sqrt{2})$. The required constraint for a solution to (6.57) is thus taken as

$$R_\eta \equiv \frac{A_{\eta \rightarrow 2\gamma}}{A_{\pi^0 \rightarrow 2\gamma}} = \frac{(F_{0\eta'} S_8 - F_{8\eta'} S_3) F_\pi}{(F_{8\eta} F_{0\eta'} - F_{0\eta} F_{8\eta'}) S_3} \quad (6.62)$$

Equations (6.33), (6.57) and (6.62) are most easily solved by employing the substitutions (6.32) in the equations which do not involve $\tilde{F}_{0\eta}$ or $\tilde{F}_{0\eta'}$, and solving for θ , F_η and $F_{\eta'}$. These will give the required $\tilde{F}_{0\eta}$ and $\tilde{F}_{0\eta'}$ using the remaining equations and thus A_η and $A_{\eta'}$, the gluonic components of the η and η' mesons. Solutions for F_η , $F_{\eta'}$, A_η , $A_{\eta'}$ and the predicted ρ are plotted as a function of R_η in Fig 6.1. The region of experimental values for ρ is superimposed on the plot indicating a preferred range of values for R_η and hence for the pseudoscalar decay constants. Choosing a value of $\rho = 4.0$ in the centre of its range, corresponding to $R_\eta = 1.1$ gives the following solution (all decay constants in GeV)

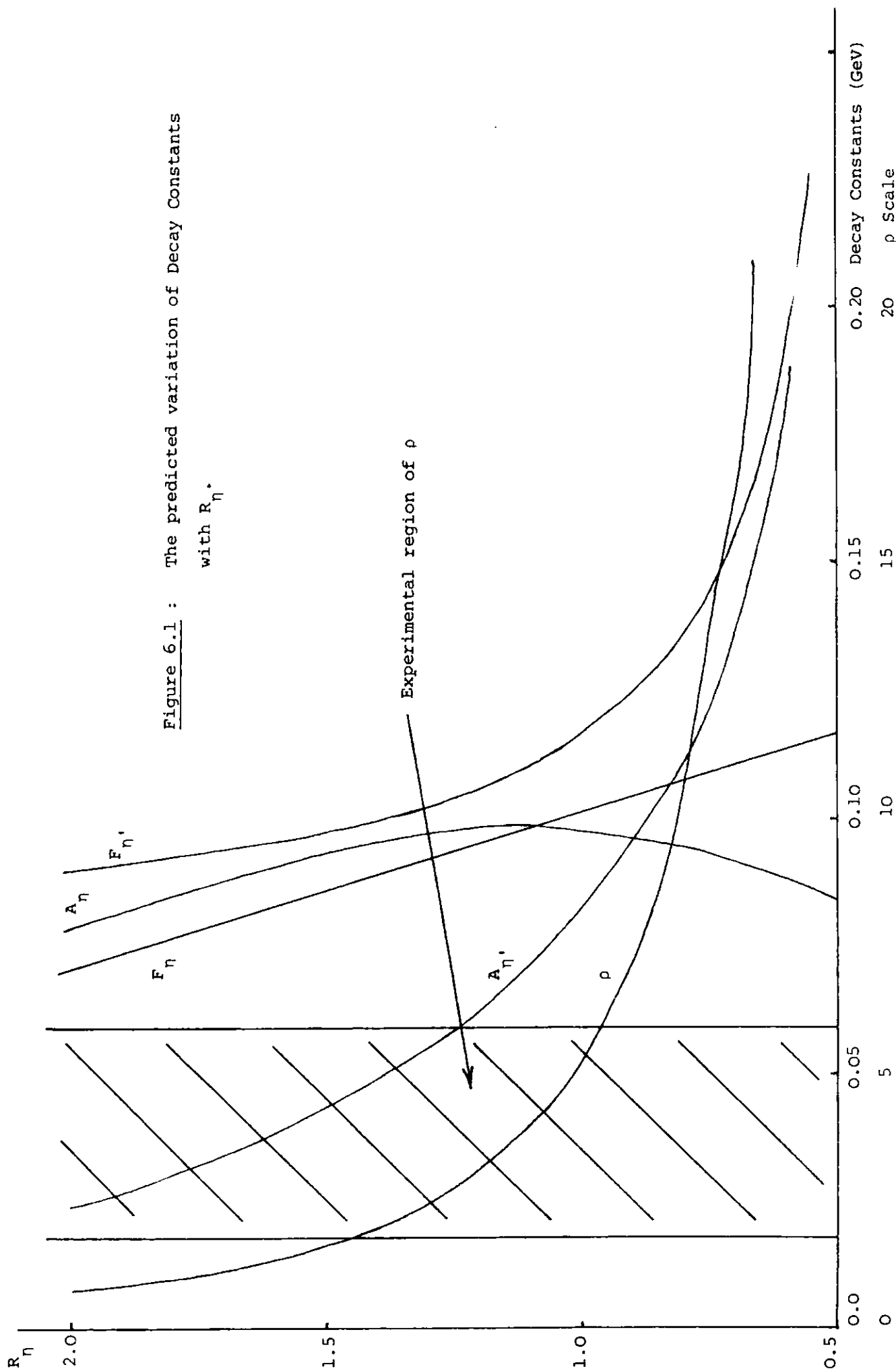


Figure 6.1 : The predicted variation of Decay Constants with R_η .

$$\begin{aligned}
 F_{\eta} &= 0.10 & F_{\eta'} &= 0.11 & \theta &= 23^{\circ} \\
 F_{8\eta} &= 0.09 & F_{8\eta'} &= -0.04 \\
 F_{\text{on}} &= 0.04 & F_{\text{on}'} &= 0.10 \\
 A_{\eta} &= 0.10 & A_{\eta'} &= 0.07
 \end{aligned}
 \tag{6.63}$$

This can be compared with results obtained from similar analyses of (i) Goldberg⁽¹⁴⁶⁾ and (ii) Williams and van Herwijnen⁽¹⁴⁷⁾ displayed in Table 6.1.

Decay Constant	(i)	(ii)	Decay Constant	(i)	(ii)
$F_{8\eta}$	0.10	0.11	$F_{\text{on}'}$	0.10	0.11
$F_{8\eta'}$	-0.02	-0.02	A_{η}	0.06	0.06
F_{on}	0.02	-0.02	$A_{\eta'}$	0.06	0.09

TABLE 6.1 : Results for Pseudoscalar decay constants obtained in analyses by (i) Goldberg and (ii) Williams and van Herwijnen. All values are quoted in GeV.

The values for $F_{8\eta}$ and $F_{\text{on}'}$ are similar in all cases, however, the 'mixing' decay constants which assume zero values in the SU(3) limit are a factor of $\times 2$ larger in magnitude than those obtained in (i) and (ii). This difference can be partially explained, for the results of (i), by the choice made for ρ . If a larger value of ρ had been chosen (Goldberg obtains $\rho = 7.3$ from (i)) the values of $F_{8\eta'}$ and F_{on} would be reduced. The discrepancy between the value of F_{on} obtained in (6.62) and that found in (ii) is not so obvious however, due to the sign difference which has a profound effect upon $A_{\eta} (= F_{\text{on}} - \tilde{F}_{\text{on}'})$ and hence $\rho (= 11.3$ from the results of (ii)). Williams

and van Herwijnen obtain their decay constants from a solution of (6.57) with two further constraints given by the ratios (6.60) whose experimental values are taken to be $A_{\eta' \rightarrow 2\gamma} : A_{\eta \rightarrow 2\gamma} : A_{\pi^0 \rightarrow 2\gamma} = 1.9 : 1.0 : 1.3$ obtained from $\Gamma(\eta \rightarrow 2\gamma) = 0.324 \pm 0.046 \text{ KeV}^{(156)}$ and $\Gamma(\eta' \rightarrow 2\gamma) = 5.9 \pm 2.8 \text{ KeV}^{(97)}$ with $\Gamma(\pi^0 \rightarrow 2\gamma) = 7.5 \pm 0.5 \text{ eV}^{(61)}$. The relative signs they find for $F_{8\eta}$, $F_{8\eta'}$, $F_{0\eta}$ and $F_{0\eta'}$ contradict (6.33) obtained from the mixing formalism.

Using the value for $\Gamma(\pi^0 \rightarrow 2\gamma)$ given above⁽⁶¹⁾ the solution (6.62) predicts (with $\rho = 4.0$)

$$\Gamma(\eta \rightarrow 2\gamma) = 0.61 \text{ KeV}$$

$$\Gamma_{\eta \rightarrow 2\gamma} = 3.1 \text{ KeV}$$

(6.64)

which are to be compared with (6.60) for $\Gamma(\eta \rightarrow 2\gamma)$ and

$$\begin{aligned} \Gamma(\eta' \rightarrow 2\gamma)_{\text{expt.}} &= 5.4 \pm 2.1 \text{ KeV}^{(96)} \\ &= 5.9 \pm 2.8 \text{ KeV}^{(97)} \end{aligned}$$

(6.65)

In view of the approximations made in deriving (6.61) these predictions are taken to be satisfactory.

6.5 SOLUTION OF THE ISOSPIN VIOLATING EQUATIONS

With the definition

$$M_1 \equiv m_d \langle \bar{d}d \rangle_0 - m_u \langle \bar{u}u \rangle_0 \quad (6.66)$$

for this isospin violating quantity the equations (6.53) can be rewritten

as

$$\begin{aligned} M_{\pi}^2 F_{\pi} F_{8\pi} + M_{\eta}^2 F_{3\eta} F_{8\eta} + M_{\eta'}^2 F_{3\eta'} F_{8\eta'} &= \frac{1}{\sqrt{3}} M_1 \\ M_{\pi}^2 \tilde{F}_{\pi} \tilde{F}_{0\pi} + M_{\eta}^2 \tilde{F}_{3\eta} \tilde{F}_{0\eta} + M_{\eta'}^2 \tilde{F}_{3\eta'} \tilde{F}_{0\eta'} &= \frac{2}{\sqrt{6}} M_1 \\ M_{\pi}^2 F_{0\pi} F_{\pi} + M_{\eta}^2 F_{0\eta} F_{3\eta} + M_{\eta'}^2 F_{0\eta'} F_{3\eta'} &= \frac{2}{\sqrt{6}} M_1 \end{aligned} \quad (6.67)$$

Footnote to page 132

The predictions $\Gamma(\eta' \rightarrow 2\gamma) = 3.1 \text{ KeV}$ made in the current quark framework is much smaller (approx. $\times \frac{1}{2}$) than the experimentally determined width. Electromagnetic decay widths of the η' predicted in chapter 4 using the constituent quark approach are, however, consistently larger than corresponding experimental widths (approx. $\times 2$). The electromagnetic decays of the η' perhaps allow a distinction between the two approaches.

These equations contain six unknowns $F_{8\pi}$, $F_{0\pi}$, $\tilde{F}_{0\pi}$, $F_{3\eta}$, $F_{3\eta'}$ and M_1 which can be reduced, with the aid of (6.32) to give three equations for $\lambda_{\pi\eta}$, $\lambda_{\pi\eta'}$ and $\tilde{F}_{0\pi}$ in terms of M_1 . To obtain a complete solution a further constraint is required. This is provided by the estimates of Langacker and Pagels for the isospin violating ratio $(m_d - m_u)/(m_d + m_u)$, as shown in Table 6.2.

Process	$(m_d - m_u)/(m_d + m_u)$
Kaon Mass difference ⁽¹²¹⁾	0.565
Baryon Mass difference ⁽¹²¹⁾	0.339
$\eta \rightarrow 3\pi$ ⁽¹²¹⁾	0.468
$\rho - \omega$ Mixing ⁽¹²²⁾	0.323

TABLE 6.2: Estimates for the Isospin violating ratio $(m_d - m_u)/(m_d + m_u)$

The values quoted are obtained by applying the techniques of chiral perturbation theory ^(34,157) to various processes which are sensitive to the required ratio. The calculations necessarily assumed SU(3) invariance of the vacuum expectation values of the bilinear products of quark fields as in equation (5.14). The magnitude of M_1 is obtained by using

$$M_{\pi}^2 F_{\pi}^2 = -(m_u \langle \bar{u}u \rangle_0 + m_d \langle \bar{d}d \rangle_0) \quad (6.68)$$

from (6.51), with (6.66) to give

$$M_1 = - \left\{ \frac{m_d - m_u}{m_d + m_u} \right\} M_{\pi}^2 F_{\pi}^2 \quad (6.69)$$

Equations (6.32), (6.67) and (6.69) provide the required solution, allowing a determination of $R = \Gamma(\psi' \rightarrow \pi^0 \psi) / \Gamma(\psi' \rightarrow n \psi)$. The variation of

R with the input value of M_1 is displayed in Fig 6.2, where the range of values obtained from Table 6.2 is included. To obtain agreement with the Mark II⁽¹³⁷⁾ and Crystal Ball⁽¹³⁸⁾ determinations of $R = (40 \pm 10) \times 10^{-3}$ and $(60 \pm 20) \times 10^{-3}$ a relatively large value of M_1 is required. Using the values in (6.63) for the isospin conserving decay constants, the largest value of M_1 given by Table 6.2 implies $R = 32 \times 10^{-3}$, a value of $R = 50 \times 10^{-3}$ consistent with both the Mark II and Crystal Ball results would require $M_1 = -0.70 M_{\pi\pi}^2$, indicating a considerable violation of SU(2) at the current quark level. The solution to (6.67) with $M_1 = -0.70 M_{\pi\pi}^2$ is

$$\begin{aligned}
 \lambda_{\pi\eta} &= 0.034 & \lambda_{\pi\eta'} &= 5.2 \times 10^{-3} & F_{0\pi} &= 1.7 \times 10^{-3} \\
 F_{3\eta} &= -3.3 \times 10^{-3} & F_{3\eta'} &= -5.8 \times 10^{-4} & F_{8\pi} &= 2.7 \times 10^{-3} \\
 \tilde{F}_{0\pi} &= -0.079 & A_{\pi} &= 0.081
 \end{aligned} \tag{6.70}$$

where all decay constants have dimensions of GeV.

The constituent quark model analysis of the strong isospin violating quark mass difference $\Delta = m_d - m_u$ yielded the value

$$(m_d - m_u)_{\text{constit.}} \approx 2.8 \text{ MeV} \tag{6.71}$$

If the constituent quark mass is defined loosely by

$$m_i^{\text{constit.}}(Q^2) \approx m_i^{\text{curr.}}(Q^2) + m_{\text{NP}}(Q^2) \tag{6.72}$$

and the non-perturbative contributions to the u and d quark masses are assumed to be equal then $\Delta^{\text{constit.}} \approx \Delta^{\text{curr.}}$ allowing the difference between current quark masses to be set approximately at

$$(m_d - m_u)_{\text{curr.}} \approx 2.8 \text{ MeV} \tag{6.73}$$

M_1 in units of $-M_\pi^2 F_\pi^2$

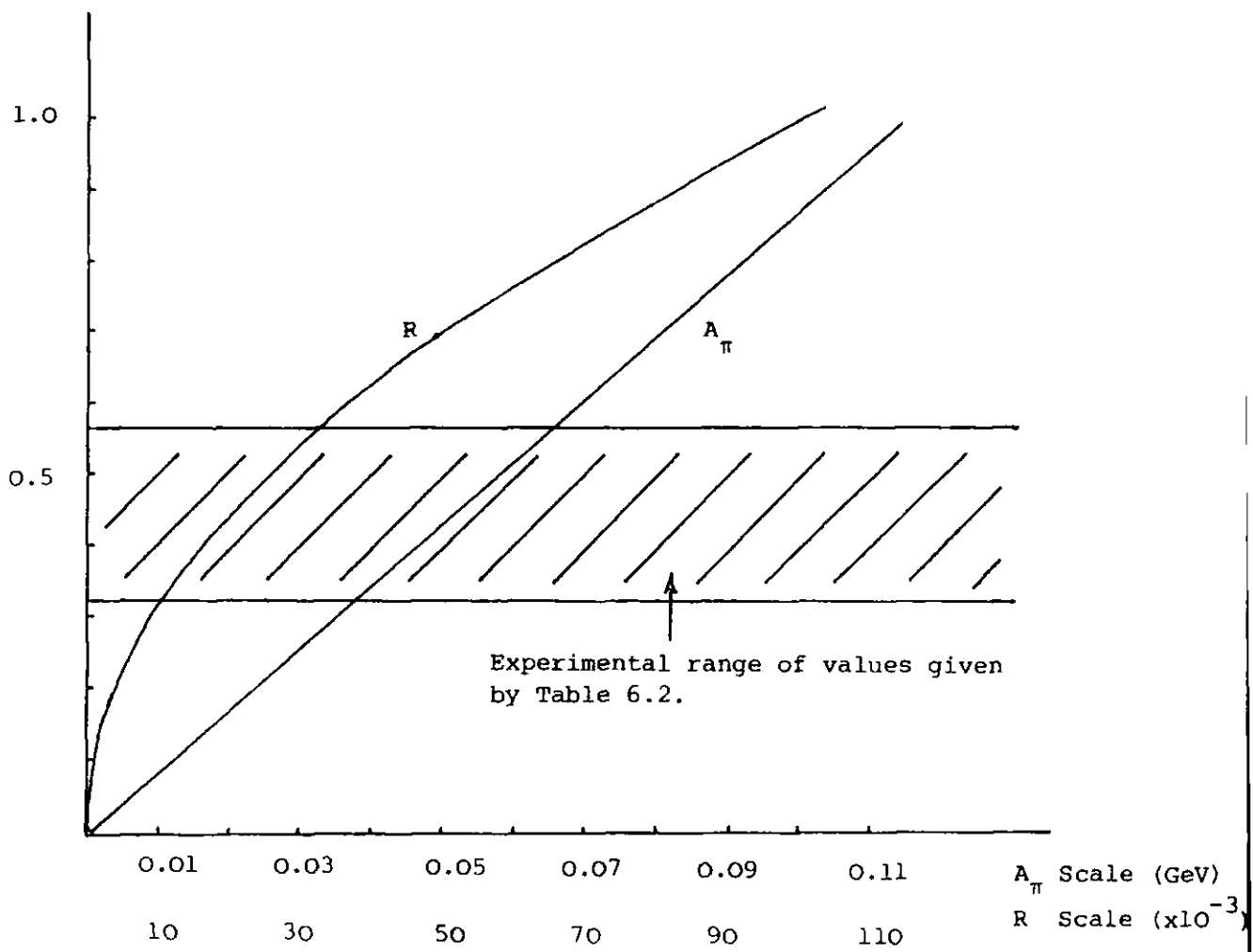


Figure 6.2 : The predicted variation of A_π and R with M_1

With $M_1 = -0.70 M_{\pi F \pi}^2$ (6.69) determines the individual current quark masses

$$m_d \approx 3.4 \text{ MeV}, \quad m_u \approx 0.6 \text{ MeV} \quad (6.74)$$

and (6.68) gives

$$\langle \bar{u}u \rangle_0 = \langle \bar{d}d \rangle_0 = \langle \bar{s}s \rangle_0 \approx -0.039 \text{ GeV}^3 \quad (6.75)$$

This quantity has been estimated using different methods by Shifman, Vainshtein and Zakharov⁽¹⁵⁸⁾ who find $\langle \bar{q}q \rangle_0 = -0.015 \text{ GeV}^3$.

Also, from (6.51)

$$m_s = 80 \text{ MeV} \quad (6.76)$$

If a smaller value of M_1 had been chosen, for example $M_1 = -0.50 M_{\pi F \pi}^2$ (corresponding to $R = 25 \times 10^{-3}$) then the following parameter values would have been obtained,

$$m_d = 4.2 \text{ MeV}; \quad m_u = 1.4 \text{ MeV}; \quad \langle \bar{q}q \rangle_0 = -0.03 \text{ GeV}^3; \quad m_s = 111 \text{ MeV}. \quad (6.77)$$

Thus, decreasing the level of isospin violation (as measured by M_1) produces an increase in the quark mass values and a corresponding decrease in $\langle \bar{q}q \rangle_0$. By demanding agreement with Shifman et al for the quantity $\langle \bar{q}q \rangle_0$ gives

$$m_u = 3.9 \text{ MeV}; \quad m_d = 6.7 \text{ MeV} \text{ and } m_s = 207 \text{ MeV} \quad (6.78)$$

Although these values appear respectable they give a poor value of $R \approx 10^{-2}$ for the ratio of the SU(2) to SU(3) violating decays of the ψ' .

CHAPTER 7SUMMARY AND CONCLUSIONS

Throughout this work various details of mixing models of the pseudo-scalar and vector mesons have been analysed, and where appropriate predictions of meson properties made using the model results. In Chapter 2 the construction of ground state mixing schemes is examined. The question of whether meson mixing is best described in terms of linear or quadratic masses is left open (the failure of early conventional linear mixing procedures being attributed to their inadequate description of meson structure) and the properties of both types of model investigated. The introduction of the quark-antiquark annihilation mechanism to the basic models explains qualitatively the differences between vector and pseudoscalar mixing. In the vector case where the annihilation interaction strength (A) is small compared to the $m_s - m_u$ mass difference an ideal mixing pattern results, however, when A and $m_s - m_u$ are of comparable magnitude, as in the pseudoscalar case, this pattern breaks down and considerable mixing occurs between the non-strange, $1/\sqrt{2} (u\bar{u} + d\bar{d})$, and purely strange, $s\bar{s}$, components. The vectors are well described in such schemes but an accurate quantitative description of the low mass pseudoscalars requires the annihilation interaction to take on a flavour dependence.

Including charmonium states in the analysis uncovers a deficiency in the model. The simple additive quark model approach where

$$M_{CC}^2 = 2M_D^2 - M_\pi^2 \quad (\text{quadratic}) \quad \text{or} \quad M_{CC} = 2M_D - M_\pi \quad (\text{linear}) \quad (7.1)$$

requires that the variation of annihilation parameters be such that $A_{CC} > A_{SS}$, which does not agree with the expectations of asymptotic freedom. Imposing $A_{uu} > A_{ss} > A_{cc}$ leads to the conclusion that mesons composed of unequal mass quarks are not adequately described by these simple models. The required

variation for A_{qq} can only be obtained by treating M_{ss} and M_{cc} as parameters which are determined by fitting to the Crystal Ball result⁽⁵⁴⁾ for the ratio $\rho = 5.88$ and the η_c mass. This approach induces an increase (decrease) in the magnitudes of M_{ss} and M_{cc} in the quadratic (linear) model when compared with their additive values as given by (7.1).

Mixing $c\bar{c}$ states in ground state models as out-lined in Chapter 2 cannot produced a complete description of meson structure since the many radial states which exist between the η' or ϕ and the charmonium levels will provide important contributions to meson wavefunctions via mixing with their ground states. Such mixing introduces the inert components in the η and η' wavefunctions which are necessary to explain the discrepancy in the strangeness exchange sum rule (3.2)⁽⁵⁶⁾. The radial mixing models of Cohen and Lipkin⁽⁵⁹⁾, described in Chapter 3, provide a reasonable description of the low mass mesons but fail, in the linear case, to reproduce the ψ - η_c splitting. The reasons for this failure appear to lie in the incomplete description of the flavour dependence of the annihilation and hyperfine interaction terms. By including the mass variation of the interaction strengths A and B the ψ - η_c splitting is easily accommodated, however, such an extension of the model necessitates the inclusion of further constraints to fix the values of the increased number of parameters. As with the ground-state models the Crystal Ball value of ρ is chosen for this purpose.

Including radial excitations in the mixing model prescriptions has a radical effect upon the predicted value of ρ , its magnitude suffering a considerable reduction compared with the ground state model predictions when the same S quark mass is used. The sensitive dependence of ρ upon the magnitude of m_s is exploited in the extended radial models described in Chapter 3 to force the prediction of ρ to coincide with its Crystal Ball value. This is achieved in both quadratic and linear models by decreasing m_s , however, such a reduction produces a poor prediction for the Kaon mass

in the quadratic case and leads to a mass variation of the annihilation strengths inconsistent with that expected from first order perturbative QCD in the linear case. Analyses of both models in Chapter 3 indicates that a mixing prescription which would provide an adequate description of the meson mass spectra in a manner consistent with first order perturbative QCD requires a value of ρ less than the Crystal Ball value.

Further problems are encountered when the linear model is used to describe the structure of the K, K^*, D, D^*, F and F^* states. Assuming the hyperfine splitting strengths appropriate to this $I \neq 0$ sector of the mass matrix are given by factorising the $I = 0$ results produces poor mass predictions for these particles. As in the ground-state case this problem could be caused by an over simplistic description of meson structure. That this may be the case is indicated by the empirical dependence of $|\psi_n(0)|$ upon n . The log potential model, from which the $|\psi_n(0)|^2 \sim 1/n$ variation used in the Cohen and Lipkin models is derived, provides an adequate description of the charmonium and upsilonium mass spectra, however, it is not clear that such a variation should be appropriate to the lower mass states. The experimental results for $V \rightarrow e^+e^-$ decays quoted in Chapter 3 indicate that the fall off of $|\psi_n(0)|$ with n is much less rapid for those states with a low mass than for those with higher masses. In the language of potential models this suggests that the lighter, more relativistic quarks, experience more of the linear confining potential which gives $|\psi_n(0)|^2 \sim \text{constant}$ than the heavier quarks which are influenced more by the $1/r$ Coulomb potential for which $|\psi_n(0)|^2 \sim 1/n^3$.

The inability of the extended mixing models described in Chapter 3 to fit both the pseudoscalar mass spectrum and the Crystal Ball measurement of ρ suggests a model preference for a smaller value of the latter quantity. In Chapter 4 the experimental status of this ratio is reviewed and a linear mixing analysis conducted to find the preferred value. The magnitude of ρ is determined by exploiting its sensitive dependence on the structure of $\eta-\eta'$ mixing and hence upon the strange quark mass m_s . Thus, when model

predictions for quantities which also depend strongly upon the η - η' mixing pattern are compared with experiment for each of the five present experimental values of ρ , a model preferred value is determined.

Attention is concentrated on the predictions for the radiative $V \rightarrow P\gamma$ and $P \rightarrow V\gamma$ decays, of which $\rho \rightarrow \eta\gamma$, $\omega \rightarrow \eta\gamma$ and $\phi \rightarrow \eta\gamma$ are of particular interest. The results displayed in Table 4.6 indicate that agreement between model predictions and experiment for the widths of these processes is best for values of ρ less than the Crystal Ball result. A precise value of $\rho = 3.1$ is determined by requiring the predicted magnitude of $\bar{\sigma}(\pi^- p \rightarrow \eta' n) / \bar{\sigma}(\pi^- p \rightarrow \eta n)$ to coincide with its experimental value as given by Stanton et al⁽⁹⁴⁾.

Predictions are also made for the masses of the radially excited pseudoscalar and vector states. The first excitations of the η and η' occur at 1.36 and 1.50 GeV respectively, the former value being close to that found by a recent Crystal Ball experiment⁽⁸¹⁾. The corresponding vector excitations of the ρ , ω and ϕ are predicted at 1.33, 1.34 and 1.59 GeV respectively. Experimental candidates for the ρ' and ϕ' exist, however no such ω' state has yet been observed. The experimentally well established $I = 1$ state with $M \approx 1600$ MeV is confirmed as the second radial excitation of the ρ .

The unitary spin wavefunctions obtained by diagonalising the linear mass matrix in Chapter 4 are also used to determine the changes induced in the strangeness exchange sum rule (3.2). The approximate agreement between experiment and theory, noted by Lipkin⁽⁵⁹⁾, which is achieved by including radial excitations in the pseudoscalar mixing scheme is further enhanced when the full flavour dependence of the interaction terms is included in the model. Also, by using an additivity procedure similar to that encountered in the derivation of (3.2) the strong two body decay amplitudes of the vector mesons are expressed in terms of the more fundamental strong $q\bar{q}$ production amplitudes. Relations among these are determined by applying G-parity and

SU(3) selection rules, allowing predictions to be made. The close agreement between experiment and the results obtained for the ground state $V \rightarrow PP$ decays justifies an investigation of similar decays of the radially excited vectors. The relationships between the decay widths for such processes are determined in Chapter 4. Accepting the uncertainties in the predictions made in this chapter resulting from the extrapolation of excitation energies from the charmonium to lower mass regions and the non-relativistic nature of the calculations, the broad agreement observed with experiment is taken to be satisfactory.

In Chapter 5 the linear mixing model with wavefunctions and parameter values as determined in Chapter 4, is used as a framework for an investigation of the suggestion that isospin is an accidental symmetry of the hadronic spectrum. The violation of isospin by the strong interactions is manifest in the magnitude of the quark mass difference $\Delta = m_d - m_u$. Δ and isospin violating electromagnetic interaction terms are included in the Hamiltonian appropriate to the linear mixing model. Diagonalisation of the resulting mass matrix in the vector and pseudoscalar sectors allows the determination of isospin violating mixing angles and meson isomultiplet mass differences. The magnitudes of the additions to the Hamiltonian are determined by comparing model predictions for the mass differences $M_{\pi^+} - M_{\pi^0}$, $M_{K^+} - M_{K^0}$ and $M_{D^+} - M_{D^0}$ with experiment to yield a value of 2.78 MeV for the strong constituent mass difference $m_d - m_u$. This agrees well with the independent determination of $\Delta \approx 3$ MeV obtained in 5.3 using a combination of current algebra and constituent quark model approaches.

The isospin violating parameters found in this manner are subsequently used to predict the vector isomultiplet mass differences displayed in Table 5.1, and the magnitudes of $B(\omega \rightarrow 2\pi)$ and $R \equiv \Gamma(\psi' \rightarrow \pi^0\psi) / \Gamma(\psi' \rightarrow \eta\psi)$. The predicted value of $B(\omega \rightarrow 2\pi) = 0.018$ is in close agreement with experiment, however, that for the ratio $R = 17 \times 10^{-3}$ is a factor of X2 to X3

smaller than its present experimental value as determined by the Mark II⁽¹³⁷⁾ and Crystal Ball⁽¹³⁸⁾ collaborations. The calculations emphasize the importance of the strong contribution to these isospin violating processes. For both $B(\omega \rightarrow 2\pi)$ and R approximately 80% of the contribution to the relevant amplitudes is given by the strong isospin violating term Δ . A further interesting point raised in the determination of R concerns the relative importance of $\pi^0-\eta$, $\pi^0-\eta'$ and $\pi^0-\eta_c$ mixing contributions. The suppression of the $\pi^0-\eta_c$ mixing angle when compared with that for $\pi^0-\eta$ mixing is compensated by the relatively greater amount of $c\bar{c}$ in the η_c wavefunction, to the extent that the $\pi^0-\eta_c$ contribution dominates in the prediction for R .

A close study of the ratios ρ and R in the constituent quark framework has allowed a quantitative estimate of the symmetry violation which occurs in constituent quark models of mesons. In Chapter 6 these ratios are examined using current algebra and PCAC techniques, and again allow a measure of symmetry violation as expressed by the different values assumed by the various current quark mass and pseudoscalar decay parameters. Relationships between the pseudoscalar meson masses and decay constants are derived using axial vector Ward Identities as outlined in Appendix 4. The poor predictions for the η' mass, $M_{\eta'} \leq \sqrt{3} M_{\pi}$ and the unacceptably large estimates of observable isospin violations (the $U(1)$ problems) are avoided by including the triangle anomaly contribution in the divergence of the $U(1)$ axial current and noting that the topological structure of the QCD vacuum implies that this anomaly will add to the mass of the $U(1)$ pseudoscalar, and hence, through symmetry breaking, to the $SU(3)$ $|8\rangle$ and $|\pi^0\rangle$ states also.

The equations which relate pseudoscalar masses and decay constants are conveniently separated into $SU(3)$ (but not $SU(2)$) and $SU(2)$ violating forms. The $SU(3)$ violating equations are solved for the pseudoscalar decay constants, $F_{\alpha P}$, by including Goldberg's analysis⁽¹⁴⁶⁾ of $A(\eta \rightarrow 2\gamma)/A(\pi^0 \rightarrow 2\gamma)$

and the ratio ρ in the problem. By using the Particle Data Group average value for the former ratio and choosing $\rho \approx 4.0$ the magnitudes of $F_{\alpha P}$ obtained compare favourably with those found by Goldberg in a similar analysis, and, considering the approximations made provide a satisfactory prediction of $\Gamma(\eta' \rightarrow 2\gamma) \approx 3.1 \text{ KeV}$.

The SU(3) violating $F_{\alpha P}$ are used in the SU(2) violating equations to predict the magnitude of R. The isospin violating decay constants are expressed in terms of

$$M_1 = - \left(\frac{m_d - m_u}{m_d + m_u} \right) M_\pi^2 F_\pi^2 \quad (7.2)$$

which has been previously determined from, for example, $\eta \rightarrow 3\pi$ decay, or ρ - ω mixing (see Table 6.2). An average value for $M_1 \approx -0.4 F_\pi^2 M_\pi^2$ yields pseudoscalar decay constants which determine $R \approx 16 \times 10^{-3}$, in agreement with the constituent quark model predictions of Chapter 5 but a factor of X2 to X3 smaller than present experimental results. If the predicted ratio is forced to agree with experiment a large degree of isospin violation is imposed on the model. M_1 then equals $-0.7 M_\pi^2 F_\pi^2$, a value much greater than any previous estimates.

Combining the isospin violating results of Chapters 5 and 6 allows a rough estimate of the current quark mass parameters $m_i(Q^2)$ at a value of Q^2 appropriate to the problem. It is found that with $M_1 = -0.70 M_\pi^2 F_\pi^2$ the $m_i(Q^2)$ have unusually small values, $m_u \approx 0.6$, $m_d \approx 3.4$, and $m_s \approx 80 \text{ MeV}$, much less than estimates by previous authors. Decreasing M_1 to values in line with other analyses increases the $m_i(Q^2)$ to give, for example, for $M_1 = -0.4 M_\pi^2 F_\pi^2$, $m_u \approx 2.1$, $m_d \approx 4.9$ and $m_s \approx 145 \text{ MeV}$, which are reasonably consistent with other current algebra estimates. Thus, the approaches of both Chapters 5 and 6 point to a consistent value of the isospin violating ratio R which is at least a factor of X2 less than its experimental determination.

The roles played by the annihilation interaction in the constituent quark framework and the triangle anomaly in the current quark approaches to meson masses are directly analogous. In Chapter 2 it was noted that in the absence of annihilation contributions to the mass matrix the η' was predicted to have a mass coincident with the π . Likewise, if the anomaly is ignored in the current algebra treatment in Chapter 6, the η' mass is upper bounded by $M_{\eta'} \leq \sqrt{3} M_{\pi}$. In both approaches the annihilation interaction, or anomaly, adds to the mass of the SU(3) singlet state, thus increasing $M_{\eta'}$, and allowing a description of the pseudoscalar mass spectrum consistent with experiment. These interaction terms also play an identical role in determining the structure of the unitary spin wavefunctions. In their absence, and with the condition $m_u < m_d < m_s$, the pseudoscalar nonet contains three non-strange states with the structure $u\bar{u}$, $d\bar{d}$ and $s\bar{s}$. If such states were manifest in the physical spectrum large violations of isospin would be observed in the particle masses, as noted in Chapter 6. This problem is circumvented when the annihilation, or anomaly, contributions are included. The structure of the unitary spin wavefunctions are determined by the relative magnitudes of the annihilation (or anomaly) mass contributions, denoted collectively by A , and the difference between the constituent (or current) quark masses. Three cases are of interest,

(i) If $A \ll m_d - m_u \ll m_s - m_d$ the three non-strange nonet states would essentially retain their $u\bar{u}$, $d\bar{d}$ and $s\bar{s}$ character.

(ii) With $m_d - m_u \ll A \ll m_s - m_d$ an approximation to the ideal mixing situation would be observed. Ideal mixing is obtained when $m_d = m_u$ and $A \ll m_s - m_d$.

(iii) $m_d - m_u \ll A \approx m_s - m_u$, which represents the physical case. This condition ensures the approximate equality of the magnitudes of $u\bar{u}$ and $d\bar{d}$ contributions to meson wavefunctions and hence the suppression of observable isospin violations in the mass spectra to their experimental level.

Thus, it is seen that the annihilation and anomaly contributions in their respective frameworks are essential to an understanding of the properties of pseudoscalar mesons.

APPENDIX 1 - CONVENTIONS

Contravariant 4-vectors are denoted by $x^\mu = (x^0, x^1, x^2, x^3)$. The corresponding covariant form is $x_\mu = g_{\mu\nu} x^\nu$ where the metric tensor is defined by

$$g_{00} = -g_{11} = -g_{22} = -g_{33} = 1$$

and

$$g_{\mu\nu} = g^{\mu\nu} = 0 \text{ for } \mu \neq \nu$$

The conventions of Bjorken and Drell⁽¹⁶³⁾ are adopted for Dirac γ matrices which obey the anticommutation relations

$$\{\gamma^\mu, \gamma^\nu\} \equiv \gamma^\mu \gamma^\nu + \gamma^\nu \gamma^\mu = 2g^{\mu\nu}$$

and $\gamma^{0\dagger} = \gamma^0$, $\gamma^{k\dagger} = -\gamma^k$ with $k = 1, 2, 3$. The γ_5 matrix is defined by

$$\gamma_5 \equiv \gamma^5 = i\gamma^0 \gamma^1 \gamma^2 \gamma^3$$

The eight Gell-Mann matrices of SU(3) are

$$\lambda_1 = \begin{pmatrix} 0 & 1 & 0 \\ 1 & 0 & 0 \\ 0 & 0 & 0 \end{pmatrix} \quad \lambda_2 = \begin{pmatrix} 0 & -i & 0 \\ 1 & 0 & 0 \\ 0 & 0 & 0 \end{pmatrix} \quad \lambda_3 = \begin{pmatrix} 1 & 0 & 0 \\ 0 & -1 & 0 \\ 0 & 0 & 0 \end{pmatrix}$$

$$\lambda_4 = \begin{pmatrix} 0 & 0 & 1 \\ 0 & 0 & 0 \\ 1 & 0 & 0 \end{pmatrix} \quad \lambda_5 = \begin{pmatrix} 0 & 0 & -i \\ 0 & 0 & 0 \\ 1 & 0 & 0 \end{pmatrix} \quad \lambda_6 = \begin{pmatrix} 0 & 0 & 0 \\ 0 & 0 & 1 \\ 0 & 1 & 0 \end{pmatrix}$$

$$\lambda_7 = \begin{pmatrix} 0 & 0 & 0 \\ 0 & 0 & -i \\ 0 & i & 0 \end{pmatrix} \quad \lambda_8 = \frac{1}{\sqrt{3}} \begin{pmatrix} 1 & 0 & 0 \\ 0 & 1 & 0 \\ 0 & 0 & -2 \end{pmatrix}$$

satisfying the commutation

$$[\lambda^\alpha, \lambda^\beta] = 2if_{\alpha\beta\gamma} \lambda^\gamma$$

and anti-commutation

$$\{\lambda^\alpha, \lambda^\beta\} = \frac{4}{3} \delta_{\alpha\beta} + 2d_{\alpha\beta\gamma} \lambda^\gamma$$

relations respectively. The non-zero antisymmetric $f_{\alpha\beta\gamma}$ and symmetric $d_{\alpha\beta\gamma}$ are

$$f_{123} = 1 ; \quad f_{458} = f_{678} = \frac{\sqrt{3}}{2}$$

$$f_{147} = -f_{156} = f_{246} = f_{257} = f_{345} = -f_{367} = \frac{1}{2}$$

$$d_{118} = d_{228} = d_{338} = -d_{888} = \frac{1}{\sqrt{3}}$$

$$d_{448} = d_{558} = d_{668} = d_{778} = \frac{1}{2\sqrt{3}}$$

$$d_{146} = d_{157} = -d_{247} = d_{256} = d_{344} = d_{355} = -d_{366} = d_{377} = \frac{1}{2}$$

Throughout the calculations of Chapter 6 covariant normalisation of physical states is chosen such that

$$\langle \vec{p}, \alpha | \vec{p}', \alpha' \rangle = 2E(2\pi)^3 \delta^3(\vec{p}-\vec{p}') \delta_{\alpha\alpha'}$$

where \vec{p} represents the momentum and α all the other quantum numbers necessary to specify a particular state. With such normalisation the completeness integrals are

$$\sum_p |p\rangle \langle p| = \int \frac{d^3p}{(2\pi)^3 2E}$$

APPENDIX 2 - INTERACTION PERTURBED SU(n) BASES

The discussion in Chapter 4 concerning the construction of meson unitary spin wavefunctions referred to two possible modes of their expression. The wavefunctions were written firstly in the $q\bar{q}$ basis of states as obtained from the direct diagonalisation of equation (4.1), and then later, in order to facilitate a comparison with more conventional schemes, in terms of an interaction perturbed SU(3) basis of states (ignoring $c\bar{c}$ contributions), where the particle wavefunction was expressed in terms of its octet and singlet components. The transposition of the state vectors from one basis to the other is straightforward once the interaction perturbed SU(3) basis, which necessarily involves the mixing of higher radial excitations with the ground state basis vectors, is defined. A convenient definition is provided by imposing the condition that the required basis states diagonalise the mass matrix (4.1) with $m_s \equiv m_u$, $B_{ss} \equiv B_{uu}$ and $A_{ss} \equiv A_{uu}$.

Results for the ground state ($n = 1$) are just the usual SU(3) eigenvectors given in Chapter 1. Increasing to $n = 4$ and hence mixing radial components in the ground state basis states, and vice versa, yields eigenvectors of the form

$$\begin{aligned} |\pi\rangle &= \sum_i \alpha_i |\pi\rangle_i \\ |8\rangle &= \sum_i \alpha_i |8\rangle_i \\ |1\rangle &= \sum_i \beta_i |1\rangle_i \end{aligned}$$

for each value of n where, with $i = 1, \dots, n$

$$|\pi\rangle_i \equiv \frac{1}{\sqrt{2}} |\bar{u}u - \bar{d}d\rangle_i, \quad |8\rangle_i = -\frac{1}{\sqrt{6}} |\bar{u}u + \bar{d}d - 2\bar{s}s\rangle_i, \quad |1\rangle_i = \frac{1}{\sqrt{3}} |\bar{u}u + \bar{d}d + \bar{s}s\rangle_i$$

and α_i and β_i give the radial expansion of octet and singlet states respectively. Using parameters obtained from the $\rho = 2.8$ fit the following results

for the ground-state eigenvectors are obtained

$$\alpha_1 = 0.922 \quad ; \quad \alpha_2 = 0.304 \quad ; \quad \alpha_3 = 0.190 \quad ; \quad \alpha_4 = 0.147$$

$$\beta_1 = 0.854 \quad ; \quad \beta_2 = -0.468 \quad ; \quad \beta_3 = 0.189 \quad ; \quad \beta_4 = -0.130$$

The hyperfine interaction is solely responsible for the non-zero values of $\alpha_2, \alpha_3, \alpha_4$, however, the mixing of radial components in the ground state SU(3) singlet state is caused by both the hyperfine and annihilation interactions, thus, while the values of α_i are identical for all fits performed those for β_i show a slight dependence upon ρ due to the variation of the magnitude of A_{uu} with this quantity.

In a completely analogous manner an SU(4) basis which includes the effects of radial excitations can be defined by including $c\bar{c}$ components in the mass matrix and diagonalising (4.1) with $m_c = m_s \equiv m_u$, $A_{cc} = A_{ss} \equiv A_{uu}$, $B_{cc} = B_{ss} \equiv B_{uu}$. Again, with $n = 1$ the usual ground state eigenvectors are obtained

$$|\pi^0\rangle = \frac{1}{\sqrt{2}} (u\bar{u} - d\bar{d}) \quad \quad \quad |\eta_8\rangle = -\frac{1}{\sqrt{6}} (u\bar{u} + d\bar{d} - 2s\bar{s})$$

$$|\chi\rangle = \frac{1}{\sqrt{12}} (u\bar{u} + d\bar{d} + s\bar{s} - 3c\bar{c}) \quad \quad \quad |1\rangle = \frac{1}{2} (u\bar{u} + d\bar{d} + s\bar{s} + c\bar{c})$$

where $|\eta_8\rangle$ and $|\chi\rangle$ are isoscalar states belonging to the 15 of SU(4) and $|1\rangle$ is the SU(4) singlet state. For $n = 4$ the radial expansion of the ground state 15-plet is again set by that of the π^0 with the result

$$\begin{aligned} |\pi\rangle &= \sum_i \alpha_i |\pi\rangle_i \\ |\eta_8\rangle &= \sum_i \alpha_i |\eta_8\rangle_i \\ |\chi\rangle &= \sum_i \alpha_i |\chi\rangle_i \\ |1\rangle &= \sum_i \beta_i |1\rangle_i \end{aligned}$$

where the α_i are as above and $\beta_1 = 0.808$; $\beta_2 = -0.534$; $\beta_3 = -0.206$; $\beta_4 = -0.140$. Although α_i can be obtained directly from the π^0 wavefunction it is necessary to diagonalise the mass matrix to obtain the β_i .

The transposition of physical wavefunctions from a $qq\bar{q}$ basis to an interaction perturbed SU(3) or SU(4) basis can be made by noting the following definitions

$$\begin{aligned}\psi_{\text{phys}} &\equiv U\psi_{qq\bar{q}} \\ &\equiv X\psi_{\text{SU}(n)} = XY\psi_{qq\bar{q}} \quad (n = 3,4)\end{aligned}$$

where

$$\psi_{\text{SU}(n)} = Y\psi_{qq\bar{q}}$$

Thus, the required matrix X is given by

$$X = UY^{-1}$$

where both U and Y are known.

Particle wavefunctions of interest are expressed in the SU(3) basis in Table 4.4. Including the charmed quark in the analysis gives corresponding wavefunctions in the SU(4) basis as

$$|\pi^0\rangle = |\pi^0_1\rangle$$

$$|\eta\rangle = 0.972|\eta_8\rangle_1 + 0.077|\chi\rangle_1 + 0.158|1\rangle_1$$

$$|\eta'\rangle = 0.213|\eta_8\rangle_1 - 0.338|\chi\rangle_1 - 0.816|1\rangle_1$$

APPENDIX 3 - UNITARY SPIN WAVEFUNCTIONS

The full unitary spin wavefunctions with radial contributions up to $n = 4$ as obtained from the $\rho = 2.8$ fit are listed for both pseudoscalar and vector mesons.

(i) $I_3 \neq 0$ Mesons

Denoting a general wavefunction for a pseudoscalar or vector meson by $\sum_i a_i |q_i \bar{q}_i\rangle$, the $I_3 \neq 0$ K, D, F, K^* , D^* and F^* wavefunctions are constructed using the coefficients in Table 1.

Meson	a_1	\hat{a}_2	a_3	a_4
π	0.922	0.304	0.190	0.147
K	0.951	0.247	0.148	0.113
D	0.994	0.091	0.050	0.037
F	0.997	0.066	0.035	0.026
ρ	0.985	-0.142	-0.068	-0.049
K^*	0.993	-0.103	-0.051	-0.036
D^*	0.999	-0.032	-0.016	-0.012
F^*	0.999	-0.022	-0.011	-0.008

TABLE 1 : Coefficients for $I_3 \neq 0$ meson wavefunctions

(ii) $I_3 = 0$ Mesons

Denoting a general unitary spin wavefunction by

$$\sum_i \left[u_i |u\bar{u}\rangle_i + d_i |d\bar{d}\rangle_i + s_i |s\bar{s}\rangle_i + c_i |c\bar{c}\rangle_i \right]$$

the particle wavefunctions are constructed using the coefficients in Tables 2, 3 and 4.

Note that the π^0 and ρ^0 coefficients can be evaluated using the charged π and ρ results in Table 1 where $u_i^{\pi^0} = -d_i^{\pi^0} = a_i^{\pi^+} / \sqrt{2}$. Also, for all isoscalar mesons $u_i = d_i$.

Meson	u_1	u_2	u_3	u_4
η	0.427	0.050	0.027	0.020
η'	-0.492	0.324	0.125	0.086
η_c	-0.019	-0.018	-0.018	-0.018
ω	0.694	-0.115	-0.055	-0.039
ϕ	0.030	-0.029	-0.010	-0.007
ψ	0.0	0.0	0.0	0.0

Table 2: $u\bar{u}$ and $d\bar{d}$
coefficients for
I = 0 mesons.

Meson	s_1	s_2	s_3	s_4
η	-0.748	-0.209	-0.126	-0.097
η'	-0.509	0.009	0.005	0.004
η_c	-0.014	-0.014	-0.014	-0.014
ω	-0.052	-0.008	-0.004	-0.003
ϕ	0.991	-0.101	-0.050	-0.036
ψ	0.0	0.0	0.0	0.0

Table 3: $s\bar{s}$ coefficients
for I = 0 mesons.

Meson	c_1	c_2	c_3	c_4
η	-0.003	-0.002	-0.001	-0.001
η'	0.005	0.003	0.002	0.002
η_c	-0.992	-0.091	-0.049	-0.037
ω	0.0	0.0	0.0	0.0
ϕ	0.0	0.0	0.0	0.0
ψ	0.999	-0.033	-0.017	-0.012

Table 4: $c\bar{c}$ coefficients
for I = 0 mesons.

APPENDIX 4

The method of calculation of meson masses (employed in Chapters 5 and 6) in terms of the current masses of their quark constituents using Current Algebra and PCAC techniques is outlined here. In all cases considered the meson masses can be evaluated from a mixed Ward Identity similar to that in (6.38),

$$\int d^4x \partial^\mu \langle 0 | T (A_\mu^\alpha(x) \partial^\nu A_\nu^\beta(0)) | 0 \rangle = \int d^4x \langle 0 | T (\partial^\mu A_\mu^\alpha(x) \partial^\nu A_\nu^\beta(0)) | 0 \rangle + \langle 0 | [Q_5^\alpha, \partial^\nu A_\nu^\beta(0)] | 0 \rangle \quad (1)$$

where $\alpha, \beta = 0, 1, \dots, 8$ with the conditions

- (i) when $\alpha = 0, Q_5^\alpha$ is replaced by \tilde{Q}_5^0 and
- (ii) when $\beta = 0, \partial^\nu A_\nu^\beta(0)$ is replaced by $\partial^\nu \tilde{A}_\nu^0(0)$

where, as described in Chapter 6,

$$A_\mu^0 = \tilde{A}_\mu^0 + \frac{2n_f}{\sqrt{6}} K_\mu \quad (2)$$

The left-hand side of (1) is expanded as follows

$$\int d^4x \partial^\mu \langle 0 | T (A_\mu^\alpha(x) \partial^\nu A_\nu^\beta(0)) | 0 \rangle = \int d^4x \partial^\mu \langle 0 | A_\mu^\alpha(x) \partial^\nu A_\nu^\beta(0) \theta(x^0) + \partial^\nu A_\nu^\beta(0) A_\mu^\alpha(x) \theta(-x^0) | 0 \rangle$$

Inserting a complete set of intermediate states with normalisation described in Appendix 1 gives

$$\begin{aligned}
 &= \sum_{\mathbf{P}} \int d^4x \left[\frac{d^3q}{2E_{\mathbf{P}}(2\pi)^3} \partial^\mu \left\{ \langle 0 | A_\mu^\alpha(0) e^{-iqx} | P \rangle \langle P | \partial^\nu A_\nu^\beta(0) | 0 \rangle \theta(x^0) \right. \right. \\
 &\quad \left. \left. + \langle 0 | \partial^\nu A_\nu^\beta(0) | P \rangle \langle P | e^{iqx} A_\mu^\alpha(0) | 0 \rangle \theta(-x^0) \right\} \right] \\
 &= \sum_{\mathbf{P}} \int d^4x \left[\frac{d^3q}{2E_{\mathbf{P}}(2\pi)^3} \left[M_{\mathbf{P}}^4 F_{\alpha\mathbf{P}} F_{\beta\mathbf{P}} (e^{-iq \cdot x} \theta(x^0) + e^{iq \cdot x} \theta(-x^0)) \right. \right. \\
 &\quad \left. \left. + iE_{\mathbf{P}} M_{\mathbf{P}}^2 F_{\alpha\mathbf{P}} F_{\beta\mathbf{P}} (e^{-iq \cdot x} + e^{iq \cdot x}) \delta(x^0) \right] \right]
 \end{aligned}$$

where translational invariance, $A(x) = e^{i \cdot P \cdot x} A(0) e^{-i P \cdot x}$ and the definitions

$$\langle 0 | A_\mu^\alpha | P \rangle = iq_\mu F_{\alpha\mathbf{P}} \quad (3)$$

have been invoked. With the identification

$$\int \frac{d^3q}{(2\pi)^3} e^{iq \cdot x} = \delta^3(\vec{x}) e^{iq_0 \cdot x^0}$$

this reduces, after integration, to zero. Thus (1) becomes the required relation

$$\int d^4x \langle 0 | T(\partial^\mu A_\mu^\alpha(x) \partial^\nu A_\nu^\beta(0)) | 0 \rangle = -\langle 0 | \left[Q_5^\alpha, \partial^\nu A_\nu^\beta(0) \right] | 0 \rangle \quad (4)$$

as given in (6.29). Pseudoscalar masses are obtained by matching the dominant

one particle contributions to the left-hand side of (4) with the $O(m_q)$ terms obtained from the commutator.

The left-hand side of (4) is evaluated by using the techniques described above, i.e. inserting a complete set of intermediate states of which particular single particle contributions are assumed to dominate. Using translational invariance and the definitions (3)

$$\int d^4x \langle 0 | T(\partial^\mu A_\mu^\alpha(x) \partial^\nu A_\nu^\beta(0)) | 0 \rangle = - \sum_P i M_P^2 F_{\alpha P} F_{\beta P} \quad (5)$$

The evaluation of the right-hand side of (4) is described in Chapter 6, equations (6.47) to (6.50). The required result is then

$$- \sum_P M_P^2 F_{\alpha P} F_{\beta P} = \frac{1}{4} \bar{q} \left[(\lambda^\beta_{M\lambda^\alpha} + \lambda^\beta \lambda^\alpha_M) \delta_{\beta\alpha} + (\lambda^\alpha_{M\lambda^\beta} + M\lambda^\alpha \lambda^\beta) \delta_{\alpha\beta} \right] q \quad (6)$$

If the pseudoscalar decay constants are assumed to be SU(3) symmetric with the octet members taking the value F_π and the singlet F_0 and the complete set of intermediate states is dominated by the relevant octet or singlet states then the formulae of (6.3) are reproduced. If, however, the SU(3) symmetry is broken and the left-hand side of (4) is saturated with physical particle states the formulae (6.51) to (6.53) are obtained.

REFERENCES

1. E. S. Abers and B.W.Lee, Phys. Rep. 9C (1973) 1.
L. Maiani, CERN 76-20 (1976) 23.
J. Iliopoulos, CERN 77-18 (1977) 36.
J. C. Taylor, "Gauge Theories of Weak Interactions",
Cambridge Univ.Press (1979).
2. H. D. Politzer, Phys. Rep. 14C (1974) 129.
W. Marciano and H. Pagels, Phys. Rep. 36C (1978) 137.
E. de Rafael in "Quantum Chromodynamics", Proc.of the X.G.I.F.T.
Int. Seminar on Th.Physics, Ed. J.L.Alonso and R. Tarrach (1980).
3. M. Gell-Mann and Y. Ne'eman, "The Eightfold Way" (1964).
4. J.J.J. Kokkedee, "The Quark Model", A. Benjamin Inc. (1969).
5. R.H.Dalitz in "Fundamentals of Quark Models", Proc.of the 17th
SUSSP (1977) 151.
6. F.E.Close, "An Introduction to Quarks and Partons", Academic Press
(1979).
B.H. Bransden, J.V.Major, D. Evans, "The Fundamental Particles",
Van Nostrand (1973).
7. H. Goldberg and Y. Ne'eman, NC 27 (1963) 1 and Ref.3.
8. E. de Rafael in Ref.2.
9. S.L. Adler, "Lectures on Elementary Particles and Quantum Field
Theory", Editors ; S. Deser, M. Grisaru and H. Pendleton
(M.I.T. Press, Cambridge, 1971) p.1.

10. F. Gursey and L. A. Radicati, PRL 13 (1964) 173.
B. Sakita, PR 136 (1964) B1756.
11. J. D. Bjorken and S.L.Glashow, PL 11 (1964) 255.
12. Z. Maki, Prog. Th. Phys. 31 (1964) 331.
Y. Hara, PR 134 (1964) B701.
D. Amati et al, PL 11 (1964) 190.
13. M.K. Gaillard, B.W.Lee and J.L.Rosner, Rev.Mod.Phys.47 (1975) 277.
14. S.L. Glashow, J. Iliopoulos, L. Maiani , PR D2 (1970) 1285.
15. J. Aubert et al, PRL 33 (1974) 1404.
J.E. Augustin et al., PRL 33 (1974) 1406.
16. W.R.Innes et al., PRL 39 (1977) 1240.
S.W.Herb et al.,PRL 39 (1977) 252.
17. M.L. Perl, PL 70B (1977) 487.
18. S.Okubu, PL5 (1963) 165.
G. Zweig, CERN preprint 8409/Th.412 (1964).
J. Iizuku, Prog.Th.Phys. 37-38 (1966) 21.
19. V.A.Novikov et al., Phys.Rep. 41C (1978) 1.
E. Eichten et al., PR D17 (1978) 3090.
20. C. Quigg and J.L.Rosner, PL 71B (1977) 153 and Phys.Rep.56 (1979) 167.
21. T. Barnes, Southampton Univ.Preprint SHEP 79/80-4.
22. V. Chaloupka et al, PL 50B (1974) 1.
23. T. Barnes, PL 63B (1976) 65.
24. R.P. Feynman et al, PR D3 (1971) 2706.

25. C.Itzykson and M. Jacob, NC 48A (1967) 909.
J.J.J. Kokkedee, PL 22 (1966) 88.
J.J.J. Kokkedee and L. van Hove, NC 42A (1966) 711.
H.J. Lipkin and F. Scheck, PRL 18 (1967) 347 and PRL 16 (1966) 71.
H. J. Lipkin, PRL 16 (1966) 1015.
26. M.P. Locher and H. Römer, PL 23 (1966) 496.
J. L. Friar and J.S.Trefil, NC 49A (1967) 642.
G. Alexander, H.J.Lipkin and F. Scheck, PRL 17 (1966) 412.
A. Bialas and K. Zalewski, NP B6 (1968) 449.
27. G. Preparata, CERN-TH, 2713.
W. Marciano and H. Pagels in ref.2.
28. J. D. Bjorken, SLAC-PUB-2372 (Dec.1979).
29. H. D. Politzer in ref.2.
30. G. Ross in "Gauge Theories and Experiments at High Energies",
Proceedings of the 21st SUSSP (1980).
31. R.J.Crewther, Acta Phys. Austr.Suppl. XIX (1978) 47.
32. S.L.Adler, PR 177 (1969) 2426.
J. Bell and R. Jackiw, NC 60A (1969) 47.
33. De Alfaro, S. Fubini, G. Furlan and G. Rossetti, "Currents in
Hadron Physics", North Holland (1973).
34. H. Pagels, Phys. Rep. 16C (1975) 219.
35. S. Coleman, J. Math.Phys. 7 (1966) 787.
36. J. Goldstone, NC 19 (1961) 154.
J. Goldstone, A. Salam and S. Weinberg PR 127 (1962) 965.

37. C.G. Callan, R. Dashen and D.J.Gross PR D17 (1978) 2717.
38. M. Gell-Mann, R.J. Oakes and B. Renner PR 175 (1968) 2195.
39. A de Rujula, H. Georgi and S.L. Glashow PR D12 (1975) 147.
40. N.H.Fuchs, PR D20 (1979) 1244.
41. D.B. Lichtenberg, "Unitary Symmetry and Elementary Particles", Academic Press (1978).
42. G. Karl, NC 38A (1977) 315.
43. N. Isgur, PR D12 (1975) 3770 and PR D13 (1976) 122.
44. H. Fritzsche and P. Minkowski, NC 30A (1975) 393.
45. H. Fritzsche and J.D. Jackson, PL 66B (1977) 365.
46. R. Barbieri et al, PL 60B (1976) 183.
47. In later treatments, which will include the effects of mixing radial excitations with their ground-states, this $1/M^2$ dependence will be replaced by $1/m_a m_b$, where m_i are the constituent quark masses. The treatment will then coincide with that of Cohen and Lipkin.
48. N. Isgur, PR D21 (1980) 779.
49. K. Iguchi and S. Minami, PL 86B (1979) 206.
50. R. van Royen and V.G. Weisskopf, NC 50A (1967) 617.
51. K. Hirata et al, PR D10 (1978) 230.
52. F.D.Gault and A.B.Rimmer, Z.fur Phys. C8 (1981) 353.
53. H.F.Jones and M.D.Scadron, NP B155 (1979) 409.
54. R. Partridge et al., PRL 44 (1980) 712.
55. W.D.Apel, PL 83B (1979) 131.
56. H.J.Lipkin, PL 67B (1977) 65.
57. F. Marzano et al., NP B123 (1977) 203.

58. R.H. Capps, PR D15 (1977) 171 and PR D17 (1978) 1862.
59. I. Cohen and H.J.Lipkin, NP B151 (1979) 16.
60. R.H.Graham and P.J.O'Donnell, PR D19 (1979) 284.
61. Particle Data Group, Rev.Mod.Phys. 52 (1980) S1.
62. B. Kumar, Rutherford Lab preprint RL-80-060 (Sept.1980).
63. J. Ballam et al, NP B76 (1974) 375.
64. S. Bartalucci et al, NC 49A (1979) 207.
65. D.P. Barber et al, Z.fur Phys. C4 (1980) 169.
66. D. Aston et al., PL 92B (1980) 211.
67. M. Conversi et al., PL 52B (1974) 493.
N.M.Budnev et al., PL 70B (1977) 365.
P. Frenkiel et al., NP B47 (1972) 61.
G. Grayer et al., NP B75 (1974) 189.
68. H. Becker et al., NP B151 (1979) 46.
69. B. Delcourt et al., P.499 ; V.Sidorov, p.398 and M.Spinetti, P.506
in the 1979 Int.Symp. on Photon-Lepton Interactions, Fermilab (1979).
70. M. S. Atiya et al., PRL 43 (1979) 1691.
71. D. Aston et al., PL 92B (1980) 215.
72. B. Esposito et al., PL 68B (1977) 389.
73. G. Barbiellini et al., PL 68B (1977) 397.
74. G. Cosme et al., PL 67B (1977) 231.
75. G. Cosme et al., NP B152 (1979) 215.
D. Aston et al., NP B174 (1980) 269.
76. F. Richard, 1979 Int.Symp. on Lepton and Photon Interactions,
Fermilab, p.469.

77. G. Capon, Invited talk to Budapest Conf. on Particle Physics, Budapest (1977).
78. N.R. Stanton et al., PRL 42 (1979) 346.
79. R. Aaron et al., BNL Preprint BNL 2842OR.
80. C. Daum et al., CERN-EP/80-219 (1980).
81. D.L.Scharre, 1981 Int.Symp.on Lepton and Photon Interⁿs. at High Energies, Bonn, (1981).
82. D. Aschman, SLAC-PUB-2550.
E.D.Bloom, SLAC-PUB-2530.
83. D.L. Scharre, SLAC-PUB-2761 (June, 1981).
84. R. Brandelik et al., Z.fur Phys. C1 (1979) 213.
85. W. Bartel et al., PL 66B (1977) 489 and PL 64B (1976) 483.
86. W. Braunschweig et al., PL 67B (1977) 243.
87. D.L. Scharre, SLAC-PUB-2519 (1980).
88. G. Cosme et al., PL 63B (1976) 352.
89. P. Langacker, PL 90B (1980) 447.
90. A.B. Rimmer, PL 103B (1981) 459.
91. B.H. Wiik and G.Wolf in "Weak and Electromagnetic Interactions at High Energies", Editors ; R. Balian and C.H.Llewellyn Smith, North Holland (1977) p 403.
92. D. Berg et al., PRL 44 (1980) 706.
93. N. Barash-Schmidt et al., Rev.Mod.Phys. 48 (1976) 521.
94. N.R.Stanton et al., PL 92B (1980) 353.
95. See also Table 4.1.

96. D.M. Binnie et al., PL 83B (1979) 141.
97. G.S.Abrams et al., PRL 43 (1979) 447.
98. D.E. Andrews et al., PRL 38 (1977) 198.
99. M. Aguilar-Benitez et al., PRL 28 (1972) 574 and PR D6 (1972) 29.
100. S. Okubu, Prog. Th.Phys. Suppl. 63 (1978) 1.
101. G.H. Trilling et al., PL 19 (1965) 427.
102. I.J. Bloodworth et al., NP B39 (1972) 525.
103. M. Bardadin-Otwinowska et al., PR D4 (1971) 2711.
104. F.D.Gault et al., NC 24A (1974) 259.
105. R.K.Rader et al., PR D6 (1972) 3059.
J.S. Danburg et al., PR D2 (1970) 2564.
106. D.S. Ayres et al., PRL 32 (1974) 1463.
D. Cohen et al., PRL 38 (1977) 269.
107. D.W.Davies et al., PR D2 (1970) 506.
J.S.Danburg et al., PR D2 (1970) 2564.
108. N. Armenise et al., NC 65A (1970) 637.
109. M.S.Farber et al., NP B29 (1971) 237.
110. W.R.Butler et al., PR D7 (1973) 3177.
111. M. Aderholz et al., NP B8 (1968) 45 ; NP B11 (1969) 259 ;
NP B14 (1969) 255.
112. H.J.Lipkin, NP B7 (1968) 321.
113. H.J.Lipkin, "Lie Groups for Pedestrians", North Holland (1965).
114. H.Pilkuhn, "The Interactions of Hadrons", North Holland (1967).
115. B. Cassen and E. U. Condon, PR 50 (1936) 846.
116. N. Isgur, PR D21 (1980) 779.

117. N. Isgur, H.R. Rubinstein, A. Schwimmer and H.J.Lipkin, PL 89B (1979) 79.
118. P. Langacker, PL 90B (1980) 447.
119. G. Segre and J. Weyers, PL 62B (1976) 91.
120. H. Genz, Lett. al. Nuovo Cim. 21 (1978) 270.
121. P. Langacker and H. Pagels, PR D19 (1979) 2070.
122. P. Langacker, PR D20 (1979) 2983.
123. D.J. Gross, S.B. Treiman and F. Wilczek, PR D19 (1979) 2188.
124. W. Marciano and H. Pagels in Ref.2.
125. R.D. Peccei, Max Planck Institut, preprint MPI-PAE/PTh. 45/80 (1980).
126. J. Ellis in "Weak and Electromagnetic Interactions at High Energies"
Editors - R. Balian and C.H.Llewellyn Smith, North Holland (1977) 1.
127. H. Georgi and H.D. Politzer, PRL 36 (1976) 1281, PRL 37 (1976)
68 and PR D14 (1976) 1829.
128. R.J.Crewther, Riv. del Nuovo Cim. 2 (1979) 63.
129. H.D.Politzer, NP B117 (1976) 397.
130. R. Dashen, PR 183 (1969) 1285.
131. R.P. Feynman, "Photon-Hadron Interactions", W.A. Benjamin, Inc.(1972).
132. G.W.Brandenburg et al., NP B104 (1976) 413.
133. A. Quenzer et al., PL 76B (1978) 512.
134. H. Alvensleben et al., PRL 25 (1970) 1373 and PRL 27 (1971) 888.
B.N. Ratcliff, PL 38B (1972) 345.
D. Benaksas, PL 39B (1972) 289.
135. S.O.Holmgren et al., PL 66B (1977) 191.
136. A.B. Wicklund et al., PR D17 (1978) 1197.
137. M. Oreglia et al., PRL 45 (1980) 959.
138. T.M.Himmel et al., PRL 44 (1980) 921.
139. S. Coleman and E.Witten, PRL 45 (1980) 100.
140. S. Weinberg, PR D11 (1975) 3583 and Proceedings of the XVII Int.Conf.
on High Energy Physics (London,1974), p.III-59.

141. R.J.Crewther, Riv.del.Nuovo Cim.2 (1979) 63 and PL 70B (1977) 349.
142. R.J.Crewther, Acta Physica Austriaca, Suppl. XIX (1978) 47.
143. A.A.Belavin et al., PL 59B (1975) 85.
144. G.'t Hooft, PRL 37 (1976) 8 and PR D14 (1976) 3432.
145. E. Witten, NP B149 (1979) 285 and NP B156 (1979) 269.
146. H. Goldberg, PRL 44 (1980) 363.
147. P.G.Williams and E. van Herwijnen, Westfield College, preprint.
148. K.A.Milton, W.F.Palmer and S.S.Pinsky, PL 100B (1981) 336.
149. B.L. Ioffe and M.A. Shifman, PL 95B (1980) 99.
150. P. Auvil and N.G. Deshpande, PR 183 (1969) 1463 and PR 185(1969)2043.
- G. Cicogna, F. Strocchi and R.V. Caffarelli, PR D6 (1972) 301.
- R. Duff, S. Eliezer and P. Nanda, PR D4 (1971) 3759.
151. J.M.Gerard, J. Pestieau and J. Weyers, PL 94B (1980) 227.
152. S.B.Treiman, R. Jackiw, D.J. Gross, "Lectures on Current Algebra and its Applications", Princeton Univ.Press (1972).
153. C. Itzykson and J.B.Zuber, "Quantum Field Theory", McGraw-Hill (1980).
154. B. Renner, "Current Algebras and their Applications", Pergamon Press (1968).
155. C. Bemporad et al., PL 25B (1967) 380.
156. A. Browman et al., PRL 32 (1974) 1067.
157. P. Langacker and H. Pagels, PR D8 (1973) 4595.
158. M.A.Shifman, A.I. Vainshtein and V.I. Zakharov, NP B147 (1979) 385.
159. D. Benaksas et al., PL 39B (1972) 289.
160. H. Alvensleben et al., PRL 25 (1970) 1373.
161. I. Peruzzi et al., PRL 39 (1977) 1301.
162. J. Pisut et al., NP B6 (1968) 325.
163. J. D. Bjorken and S.Drell, "Relativistic Quantum Fields", McGraw-Hill (1965).
164. N.G. Deshpande et. al. PRD 15 (1977) 1885
165. S. Coleman and H.J. Schnitzer, PR 136 (1964) 223

